WITH NO LYSINE 1 (WNK1): A POTENTIAL REGULATOR OF
THE LYSOSOMAL DEGRADATION PATHWAY

APPROVED BY SUPERVISORY COMMITTEE

_____
Melanie H. Cobb

_____
Michael White

_____
Paul Sternweis

_____
Joseph Albanesi

_____
James Waddle

DEDICATION

I dedicate my work to my parents George and Yvonne Lenertz, my brother Leon, and my husband Kyle Lindemer. I also dedicate my work to my wonderful parrots that have made living in this fundamentalist third-world country known as Texas to not be so bad.

WITH NO LYSINE 1 (WNK1): A POTENTIAL REGULATOR OF THE LYSOSOMAL DEGRADATION PATHWAY

by

LISA YVONNE LENERTZ

DISSERTATION

Presented to the Faculty of the Graduate School of Biomedical Sciences

The University of Texas Southwestern Medical Center at Dallas

In Partial Fulfillment of the Requirements

For the Degree of

DOCTOR OF PHILOSOPHY

The University of Texas Southwestern Medical Center at Dallas

Dallas, Texas

November, 2006

AN ANALYSIS OF WNK1 ACTIVATORS, SUBSTRATES,
AND INTERACTING PROTEINS

LISA YVONNE LENERTZ, Ph.D.

The University of Texas Southwestern Medical Center at Dallas, 2006

MELANIE H. COBB, Ph.D.

With no Lysine (K) 1 (WNK1) is an atypical serine/threonine protein kinase that has its catalytic lysine positioned in a unique location. This kinase, along with another member of the WNK family, WNK4, has been genetically linked to pseudohypoaldosteronism type II (PHAII), which is characterized by both hypertension and hyperkalemia. Several groups have used reconstitution assays in *Xenopus* oocytes and mammalian cell lines to show WNKs regulate the surface expression and/or activity of various ion transporters and channels, including the epithelial sodium channel (ENaC) and the sodium chloride co-transporter (NCCT).

Although the mechanisms for regulating these cell surface proteins are not well defined, it appears that WNKs may modulate the intracellular trafficking of these channels and transporters. To help define the mechanisms WNK1 utilizes to influence blood pressure and to characterize this kinase biochemically, I performed a WNK1 kinase activation screen and a WNK1 yeast-two-hybrid screen. I have shown that WNK1 kinase activity increases in response to osmotic stress, which may imply its kinase activity is important for regulating ion homeostasis in response to a change in cell volume. I have also shown that a proline-rich region of WNK1 interacts with vacuolar protein sorting 4a (VPS4a), an ATPase that helps sort cargo from the plasma membrane to lysosomes. Cells expressing a VPS4 ATP-hydrolysis mutant trap cargo from the cell surface in an aberrant endosomal structure, slowing protein degradation via the lysosomal pathway. I hypothesize that WNK1 delivers cargo to VPS4a to facilitate the degradation of plasma membrane proteins.

Table of Contents

List of Figures and Tables

Chapter 1

Chapter 2

Chapter 3

Chapter 4

List of Abbreviations

AAA: ATPases associated with diverse cellular activities
CCD: cortical collecting duct
DCT: distal convoluted tubule
EEA1: early endosome antigen 1
EGF: epidermal growth factor
ENaC: epithelial sodium channel
ERK: extracellular regulated kinase
ESCRT: endosomal sorting complex required for transport
KCC: potassium chloride cotransporter
LC3: microtubule-associated protein (MAP) light chain 3
MAPK: mitogen activated protein kinase
MIT: microtubule interacting trafficking domain
MVB: multivesicular body
NCCT: sodium chloride co-transporter
NKCC: sodium potassium chloride co-transporter
OSR: osmotic stress responsive
PAK: p21-activated kinase
PHAII: pseudohypoaldosteronism type II
PI(3)P: phosphatidyl inositol-3-phosphate
ROMK: renal outer medullary potassium channel
SGK: serum and glucocorticoid-regulated kinase
SKD1: suppressor of K^+ transport growth defect 1
SPAK: STE20/SPS1-related proline/alanine-rich kinase
TRPV: transient receptor potential vanilloid
VPS: vacuolar protein sorting
WNK: With no Lysine (K)

Chapter 1

Introduction

Introduction- With no Lysine (K) (WNK) kinases are atypical serine/threonine protein kinases that gathered much interest after two family members, WNK1 and WNK4, were linked to the familial form of hypertension pseudohypoaldosteronism type II (PHAII) (Wilson *et al.* 2001). This kinase family is unique because the lysine required for phosphoryl transfer is located in subdomain I instead of in subdomain II as in all other protein kinases. There are four mammalian homologs, one in *C. elegans* and *D. melongaster*, and at least nine in *A. thaliana* (Verissimo *et al.* 2001; Nakamichi *et al.* 2002). WNK kinases are relatively large proteins that contain a kinase domain located near the N-terminus, an autoinhibitory domain, putative coiled-coil domains, and large stretches of proline (Figure 1). All four family members also contain significantly large regions that have no sequence similarity to known domains.

Since mutations in WNK kinases were linked to hypertension, many groups began studying how over-expression or deletion of these proteins modulates the cell surface expression and activity of various ion transporters and channels, while others have focused on linking the WNK1 and WNK4 mutations to essential hypertension. These studies have lead to the discovery that WNK kinases modulate the cell surface presentation of several plasma membrane proteins and that mutations in WNKs may contribute to the severity of hypertension in the general population. Many questions remain to be answered

though about the mechanisms and signaling pathways by which WNK kinases regulate ion homeostasis and ultimately blood pressure.

My dissertation work has focused on characterizing a WNK1 protein interaction that may provide clues about how WNK1 regulates the cell surface expression of ion channels and transporters and studying the biochemical properties of the WNK kinases. As will be discussed in further chapters, I have evidence that WNK1 may play a role in the lysosomal degradation pathway. This chapter is a summary of what has been reported in the literature about the WNK kinases.

Mutations of WNK Kinases in PHAII- Mutations in WNK1 and WNK4 were found in Caucasian families that have PHAII, which is also known as Gordon's syndrome. Patients with this disease are characterized as having hypertension, hyperkalmeia (high serum potassium), hyperchloremia, suppressed plasma renin activity, reduced biocarbonate, but a normal glomerular filtration rate. The prevalence of PHAII is unknown since many people with the disease remain undiagnosed, but it has gained more interest in the medical community after the gene mapping study linking WNK1 and WNK4 to the disease was conducted (Wilson *et al.* 2001).

The mutations in WNK1 are intronic, resulting in a 5-fold increase in transcript level, and the mutations in WNK4 are charge-changing substitutions just distal to the first putative coiled-coil domain (Wilson *et al.* 2001). Many

experiments in cell lines and *Xenopus* oocytes have been conducted to determine how WNK kinases regulate blood pressure. These studies have shown WNKs modulate the surface expression and/or activity of several ion transporters and channels, but the mechanisms are largely undefined.

Linking Mutations in WNK Kinases to Other Forms of Hypertension- Human hypertension is a major health problem that can lead to stroke, myocardial infarction, and congestive heart failure. Hypertension is often a complex disorder caused by the input of multiple environmental and genetic factors. Genetic mutations have been found to contribute to specific forms of hypertension. For example, mutations in the epithelial sodium channel (ENaC) cause Liddle's syndrome, mutations in the thiazide-sensitive channel the sodium chloride cotransporter (NCCT) cause Gittleman's syndrome, and as described above, mutations in WNK1 and WNK4 cause PHAII.

A few human genetic studies have been conducted to determine whether mutations in WNK1 and WNK4 are found in individuals with high blood pressure who are unaware of a specific genetic component to their disorder. A study conducted in Britain of severely hypertensive Caucasian families showed that one single nucleotide polymorphism (SNP) located 3 kilobases (kb) from the WNK1 promoter is associated with the severity of both systolic and diastolic blood pressure (Newhouse *et al.* 2005). In another European study, the ambulatory blood pressure of subjects from a population-based sample was measured and

correlated with the presence or absence of WNK1 gene polymorphisms or haplotypes (Tobin *et al.* 2005). The researchers found statistically significant correlations between several common SNPs and haplotypes in WNK1 with increased blood pressure. These data support the idea that studying WNK kinases is not only critical for better understanding PHAII but is also important in better understanding hypertension in the general population.

WNK1- The first WNK kinase was cloned in the Cobb laboratory in a PCR screen to identify additional mitogen activated protein kinase kinases (MAP2K), or MAP/extracellular signal-regulated protein kinase (ERK) kinases (MEKs) (Xu *et al.* 2000). These screens lead to the identification of WNK1, an unusual protein of 2126 amino acids (rat sequence) that contains 24 PxxP motifs and at least two putative coiled-coil domains.

As mentioned above, the catalytic lysine of WNK1 was found to be positioned in subdomain I/beta strand 2 of the kinase domain instead of in subdomain II/beta strand 3. This was surprising because this critical lysine in all other protein kinases resides in subdomain II. Figure 2 shows an alignment of subdomains I and II of the WNK1 and protein kinase A (PKA) kinase domains. In WNK1, a cysteine resides at the equivalent position that the catalytic lysine of PKA is located. Mutation of this cysteine in WNK1 (C250) to alanine does not alter its activity, but mutation of it to lysine greatly reduces it, possibly because adding this bulky amino acid induces a conformational change that inhibits its

catalytic activity. The catalytic lysine, K223, is positioned where a conserved glycine in the phosphate anchor ribbon is normally located.

The ERK2 G35K/K52A double mutant was generated to determine whether the WNK catalytic lysine placement could function in other protein kinases. Interestingly, ERK2 G35K/K52A displayed similar kinase activity in comparison to wild-type ERK2, illustrating the idea that the unique placement of the WNK catalytic residue could theoretically work in other protein kinases (Xu *et al.* 2000; Xu *et al.* 2002).

In the early WNK1 characterization studies from our laboratory, the WNK1 autoinhibitory domain and regulation of WNK1 autophosphorylation were also described. *In vitro* kinase assays were used to show recombinant WNK1 485-55 inhibits an N-terminal WNK1 fragment (residues 1-491) that contains the kinase domain, and mutation of two phenylalanine residues within the autoinhibitory domain that are conserved among the WNK family members drastically reduces the ability of WNK1 485-555 to inhibit WNK1 kinase activity. In addition, it was shown that two serine residues within the WNK1 activation loop (serine 378 and 382) are required for its full autophosphorylation activity and activity towards a substrate (Xu *et al.* 2002).

Initial characterization studies also addressed WNK1 expression patterns, activators, and downstream targets. It was originally shown that WNK1 is expressed in brain and HEK293 cells, and later reports showed WNK1 is found in

polarized epithelia including those of the kidney, colon, gallbladder, sweat duct, skin, esophagus, pancreatic ducts, hepatic biliary ducts, and epididymis (Xu *et al.* 2000; Choate *et al.* 2003). It was also reported that WNK1 is cytoplasmic in some polarized epithelia but is localized on the lateral membrane in others (Choate *et al.* 2003). We have since found WNK1 expression is ubiquitous and displays a distinct localization pattern in the cytoplasm of the cell lines we have analyzed. This will be discussed further in Chapters 2 and 4.

In attempts to understand WNK1 signaling, several agents were tested to determine whether they activate WNK1, and the activation of MAPK pathways by over-expressed WNK1 was assessed. These studies led to the findings that WNK1 is activated by high molar salt and can act as a MAP4K in the ERK5 MAPK pathway (Xu *et al.* 2000; Xu *et al.* 2004). ERK5 is one of the less studied members of the MAPK family. It is activated by growth factors and plays important roles in cell proliferation, cardiovascular development, and neural differentiation (reviewed in Nishimoto and Nishida 2006). ERK5 is activated by MEK5, which is presumably activated by the MAP kinase kinase kinases (MAP3K) MEKK2 and MEKK3. WNK1 phosphorylates and co-immunoprecipitates with MEKK2 and MEKK3, and reducing WNK1 protein expression by RNA interference (RNAi) in HeLa cells reduces the ability of ERK5 to be activated by epidermal growth factor (EGF). Corroborating this finding, a recent report has shown that knocking down WNK1 expression in a

neural progenitor cell line decreases the activation of ERK5 by EGF (Sun *et al.* 2006). In Chapters 2 and 3 I will discuss my attempt to identify additional WNK1 stimuli and WNK1 substrates.

Although the first WNK1 paper was published in 2000, there is still relatively little known about its signaling. Only a handful of WNK1 substrates and two kinases that phosphorylates WNK1 have been reported. The list of known WNK1 substrates includes MEKK2, MEKK3, oxidative stress responsive 1 (OSR1), STE20/SPS1-related proline/alanine-rich kinase (SPAK), synaptotagmin II (SytII), WNK2, WNK4, and as I will discuss later, p21-activated kinase 1 (PAK1) (Xu *et al.* 2004; Vitari *et al.* 2005; Moriguchi *et al.* 2005; Anselmo *et al.* 2006; Lee *et al.* 2004; Lenertz *et al.* 2005). OSR1 and SPAK are both members of the STE20 family, MAP4 kinases that are involved in osmosensing and cell volume regulation (reviewed in Strange *et al.* 2006). SytII is a member of the synaptotagmin family, C2 domain-containing proteins that regulate membrane trafficking and vesicle fusion (reviewed in Sudhof 2002). See figure 3 for an illustration of WNK1 with its known substrates. One of the only known kinases that phosphorylates WNK1 is protein kinase B (PKB)/Akt, which phosphorylates WNK1 T60 (human sequence) in response to insulin-like growth factor (IGF-1) (Vitari *et al.* 2004). We have reported that WNK4 also phosphorylates WNK1 (Lenertz *et al.* 2005). Akt is a target of phosphatidylinositol 3-kinase (PI3K) and has been extensively studied because of

its complex role in tumor development and metastasis (reviewed in Yoeli-Lerner and Toker 2006).

Function of WNK1- WNK1 gene-deleted mice were generated and display a phenotype that is consistent with the finding that over-expression of WNK1 results in PHAII (Zambrowicz *et al.* 2003). WNK1 homozygous deleted mice die during embryonic development, but WNK1 heterozygous mice have low blood pressure. The result showing animals deleted for WNK1 are not viable implies that WNK1 is an essential gene for development and suggests it may perform functions in addition to regulating blood pressure. To support this idea, it was recently reported that knocking down WNK1 expression in the mouse neural progenitor cell line C17.2 reduces cell growth and migration (Sun *et al.* 2006).

Because mutations in WNK1 and WNK4 were found in patients with PHAII, many groups have focused on the physiological mechanisms by which these proteins regulate ion homeostasis. The general theme is that WNK1 and WNK4 modulate the surface expression and/or activity of multiple ion transporters and channels but the biochemical mechanisms are poorly understood. These ion channels and transporters include but are not limited to ENaC, NCCT, and the sodium potassium two chloride cotransporter (NKCC). The details of these findings will be discussed later in this chapter.

WNK2- WNK2 is the least studied of the four mammalian WNK family members and is approximately 2300 amino acids (Figure 1). There have been no

reports to date about the function of WNK2, but I have reported that WNK1 phosphorylates WNK2 within its kinase domain and that the WNK1 autoinhibitory domain inhibits WNK2 kinase activity (Lenertz *et al.* 2005). A tissue expression profile of the four WNK homologs was conducted, and the presence of WNK2 mRNA was limited to human fetal brain and heart and adult liver and colon, while WNK1 mRNA was expressed in multiple tissues including fetal heart, skin, small intestine, spleen, macrophages and liver, and adult liver, brain, colon and adrenals (Verissimo *et al.* 2001).

WNK3- As with WNK2, little is known about WNK3 in comparison to WNK1 and WNK4, but there have been some reports showing it also regulates the activity of ion channels and transporters. WNK3 is approximately 1750 amino acids and contains fewer proline residues than the other WNK family members; there is a small proline-rich region at the distal C-terminus (Figure 1). In the tissue distribution study conducted by Peter Jordan's group, WNK3 transcripts were found in human fetal brain but not in fetal heart, skin, small intestine, spleen, or macrophages or in adult liver, colon, or adrenals (Verissimo *et al.* 2001). Immunofluorescence experiments have shown WNK3 protein is expressed in epithelia of the small intestine, stomach, pancreatic ducts, bile ducts, and epididymis (Kahle *et al.* 2005).

There is evidence that WNK3 modulates the activity of the renal outer medullary potassium channel (ROMK) and the chloride regulators NKCC1 and

the potassium chloride cotransporters 1 and 2 (KCC1/2) (Kahle *et al.* 2005; Leng Q *et al.* 2006). ROMK is present on the apical membranes of the distal renal tubules and secretes potassium into the distal convoluted tubule (DCT) and cortical collecting duct (CCD). NKCC is a major mediator of chloride entry into the cell while KCC is a major mediator of chloride exit. Studies conducted in *Xenopus* oocytes have shown that WNK3 inhibits ROMK and KCC but stimulates NKCC1 activity (Kahle *et al.* 2005; Rinehart *et al.* 2005; Leng *et al.* 2006).

In addition to the involvement of WNK3 in regulating the activity of these ion transporters and channels, it has been reported that WNK3 increases the survival of HeLa cells via procaspase-3. Reducing WNK3 protein levels by RNAi promotes the activation of caspase-3 and accelerates apoptosis (Verissimo *et al.* 2006). As with WNK1, it appears that WNK3 may perform functions in addition to regulating electrolyte balance through the modulation of several cell surface proteins.

WNK4- WNK4 is the other WNK family member mutated in patients with PHAII, and these mutations are missense and cluster within a stretch of four amino acids distal to the first putative coiled-coil domain (Wilson *et al.* 2001). The significance of these mutations in the development of hypertension is not well understood, but a few studies have shown that these mutations alter the regulation of specific ion transporters and channels (Kahle *et al.* 2003; Yang *et al.* 2003). WNK4 is the smallest of the WNK kinases; the mouse homolog is 1222

amino acids (Figure 1). The expression of WNK4 is not limited to the kidney, as was initially suggested, but appears more limited than WNK1 expression (Verissimo *et al.* 2001). It has been reported that WNK4 protein is expressed in kidney, brain, testis, colon, heart, liver, prostate, and lung (Kahle *et al.* 2004).

Regulation of Ion Channel and Transporter Activity by WNK Kinases- As previously discussed, results from cell-based studies have suggested that WNK kinases regulate several different ion transporters and channels. It has been reported that WNK1 regulates ENaC, NCCT, NKCC, ROMK, and the transient receptor potential vanilloid 4 (TRPV4), WNK4 regulates NCCT, ROMK, NKCC, KCC, TRPV4 and TRPV5, and WNK3 regulates ROMK, NKCC, KCC and NCCT. These observations will be described in detail below.

Regulation of the Sodium Channel ENaC- Two different groups have provided evidence that WNK1 increases the amount of sodium influx through ENaC. ENaC plays a critical role in fluid reabsorption in the kidney, colon and lung, consists of three homologous subunits: alpha, beta and gamma, and is pharmacologically blocked by amiloride (reviewed in Malik *et al.* 2006). As with other cell surface proteins, the length of time it resides on the plasma membrane is a key factor in the regulation of its activity. The C-terminus of ENaC contains a PPxY motif, which binds to the E3 ubiquitin ligase developmentally downregulated protein (Nedd4-2) and is degraded via the proteasome. Nedd4-2 is downregulated via phosphorylation by serum and glucocorticoid inducible kinase

(SGK1) (reviewed in Pearce 2003), which is a target of WNK1 (Xu *et al.* 2005a; 2005b).

The Cobb laboratory has found that WNK1 increases the surface expression and activity of ENaC through its N-terminus. The N-terminus of WNK1 (residues 1-491) co-immunoprecipitates with exogenous SGK1, and expression of WNK1 1-220 increases the kinase activity of SGK1. Interestingly, this connection appears to be indirect because WNK1 does not directly phosphorylate SGK1, but the activation of it by WNK1 1-220 is PI3K-dependent as shown by its sensitivity to wortmannin. In addition, phosphorylation of WNK1 T58 (the Akt phosphorylation site) contributes to the activation of SGK1, and as determined by RNAi experiments, SGK1 activation by IGF-1 is dependent on WNK1 (Xu *et al.* 2005a; 2005b).

In contrast to our findings, another group showed that kidney-specific WNK1 (KS-WNK1), an isoform of WNK1 lacking the N-terminus and kinase domain, increases transepithelial sodium current in Fisher rat thyroid FRT epithelia transfected with ENaC and increasing amount of KS-WNK1. In this study, KS-WNK1 expression but not expression of the long WNK1 isoform containing the kinase domain (L-WNK1) was induced by aldosterone, and treatment with aldosterone increased the sodium transepithelial current (Naray-Fejes-Toth *et al.* 2004). The reasons for the different results between our laboratory and the other group are currently not understood at this time.

Regulation of the Potassium Channel ROMK- WNK1, WNK3 and WNK4 have been shown to decrease the surface expression and activity of the potassium channel ROMK (Kahle *et al.* 2003; Lazrak *et al.* 2006; Leng *et al.* 2006; Cope *et al.* 2006; Wade *et al.* 2006). ROMK-induced current is increased in HEK293 cells where WNK1 expression is knocked down using RNAi, and over-expression of L-WNK1 or WNK1 1-491 decreases ROMK activity as assessed by whole-cell patch-clamp recordings. Interestingly, over-expression of KS-WNK1 alone has no effect on ROMK but it does reverse the inhibition induced by L-WNK1 (Lazrak *et al.* 2006), and this finding was supported by another group who used *Xenopus* reconstitution experiments to show KS-WNK1 negatively regulates L-WNK1 (Wade *et al.* 2006). Furthermore, it was reported that the WNK1-mediated inhibition of ROMK does not depend on its catalytic activity (Cope *et al.* 2006). It is possible that the presence of the WNK1 N-terminus is important for down-regulating ROMK but it does not have to possess kinase activity.

As with WNK1, reconstitution studies in *Xenopus* oocytes have been conducted to show WNK3 and WNK4 also inhibit the surface expression and activity of ROMK. It appears these effects are kinase-independent but that the inhibition of ROMK is more pronounced with the WNK4 PHAII mutants or the WNK3 homologous PHAII point mutants in comparison to the wild-type counterparts (Kahle *et al.* 2003; Leng *et al.* 2006). The inhibition of ROMK by WNK1, WNK3 and WNK4 may account for the hyperkalemia observed in PHAII

patients where WNK1 is presumably over-expressed and specific WNK4 residues are mutated.

Regulation of the Sodium Chloride Cotransporter NCCT- The mechanisms of regulation for NKCC, ENaC, and ROMK by WNK1 appear to be different from one another and how WNK1 regulates NCCT appears to be no exception. Different groups have provided evidence that WNK1 activates NCCT through inhibition of WNK4. WNK4 has been shown to prevent NCCT from being expressed on the cell surface and that WNK1 relieves this inhibition (Yang *et al.* 2003; Yang *et al.* 2005; Cai *et al.* 2006; Golbang *et al.* 2006). In the first study to suggest WNK kinases may regulate other WNK family members, *Xenopus* oocytes were injected with WNK1, WNK4 and NCCT. NCCT alone was expressed on the plasma membrane, but when WNK4 was added no surface expression was detected. Interestingly, the addition of WNK1 relieved the WNK4-mediated inhibition (Yang *et al.* 2003). The same group conducted another study to show the effects mediated by WNK1 and WNK4 are dependent upon the presence of the kinase domains (Yang *et al.* 2005). The study performed by Golbang *et al.* corroborated some of the findings of Yang *et al.* except they concluded the WNK1 effect is kinase-independent. The debate over whether WNK-mediated events are kinase-dependent or kinase-independent is still ongoing and merits further investigation.

The study conducted by Cai *et al.* offered a mechanistic explanation for how WNK4 down-regulates NCCT by showing clathrin-mediated endocytosis of NCCT is not affected by WNK4 and suggesting WNK4 may increase the degradation of the cotransporter via the lysosomal degradation pathway (Cai *et al.* 2006). Exogenous WNK4 reduces the amount of NCCT expressed on the plasma membrane, but over-expression of wild-type or dynamin K44A does not appear to influence this WNK4-mediated effect. In addition, Cai *et al.* reported that WNK4 over-expressed in COS-7 cells co-localizes with the lysosomal marker cathepsin D.

To further complicate the story linking WNK kinases to NCCT, *Xenopus* reconstitution studies were used to show that wild-type WNK3 but not kinase-dead WNK3 promotes NCCT localization on the plasma membrane (Rinehart *et al.* 2005). It is not known whether this effect is mediated through the inhibition of WNK4, as it is presumed for the regulation of NCCT by WNK1.

Regulation of the Sodium Potassium Chloride Cotransporter NKCC- The modulation of NKCC activity by WNK kinases has not been as extensively studied as the relationships between WNKs with ROMK or NCCT. The few available reports suggest that WNK1, WNK3 and WNK4 all increase NKCC activity and that this is kinase-dependent (Rinehart *et al.* 2005; Anselmo *et al.* 2006; Gagnon *et al.* 2006).

As for the regulation of NKCC by WNK1, WNK1 interacts with and phosphorylates OSR1, resulting in increased activity of the cotransporter as assessed by radioactive rubidium uptake, which mimics the influx of sodium and potassium. WNK1 and OSR1 strongly interact, which is supported by co-immunoprecipitation of the endogenous proteins, and knocking down WNK1 or OSR1 protein levels by RNAi in HeLa cells reduces NKCC activity (Anselmo *et al.* 2006). In the case of WNK4, studies in *Xenopus* oocytes were conducted to show WNK4 interacts with the OSR1 homolog SPAK, and mutation of the WNK4 and SPAK kinase domains or of the SPAK interaction motif in WNK4 decreases NKCC activation (Gagnon *et al.* 2006). It is not known whether WNK3 also phosphorylates OSR1 or SPAK, but wild-type and not kinase-dead WNK3 is thought to increase NKCC activity (Rinehart *et al.* 2005).

Regulation of the Potassium Chloride Cotransporter KCC- The list of cell surface proteins reportedly regulated by WNK kinases continues to expand. There have been a few studies conducted to show WNK3 and WNK4 inhibit KCC, a neuronal-specific KCl cotransporter responsible for chloride exit from the cell (Kahle *et al.* 2005; Gagnon *et al.* 2006). At least in the case of WNK3 it appears this effect is kinase-dependent (Kahle *et al.* 2005). As for many of the WNK studies, *Xenopus* reconstitution assays were used in these reports to connect WNK3 and WNK4 with KCC.

Regulation of the Nonselective Cation Channels TRPV4 and TRPV5- The most recent channels that WNK kinases have been reported to regulate are TRPV4 and TRPV5. TRPV4 is a nonselective cation channel expressed in many tissues that participates in thermosensation, mechanosensation, and osmoregulation (Fu *et al.* 2006; reviewed in Nilius *et al.* 2004), and TRPV5 is essential for calcium reabsorption in epithelia (reviewed in Thebault *et al.* 2006). Exogenous WNK1 and WNK4 inhibit the cell surface presentation of over-expressed TRPV4 (Fu *et al.* 2006), but conversely, WNK4 appears to increase the amount of TRPV5 expressed on the plasma membrane (Jiang *et al.* 2006). The mechanisms by which WNK1 and WNK4 modulate these channels are not known and the consequences of these regulatory events remain to be determined.

Conclusions- Much information about WNK kinases has been obtained since the first cloning paper and the human genetics study linking WNK1 and WNK4 to PHAII were published (Xu *et al.* 2000; Wilson *et al.* 2001). Since then many studies have been conducted to better understand the physiology of WNK kinases and they have shown WNKs regulate the surface expression and activity of several ion transporters and channels. See figures 5-7 for schematics. Connecting WNKs to the up-regulation of the sodium channels ENaC, NCCT and NKCC and to the down-regulation of ROMK may help explain how PHAII patients are both hypertensive and hyperkalemic.

Although these experiments have provided significant insight into WNK biology, many questions remain about the mechanisms and signaling by which WNKs modulate the surface expression of these proteins. It is not clear whether the kinase activity of the WNK family members is important for the regulation of transporters and channels, and it is not known how WNK1 and WNK4 interplay to regulate the cell surface expression of NCCT. What seems clear, however, is that the WNKs may regulate the intracellular trafficking of these plasma proteins as a method of influencing their activity. I will later describe how I may have discovered a link between WNK1 and protein sorting.

In addition, relatively little work has been done to identify WNK1 stimuli, interacting partners, substrates, and the signaling pathways in which WNKs act. Our laboratory has been the major contributor to the efforts to understand the biochemical properties of WNK kinases and the basic mechanisms by which these kinases may regulate ion homeostasis. We have determined WNK1 is activated by osmotic stress and have identified several WNK1 substrates and interacting partners. Information from these studies will hopefully improve our knowledge of WNK biology. These studies will have implications not only for individuals with PHAII but also for those in the general population with essential hypertension.

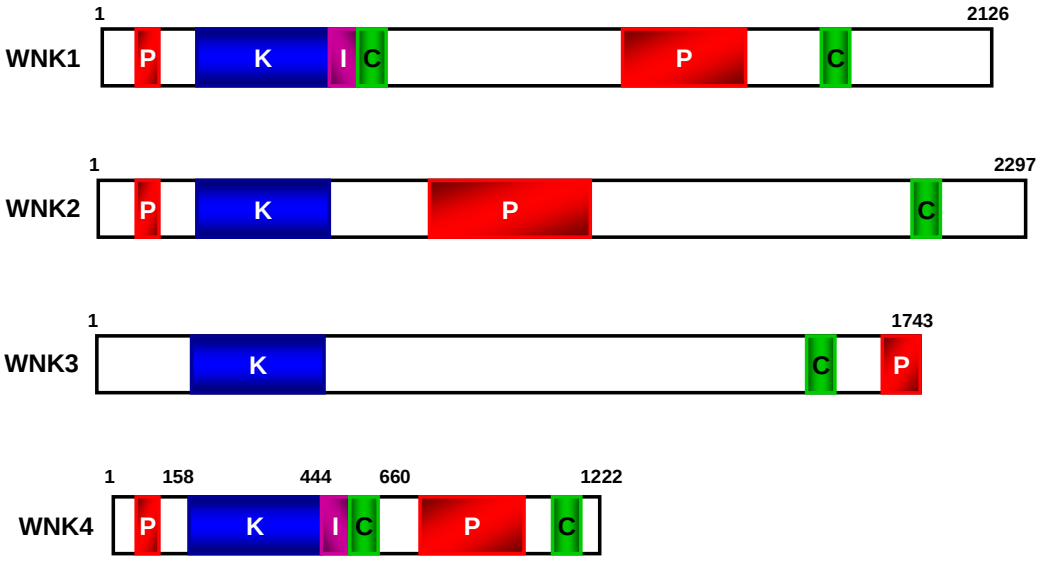

Fig. 1: Architecture of the mammalian WNK kinases. The following accession numbers from NCBI were used to generate these illustrations: rat WNK1 AAF74258, human WNK2 Q9Y3S1, human WNK3 CAI43129, and mouse WNK4 AAO21955. WNK2 and WNK3 contain a putative autoinhibitory domain directly distal to the kinase domain, but they were not included in the figure because the existence of these domains has not been tested experimentally. P: proline-rich; K: kinase domain; I: autoinhibitory domain; C: coiled-coil domain.

PKA residue	G^{55}	K^{72}		
Role in PKA	Conserved Gly	Catalytic Lys		
Role in WNK1	Catalytic Lys	Does not impact catalytic activity	Does not impact catalytic activity	Does not impact catalytic activity
WNK1 residue	K^{233}	C^{250}	K^{256}	K^{259}

Fig. 2: Catalytic domains of WNK1 and PKA. The catalytic lysine of WNK1 is positioned in subdomain I instead of in subdomain II as in all protein kinases. The WNK1 catalytic lysine replaces a conserved glycine. This figure was modified from Xu *et al.* 2000.

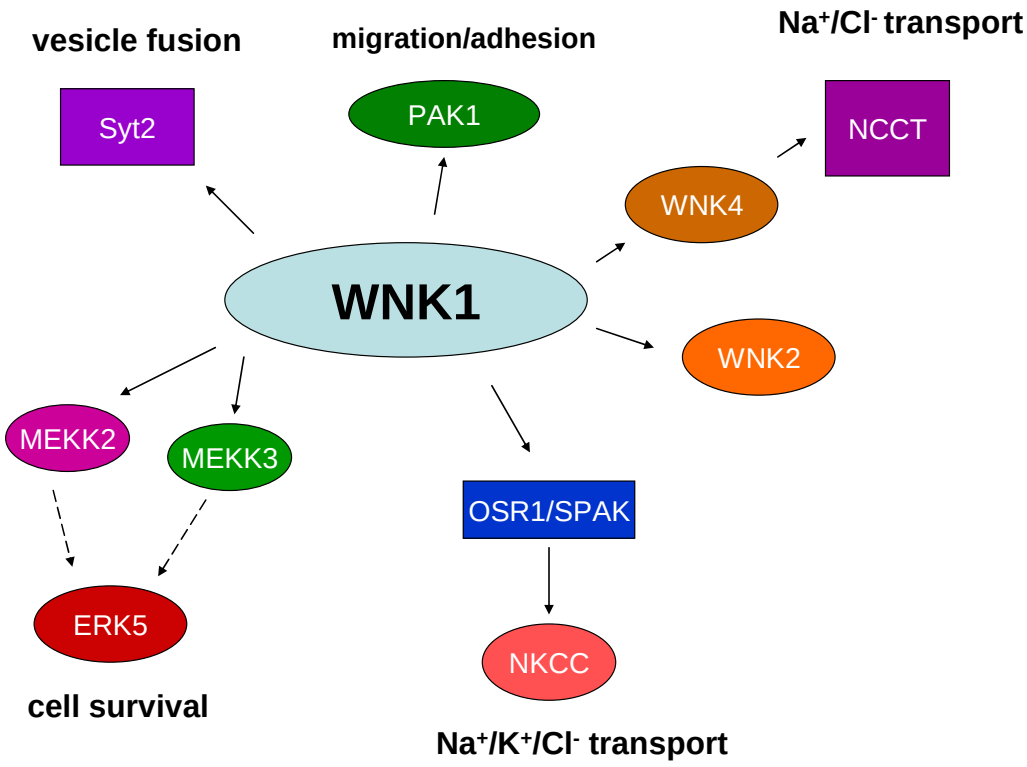

Fig. 3: WNK1 substrates. WNK1 phosphorylates MEKK2/3, the upstream MAP3Ks of ERK5, to influence cell survival (Xu *et al.* 2002; Sun *et al.* 2006). WNK1 also phosphorylates OSR1/SPAK to regulate ion transport through NKCC (Vitari *et al.* 2005; Moriguchi *et al.* 2005; Anselmo *et al.* 2006), and phosphorylates Syt2 to modulate Syt2 binding to phospholipids vesicles (Lee *et al.* 2004). I have reported that WNK1 phosphorylates WNK2 and WNK4 (Lenertz *et al.* 2005) and have evidence showing WNK1 phosphorylates PAK1. The connection between WNK1 and WNK4 is potentially interesting because work from David Ellison's group is suggestive that WNK1 relieves WNK4's inhibitory effect on NCCT surface expression and that these events are dependent on a functional WNK1 kinase domain (Yang *et al.* 2003; 2005). The WNK1/PAK1 connection will be discussed in Chapter 3.

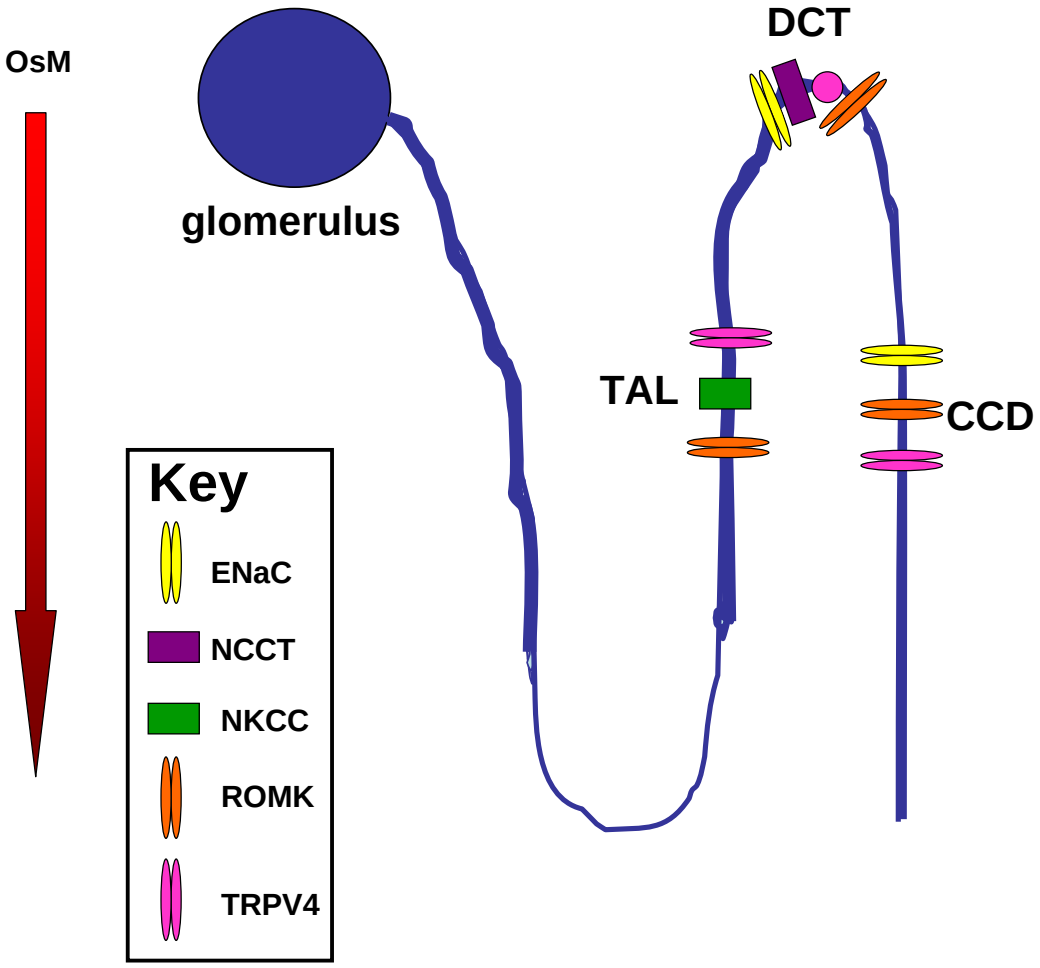

Fig. 4: Location of various ion transporters and channels in the nephron. Reviewed in Roosier 2003. TAL: thick ascending limb; DCT: distal convoluted tubule; CCD: cortical collecting duct.

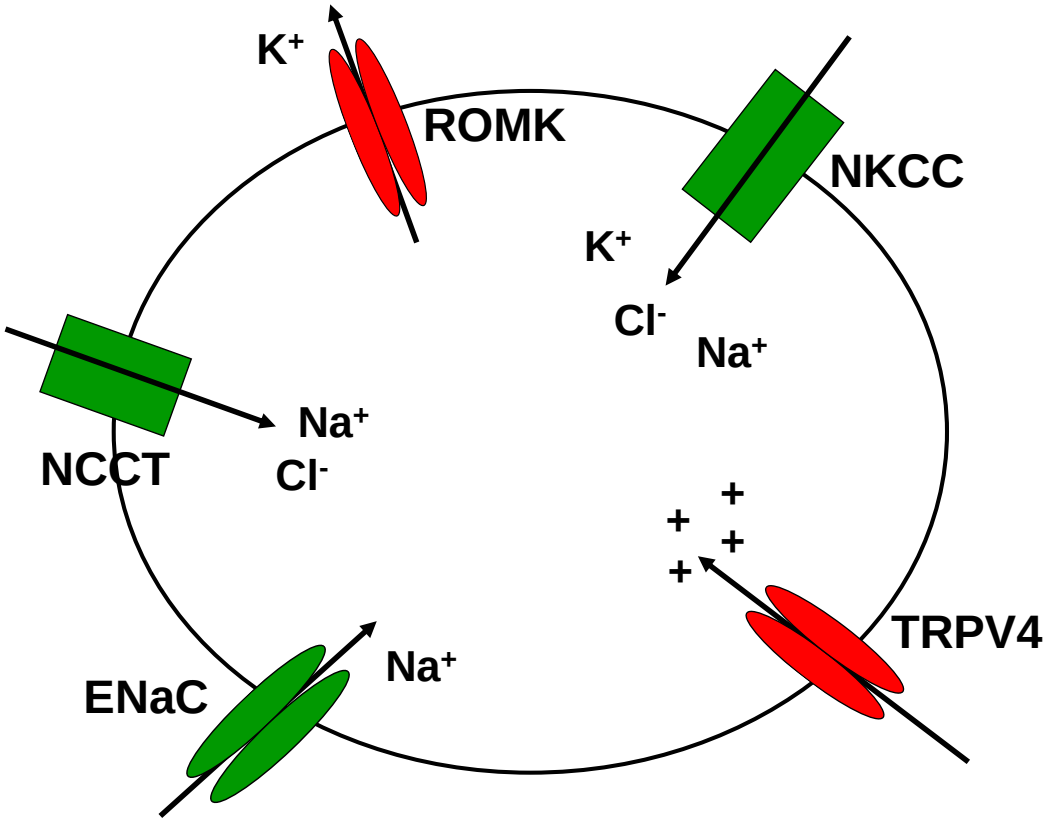

Fig. 5: Channels and transporters modulated by WNK1. WNK1 has been shown to positively regulate ENaC, NKCC and NCCT (denoted in green) and to negatively regulate ROMK and TRPV4 (denoted in red). See text for details.

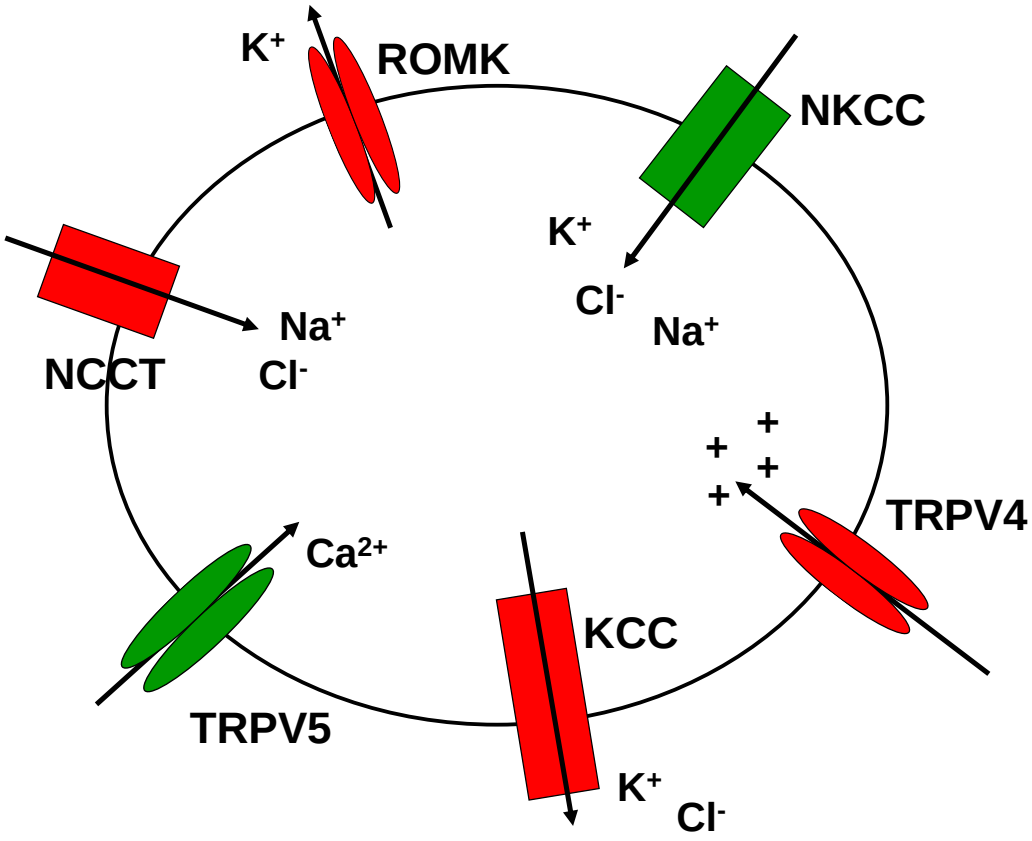

Fig. 6: Channels and transporters modulated by WNK4. WNK4 has been shown to positively regulate NKCC and TRPV5 (denoted in green) and to negatively regulate ROMK, NCCT, KCC and TRPV4 (denoted in red). See text for more details.

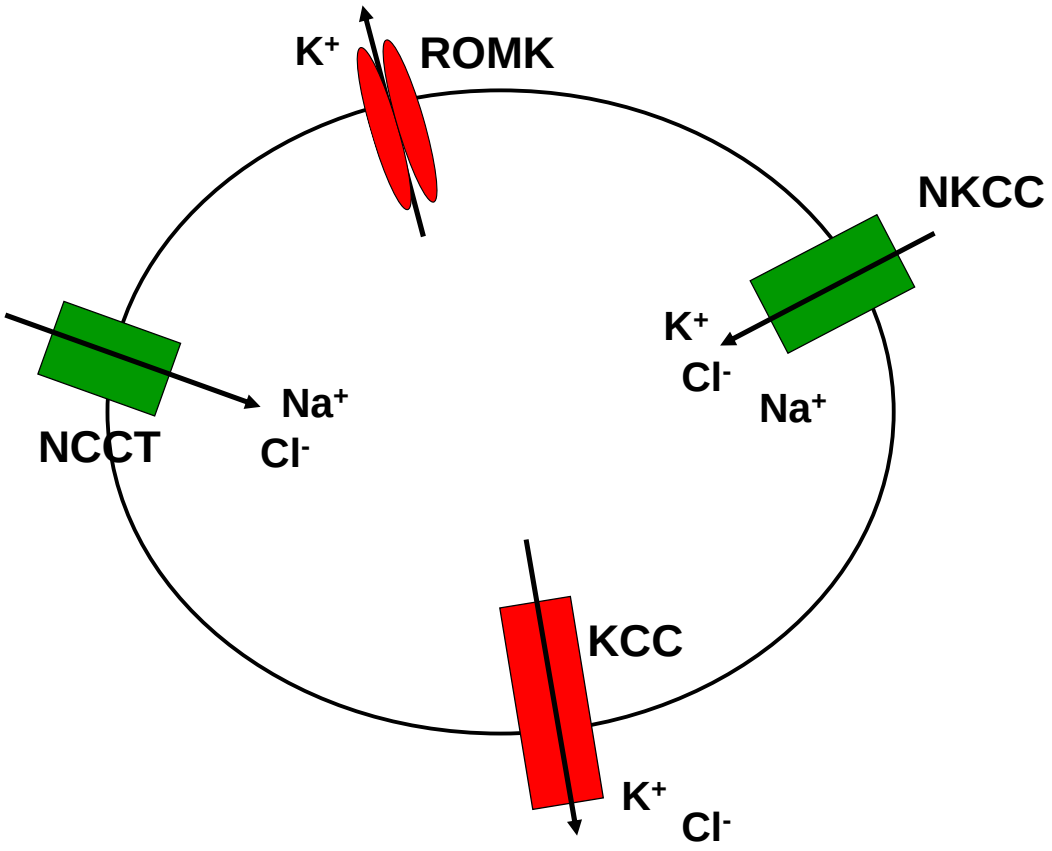

Fig. 7: Channels and transporters modulated by WNK3. WNK3 has been shown to positively regulate NCCT and NKCC (denoted in green) and to negatively regulate KCC and ROMK (denoted in red). See text for more details.

Chapter 2

Biochemical Characterization of WNK1

Introduction

When I first began working on WNK1, relatively little was known about its signaling, its expression patterns, its interacting partners, its substrates, or how over-expression of the protein results in hypertension. During my early studies in the Cobb laboratory, I performed a series of biochemical experiments in efforts to better understand the kinase behavior of the WNK family members. Specifically, I sought to identify WNK1 stimuli, to determine what cell lines express the protein, and to pursue a finding showing WNK1 phosphorylates WNK4.

When WNK1 and WNK4 were genetically linked to hypertension in 2001 (Wilson *et al.* 2001), many people thought the expression of WNK1 and WNK4 would prove to be rather limited. Previous work from our laboratory, however, showed that WNK1 protein is not only expressed in human embryonic kidney (HEK293) cells but is also highly expressed in brain and COS cells (Xu *et al.* 2000). This prompted me to determine what other cell types express WNK1. I had several reasons for screening different lines: 1) To find a cell line besides HEK293 or COS that would be more biologically relevant to hypertension in which to conduct a WNK1 kinase activity stimulus screen. 2) To assess any pattern of WNK1 expression among normal cell lines, noninvasive cancer lines, and invasive lines. I wanted to know if cancer cells express more WNK1 than non-transformed cell types. This idea arose from preliminary data showing WNK1 may cooperate with Raf1 to induce the formation of foci in NIH3T3 cells.

In addition to the lack of knowledge concerning the expression patterns of WNK1, little was known about its signaling. We had evidence that WNK1 acts as a MAP4K in the ERK5 MAPK pathway and that WNK1 associates with SGK1 (Xu *et al.* 2004; 2005b). In efforts to map WNK1 pathways and to obtain active WNK1 that could be used in further biochemical analyses, I conducted a kinase activation screen by immunoprecipitating WNK1 from treated cell lines. Knowing what stimuli activate a kinase potentially provides clues about the identity of upstream regulators and downstream effectors. At the time, there were no known kinases upstream of WNK1 and the only known substrate was MBP. Shortly thereafter we discovered WNK1 phosphorylates WNK4.

The result showing WNK4 is a WNK1 substrate was interesting because as previously discussed, a report from David Ellison's group suggested that WNK1 may modulate WNK4's ability to influence the amount of NCCT present on the plasma membrane of *Xenopus* oocytes (Yang *et al.* 2003). WNK4 prevented NCCT from being expressed on the cell membrane, and the addition of WNK1 relieved the WNK4-mediated inhibition. In continuation, this group also showed that WNK1's effect on WNK4 depends on the presence of a functional WNK1 kinase domain (Yang *et al.* 2005).

These data are suggestive that WNK kinases may influence the activity of one another to modulate a biological output. Since this was a largely unexplored area in the WNK field, I sought to further define the relationships between the

WNK family members. I tested the ideas that WNKs phosphorylate one another and that the autoinhibitory domain of one WNK kinase may inhibit other family members. Information from this characterization shows that WNK1 is ubiquitous, WNK1 is activated by osmotic stress, and WNK family members may belong to the same signaling cascade.

Methods

Cell Culture and Harvesting- Cell lines were cultured in Dulbecco's modified Eagle's medium (DMEM) with 10% fetal bovine serum and 1% L-glutamine at 37 °C under 5% CO_2. Mouse distal convoluted tubule (DCT) cells were cultured as described above with 110 mg/L sodium pyruvate under 10% CO_2. Confluent cells were generally harvested in lysis buffer containing 1% Triton X-100, 50 mM HEPES (pH 7.5), 150 mM NaCl, 1.5 mM $MgCl_2$, 1 mM EGTA, 10% glycerol, 100 mM NaF, 0.2 mM Na_3VO_4, 50 mM β-glycerophosphate, 1 mM dithiothreitol, 1 mM benzamidine hydrochloride, 10 mg/L leupeptin, 0.5 mg/L pepstatin A, and 1.5 mg/L aprotinin. The cells were vortexed for 30 s, incubated on ice for 10 min, and centrifuged for 15 min at 14,000 rpm to remove insoluble material.

Cell Lines- MDA-MB-231, MCF7, HME31, HME50, and ME16C were kindly provided by Jerry Shay and Woody Wright (UT Southwestern, Department of Cell Biology). HT-29 and SW40 were provided by Richard Gaynor (formerly

UT Southwestern, Department of Internal Medicine), and DCT were provided by Orson Moe (UT Southwestern, Department of Internal Medicine).

Antibodies and Proteins- The anti-WNK1 antibody Q256 was previously described (Xu *et al.* 2000). The purified kinase domains of rat WNK1 (residues 194-483), WNK4 (141-436), and the autoinhibitory fragment of WNK1 (residues 485–614) were provided by Xiaoshan Min. WNK1 (194-483) and WNK1 (485-614) were purified from Rosetta cells and WNK4 (141-436) was purified from Sf9 cells (Min *et al.* 2004). I prepared His_6-WNK4 (141-426) S332A using the Bac-to-Bac® system. Briefly, site-directed mutagenesis was used to mutate serine 332, a baculovirus was generated, Sf9 cells were infected with the virus, and nickel beads were used to purify the protein. GST-WNK1 (1-555) was provided by Bing-e Xu, and the GST-tagged WNK2 kinase domain was provided by Kyle Wedin.

Western Blotting- Proteins from cell lysates were resolved on 7.5% polyacrylamide gels in sodium dodecyl sulfate (SDS) and transferred to nitrocellulose at 400 mA and room temperature for 1 h in fresh 1X transfer buffer (25 mM Tris, 187 mM glycine) containing no methanol but 0.1% SDS. The nitrocellulose membranes were blocked in 5% nonfat dry milk, incubated with 1:1000 Q256 and 1:5000 anti-rabbit secondary antibody, and visualized by enhanced chemiluminescence.

In Vitro Kinase Assays of Immunoprecipitated WNK1- Confluent DCT cell cultures were incubated overnight in 1% fetal bovine serum, treated with a stimulus, and WNK1 was immunoprecipitated using Q256. Other cell lines were starved overnight without serum. Immunoprecipitated WNK1 was washed three times with 1 M NaCl, 20 mM Tris-HCl (pH 7.4) and once with 10 mM $MgCl_2$, 10 mM HEPES (pH 8.0). The beads were then incubated with 10 mM HEPES (pH 8.0), 10 mM $MgCl_2$, 50 μM ATP (~5000 cpm/pmol [γ-^{32}P]ATP), 1 mM benzamidine hydrochloride, and 1 mM dithiothreitol at 30°C for 15-30 min. The samples were then subjected to SDS polyacrylamide gel electrophoresis (SDS-PAGE), the gels were dried to generate an autoradiogram, and the WNK1 bands were excised and counted using a scintillation counter.

In Vitro Kinase Assays With Purified Proteins- The *in vitro* kinase assays were generally performed as follows. For the experiments to determine whether WNKs can phosphorylate one another, equimolar amounts of each WNK were incubated at 30°C for 20-30 min in kinase buffer (10 mM HEPES (pH 8.0), 5 mM $MgCl_2$, 0.5 mM benzamidine hydrochloride, 0.5 mM dithiothreitol, and 0.3 mg/mL bovine serum albumin (BSA)). BSA was added to stabilize the substrates and kinases. The samples were subjected to SDS-PAGE, and the gels were dried and exposed to x-ray film. For the assays to test whether the WNK1 autoinhibitory domain can inhibit other WNKs, 0-4.5 μg of the purified WNK1 autoinhibitory domain (residues 485-614) were incubated with 1 μg WNK4

(residues 141-436) or the WNK2 kinase domain. The proteins were resolved by SDS-PAGE, the gels were dried, and an autoradiogram was generated. The bands corresponding to WNK2 and WNK4 were excised and counted in order to determine the percent inhibition.

Two-Dimensional Phosphopeptide Mapping- Rat WNK1 wild-type (residues 194–483), WNK1 S378A (residues 194–483), and WNK4 wild-type (residues 141–436) were phosphorylated *in vitro*, subjected to electrophoresis, and transferred to polyvinylidene difluoride membranes (PVDF) membranes. The excised protein bands were soaked in 0.5% polyvinylpyrrolidone in 0.1 M acetic acid for 30 min at 37 °C, washed with water, and soaked in 50 mM ammonium bicarbonate. The peptides were digested with 50 ng/ml trypsin in 50 mM ammonium bicarbonate for 2 h at 37 °C; a second aliquot of trypsin was added for an additional 2 h. The digested peptides were lyophilized and suspended in electrophoresis buffer (2.2% formic acid, 7.8% acetic acid (pH 1.9)) and separated by thin layer electrophoresis. The digested peptides were then subjected to chromatography in the second dimension (*n*-butanol:pyridine:acetic acid:water, 15:1:3:12). I performed the *in vitro* kinase assays, while a research associate, Svetlana Earnest, performed the two-dimensional electrophoresis.

Results

WNK1 Protein Expression is Ubiquitous- To determine what cell types express WNK1 protein I obtained multiple cell lines from diverse sources including epithelial-derived lines of the colon, kidney and breast, neuroendocrine cells, and fibroblasts. I found WNK1 to be expressed in every cell line I analyzed via a Western blot and/or an *in vitro* kinase assay. These cell lines include HEK293 (human embryonic kidney), HeLa (human cervical cancer), Ins-1 (insulin-secreting beta cell), DCT (mouse distal convoluted tubule), PC12 (rat neuronal), MDA-MB-231 (human breast cancer), MCF7 (human breast cancer), HME31 ($p53^{+/+}$ human mammary epithelium), HME50 ($p53^{+/-}$ human mammary epithelium), ME16C (HME31 immortalized with the catalytic subunit of telomerase (hTERT)), HT-29 (human colon cancer), and SW480 (human colon cancer). The bottom half of figure 2 is a representative Western blot for a few of the cell lines. Equal amounts of total protein were analyzed in this experiment. It should be noted that the kidney cell line DCT does not express as much WNK1 as other lines, including the epithelial-derived colon cancer cells HT-29 and SW480. Because the only known physiological process that WNK1 regulates is blood pressure, I originally thought WNK1 would be most highly expressed in the kidney, and if it was expressed in other cell lines, it would be present at lower levels. Because WNK1 protein expression appears to be ubiquitous though, it is

likely that WNK1 performs multiple functions and may regulate ion balance in multiple cell types.

WNK1 is Activated by Hypertonic and Hypotonic Stress- I performed a WNK1 kinase activation screen in efforts to better understand its signal transduction and to obtain activated kinase to use in further biochemical analyses. I identified both hypertonic and hypotonic stress as WNK1 activators. Mouse DCT cells were used in the majority of these experiments while some assays included MDA-MB-231, MCF-7, HT-29, SW480, and HeLa. High millimolar NaCl, KCl, glucose, sucrose, and sorbitol activate WNK1 within at least 15 minutes (Figure 1), and DCT cells were treated with 0.5 M NaCl to show WNK1 can be appreciable activated by at least 5 minutes of stimulation (data not shown). The extent of activation varies among cell types. WNK1 from DCT cells is activated approximately 10-fold, while WNK1 from SW480, HT-29, MDA-MB-231, and MCF-7 is activated to a lesser extent (Figure 2). In addition, I have preliminary data showing over-expressed WNK4 from HEK293 cells is activated within 15 min by 0.5 M NaCl (data not shown). The hypotonic solutions were prepared by diluting DMEM in water to make 77 mOsM, 39 mOsM, and 19 mOsM solutions. Hypotonic stress resulted in a reproducible 2-3 fold increase in WNK1 activity in DCT cells (Figure 3).

I did not add exogenous substrate in these assays for two reasons. At the time I conducted these assays there were no identified substrates of WNK1 except

MBP, and the phosphorylation of MBP appeared to correlate with WNK1 autophosphorylation (Xu *et al.* 2002).

These data support the notion that WNK1 responds to changes in cell volume. At this point it remains unclear what the consequences of WNK1 kinase activation are, but it is conceivable that cells under osmotic stress may utilize WNK1 to modulate the amount of ion transporters and channels on the cell surface. Altering the composition of transporters and channels at the plasma membrane after osmotic stress will help normalize the salt balance and volume of a cell. As discussed later, there is evidence that the modulation of one transporter, NCCT, may be dependant upon the kinase activity of WNK1.

To date, there are no other known activators of WNK1. As mentioned previously, it has been shown that IGF-1 treatment results in the phosphorylation of human WNK1 at T60 via Akt/PKB but this does not increase WNK1 kinase activity (Vitari *et al.* 2004).

Other Agents Do Not Activate WNK1- Aside from osmotic stress, I also treated cells with serum, H_2O_2, EGF, transforming growth factor-β (TGF-β), insulin, IGF-1, UV light, parathyroid hormone, dexamethasone, and vasopressin in efforts to find a WNK1 stimulus, but none of these agents produced a consistent, appreciable change in WNK1 kinase activity. Parathyroid hormone, dexamethasone, and vasopressin were chosen because they are known regulators of kidney function. EGF was tested because we knew expression of exogenous

WNK1 activated ERK5 (Xu *et al.* 2004), and IGF-1 was tested because we had evidence that WNK1 associated with the IGF-1-responsive kinase SGK-1. I tried TGF-β because we had yeast-two-hybrid data showing the WNK1 kinase domain and Smad2 interact.

WNK Kinases Phosphorylate One Another- As mentioned before, we had preliminary data that WNK4 was phosphorylated by WNK1. This was interesting to me because work from other groups had shown WNK1 modulates WNK4's ability to regulate the surface expression of NCCT, and this regulation may be kinase-dependent (Yang *et al.* 2003; Yang *et al.* 2005; Golbang *et al.* 2006). When pursing our previous finding, I used mutants to show that WNK1 phosphorylates WNK4 on serine 332 (Figure 4). Serine 332 resides within the activation loop and is equivalent to serine 382 in WNK1, which is required for full kinase activity (Xu *et al.* 2002). In addition, I showed that WNK1 phosphorylates WNK2 within its kinase domain (Figure 5), and WNK4 phosphorylates the kinase domain of WNK1 (Figure 6).

These results were not surprising because WNKs can autophosphorylate within their kinase domains and the four WNK family members share 85% sequence identity within this domain (Figure 7). Aside from showing WNKs phosphorylate one another, these data suggest that one family member may be capable of activating another. To support this point, we know that at least WNK4 is phosphorylated by WNK1 on a site that is important for its autophosphorylation

activity (Figure 6). Although the biological function of these phosphorylation events remains to be determined, these results provide potential information about WNK signaling pathways and the relationships among the four WNK proteins.

WNK1 and WNK4 Do Not Co-Immunoprecipitate- In continuation of the characterization studies, I sought to determine whether WNK1 and WNK4 interact. I attempted to co-immunoprecipitate over-expressed WNK1 and WNK4 from HEK293 cells but did not observe an association. I attempted to co-immunoprecipitate WNK1 1-1000, 1-640, and 1-491 with WNK4 1-444, pieces that contain the kinase domain. It is possible that their interaction is transient and is difficult to detect using my methodology. Yang *et al.* were able to show that the kinase domains of WNK1 and WNK4 associate. In their experiment, the N-terminal regions of WNK1 and WNK4 were over-expressed in HEK293 cells and co-immunoprecipitated (Yang et al. 2005). WNK1 and WNK4 may transiently bind to one another, rendering their association difficult to observe experimentally, but if enough of these proteins are over-expressed, an association may be detected. The interaction between a kinase and its substrate is often transient.

WNK1 Ser378 and Ser382 and WNK4 Ser332 Are Major Autophosphorylation Sites- Another question about WNK kinases is how many autophosphorylation sites are within their kinase domains and where are they located. Knowing where WNKs are phosphorylated within their kinase domains may help us better understand how the kinase activity of each family member is

regulated. If it is later determined that an upstream kinase phosphorylates a particular residue within its kinase domain, we will have a better understanding if the phosphorylation event is stimulatory. Figure 7 is an alignment of the kinase domains of human WNKs 1-4. As mentioned above, previous work from our laboratory had shown that WNK1 S382A has significantly less activity than wild-type protein, and results from my studies showed that mutation of the equivalent site in WNK4, S332A, produced a similarly low activity protein (Xu *et al.* 2002). We wanted to know if S382 in WNK1 and S332 in WNK4 are the predominant sites autophosphorylated in the kinase domains and how many other sites are phosphorylated. To test these questions, two-dimensional peptide maps were generated.

In addition, our laboratory had data showing mutation of another WNK1 serine to alanine, S378, also results in lower kinase activity but not to the same extent as S382A. Therefore, we expected WNK1 to have at least two major autophosphorylation sites and S332 to be a major site in WNK4. Phosphorylation of WNK1 S382 and S378 alone is expected to generate up to nine tryptic phosphopeptides (Figure 8A). The WNK1 wild-type map revealed more than a dozen phosphopeptides, suggesting S378 and S382 are not the only sites that are autophosphorylated within the kinase domain (Figure 8B). We also mapped phosphopeptides in WNK1 S378A and observed at least seven tryptic phosphopeptides; phosphorylation of S382 alone should only account for up to

three phosphopeptides (Figure 8C). The major peptide missing from this map relative to that from the wild-type WNK1 map (labeled *7*/*8* in Figure 8B) most likely contains phospho-Ser378. Major phosphopeptides present in both maps (labeled *1* and *4*) most likely contain phospho-Ser382, based on the differences between these two maps and the predicted mobilities of the peptides based on their charge and hydrophobicity. These results are most consistent with the presence of at least one additional WNK1 autophosphorylation site within its kinase domain, with S378 and S382 being the major phosphorylation sites.

A phosphopeptide map of the WNK4 kinase domain was also generated, showing that the major phosphorylation site within that region is S332 (Figure 8D). Interestingly, this is the site that is phosphorylated by WNK1 (Figure 4), and mutation of this site greatly impacts its kinase activity (Figure 6). These peptide maps show that WNK1 and WNK4 are phosphorylated on multiple sites within their kinase domains and that the phospho sites that most greatly influence their kinase activities are also the most strongly phosphorylated (S378 and S382 in WNK1; S332 in WNK4).

The WNK1 Autoinhibitory Domain Inhibits the Kinase Activities of WNK2 and WNK4- In addition to the possibility that WNK kinases influence the catalytic activity of other family members through phosphorylation, I tested the idea that the WNK autoinhibitory domains may inhibit one another. Previous work from our laboratory showed WNK1 contains an autoinhibitory domain that is directly

C-terminal to the kinase domain. As mentioned in Chapter 1, this domain (residues 485-555) drastically inhibits WNK1 1-491 autophosphorylation and its phosphorylation towards MBP. As a control, the autoinhibitory domain of PAK1 (residues 1-231) was incubated with WNK1 1-491 to show it does not inhibit WNK1 (Xu *et al.* 2002).

In vitro kinase assays with recombinant proteins were conducted to determine that the WNK1 autoinhibitory domain (residues 485-614) can decrease the catalytic activity of both WNK2 and WNK4 (Figure 9). The graph shown in Figure 9 is a quantitative representation of the data shown in the above autoradiogram. These data are suggestive that the WNK1 autoinhibitory domain is capable of acting upon other substrates besides itself. In further support that WNKs can inhibit one another, David Ellison's group conducted an *in vitro* kinase assay showing the autoinhibitory domain of WNK4 can inhibit the kinase activity of WNK1 (Wang *et al.* 2004).

Discussion

Data from these studies supports the idea that WNK kinases can modulate the catalytic activity of other family members. I have shown that WNK1 is ubiquitously expressed, activated by osmotic stress, and phosphorylates WNK4 on a major phosphorylation site required for full kinase activity. In addition, I

have shown that the autoinhibitory domain of WNK1 can inhibit the kinase activity of other WNK family members.

In order to elaborate further on this story, key questions remain to be answered: 1) When and where are WNK kinases found at the same subcellular localization in order to act upon one another? 2) Do WNKs activate/inactivate one another to influence the surface expression and activity of ion channels and transporters? Addressing these issues may provide a mechanism(s) for how WNKs regulate ion homeostasis, a topic that is largely undefined in the WNK field.

A fundamental problem for addressing question one was that at the time I was conducting my characterization experiments, few WNK antibodies were available. Consequently, there has not been an extensive study conducted to determine what tissues and cell lines express each WNK family member. As discussed in the introduction, it was shown that both WNK1 and WNK4 are expressed in epithelial tissues (Kahle *et al.* 2004; Choate *et al.* 2003). Depending on the tissue type, WNK1 was shown to be located in the cytoplasm or on the lateral membrane, and WNK4 was shown to be localized at tight junctions, lateral membranes, or within the cytoplasm. A more thorough analysis is required to know specifically where each WNK kinase localizes to within the cytoplasm and to determine whether any of the WNKs co-localize under specific conditions. I have begun to address this issue for WNK1 as will be discussed in Chapter 4.

As for question 2, it appears that the kinase activity of WNK1 and WNK4 is important for regulating the surface expression and activity of certain ion transporters and channels but is negligible for others. As discussed in Chapter 1, it appears that only the N-terminal 220 residues of WNK1 and not its kinase domain are important for increasing ENaC activity. WNK1 1-220 increases the activity of SGK-1, thereby preventing the ubiquitination of ENaC by Nedd4-2 (Xu *et al.* 2005b). Conversely, the regulation of NKCC and NCCT by WNKs appears to be kinase-dependent. To recap, WNK1 activates NKCC through phosphorylation of OSR1 (Vitari *et al.* 2005; Moriguchi *et al.* 2005; Anselmo *et al.* 2006), and the kinase activity of WNK1 appears important for relieving WNK4-mediated inhibition of NCCT (Yang *et al.* 2003; 2005)

It is possible that the phosphorylation of WNK4 by WNK1 prevents WNK4 from inhibiting NCCT. The activation of WNK1 in response to osmotic challenge may promote the expression/retention of NCCT on the plasma membrane by activating WNK4 via phosphorylation of S332. See figure 10 for a model. In order to resolve this, WNK4 S332A needs to be tested in NCCT surface expression and activity assays. I predict that NCCT will be expressed on the cell surface in the presence of WNK4 S332A but not when wild-type WNK4 is expressed.

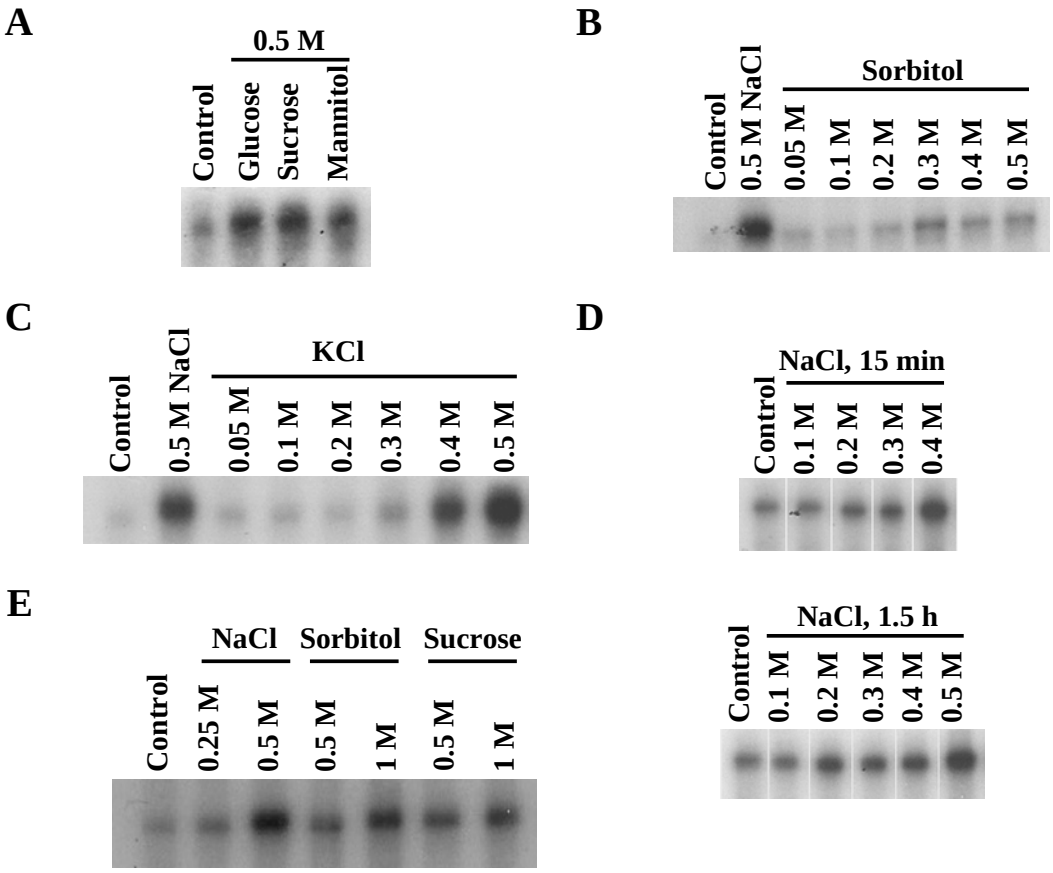

Figure 1: WNK1 is activated by osmotic stress. *In vitro* kinase assays of endogenous WNK1 immunoprecipitated from DCT cells treated with osmotic stress. WNK1 autophosphorylation is depicted here. ***A,*** 0.5 M glucose, sucrose and mannitol for 15 min. ***B,*** 0.05-0.5 M sorbitol for 15 min. ***C,*** 0.05-0.5 M KCl for 15 min. ***D,*** 0.1-0.4 M NaCl for 15 min or 0.1-0.5 M NaCl for 1.5 h. ***E,*** 0.25 and 0.5 M NaCl, 0.5 and 1 M sorbitol, and 0.5 and 1 M sucrose for 15 min.

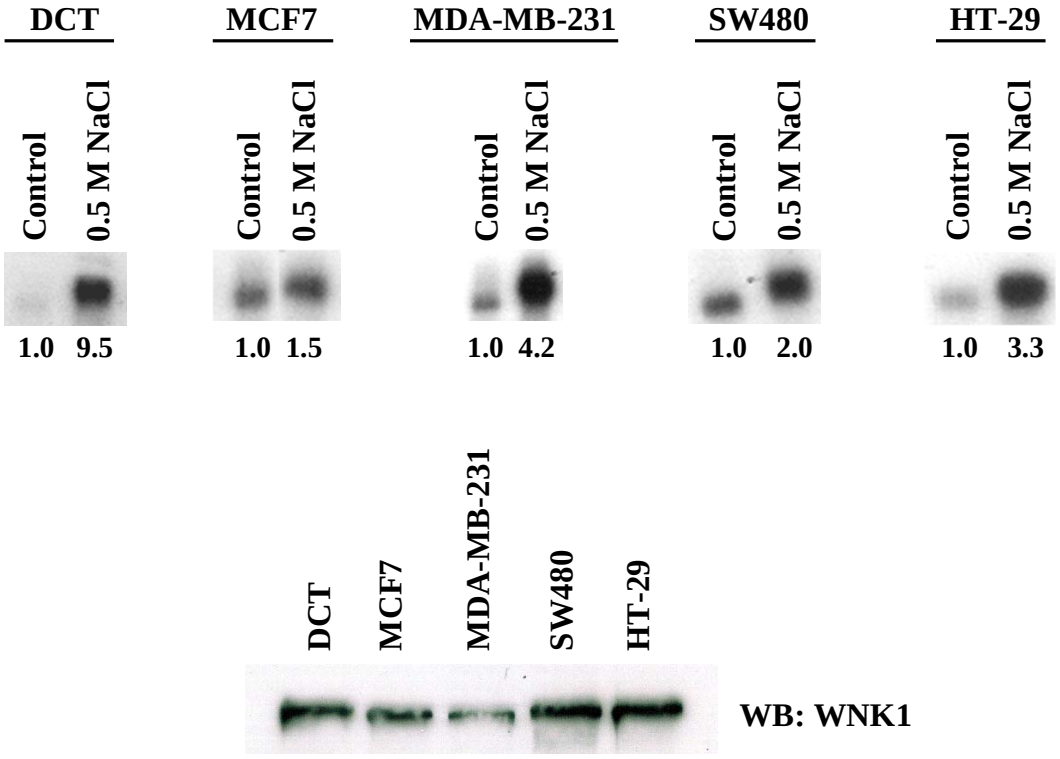

Fig. 2: The extent of WNK1 activation by osmotic stress varies among cell types. Top: *In vitro* kinase assay of endogenous WNK1 immunoprecipitated from mouse distal convoluted cells, the breast cancer cell lines MCF7 and MDA-MB-231, and the colon cancer cell lines SW480 and HT-29. Bottom: A WNK1 Western blot of cell lysates containing equivalent amounts of total protein.

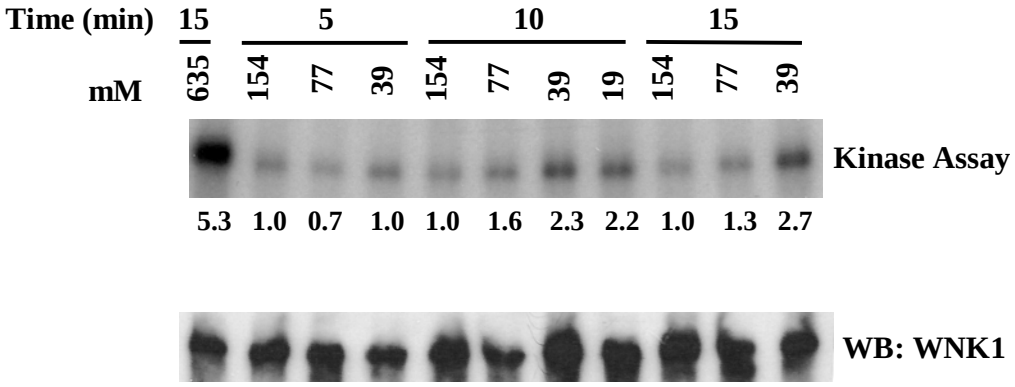

Fig 3: WNK1 is activated by hypotonic stress. Top: *In vitro* kinase assay of endogenous WNK1 immunoprecipitated from DCT cells treated with hypotonic stress. Bottom: Western blot of immunoprecipitated WNK1 to show relatively equal amounts of WNK1 were extracted.

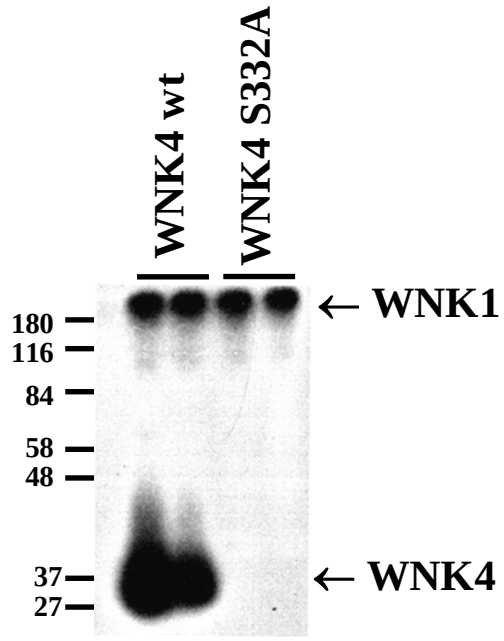

Fig 4: WNK1 phosphorylates WNK4 within its activation loop on S332. *In vitro* kinase assay of full-length GST-WNK1 with the kinase domain of wild-type and S332A WNK4.

Fig 5: WNK1 phosphorylates WNK2 within its kinase domain. *In vitro* kinase assay of WNK1 (194-483) with the GST-tagged kinase domain of WNK2.

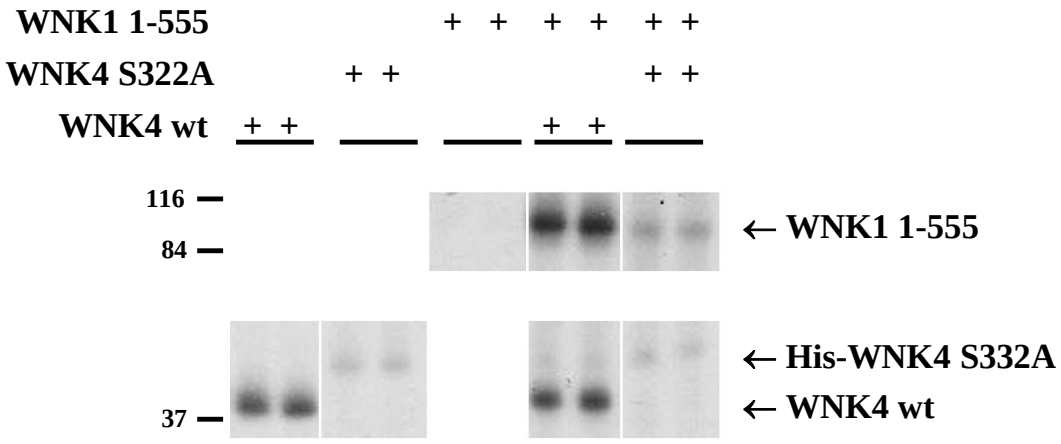

Fig 6: WNK4 phosphorylates WNK1. *In vitro* kinase assay of wild-type and S332A WNK4 with GST-tagged WNK1 1-555. WNK1 1-555 has negligible kinase activity because it contains the autoinhibitory domain without any downstream residues to relieve the inhibition.

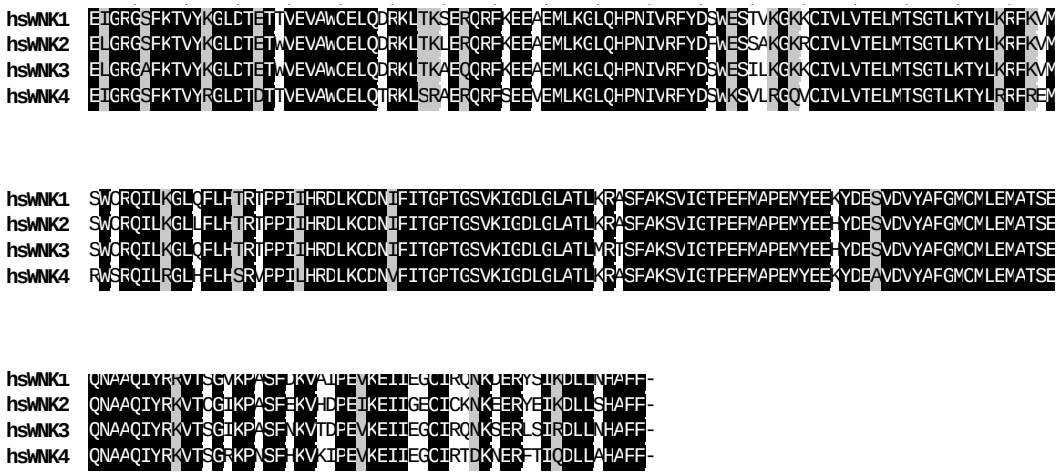

Fig. 7: The four mammalian WNK family members share a high sequence identity within their kinase domains. This alignment was created by Chick Heise.

A

WNK1: ^{366}IGDLGLATLKRASFAK**S**VIGTPEFMAPEMYEEK^{398}
WNK4: ^{316} ^{348}

(* marks the Ser phosphorylation site)

Peptide 1	RASFAK**pS**VIGTPEFMAPEMYEEK
Peptide 2	RA**pS**FAKSVIGTPEFMAPEMYEEK
Peptide 3	RA**pS**FAK**pS**VIGTPEFMAPEMYEEK
Peptide 4	ASFAK**pS**VIGTPEFMAPEMYEEK
Peptide 5	A**pS**FAKSVIGTPEFMAPEMYEEK
Peptide 6	A**pS**FAK**pS**VIGTPEFMAPEMYEEK
Peptide 7	RA**pS**FAK
Peptide 8	A**pS**FAK
Peptide 9	**pS**VIGTPEFMAPEMYEEK

B **C** **D**

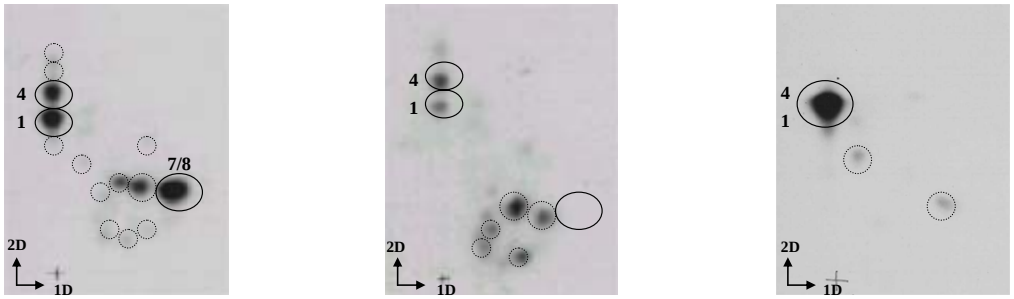

WNK1 wild-type **WNK1 S378A** **WNK4 wild-type**

Fig. 8: Phosphopeptide analysis of WNK1 and WNK4 autophosphorylation. ***A,*** The activation loop sequence of WNK1 and WNK4 and the peptide fragments predicted to be generated after digestion with trypsin. WNK1 Ser^{382} and WNK4 Ser^{332} are marked with an *asterisk.* ***B,*** Phosphopeptide map of WNK1 (194–483). Peptide identities were predicted based on their electrophoretic mobility as noted in the text. ***C,*** WNK1 S378A (194–483). ***D,*** WNK4 (141–436).

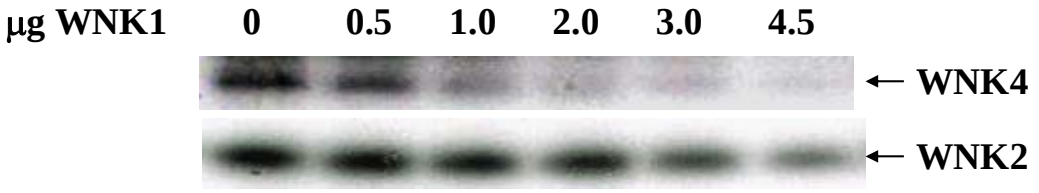

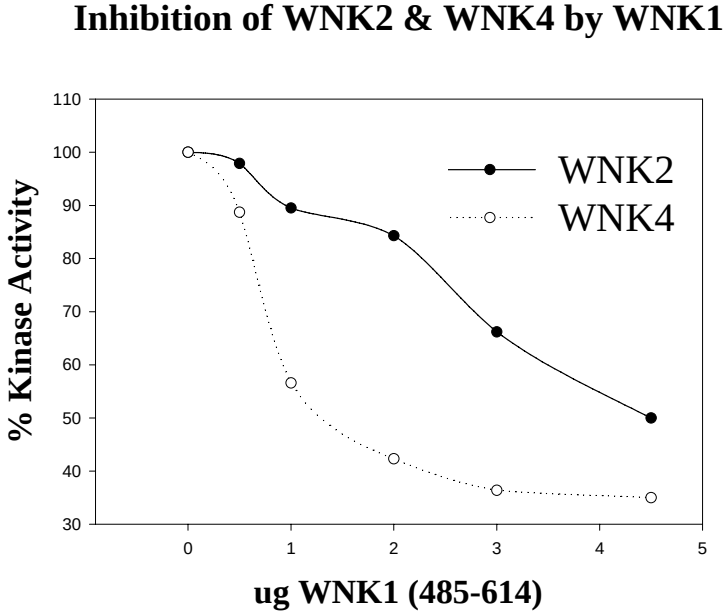

Fig 9: The WNK1 autoinhibitory domain inhibits the catalytic activity of WNK2 and WNK4. Top: Increasing concentrations of the WNK1 autoinhibitory domain (residues 485-614) were incubated with the kinase domains of WNK2 and WNK4 in an *in vitro* kinase assay. Bottom: Graphical representation of the kinase assay shown above.

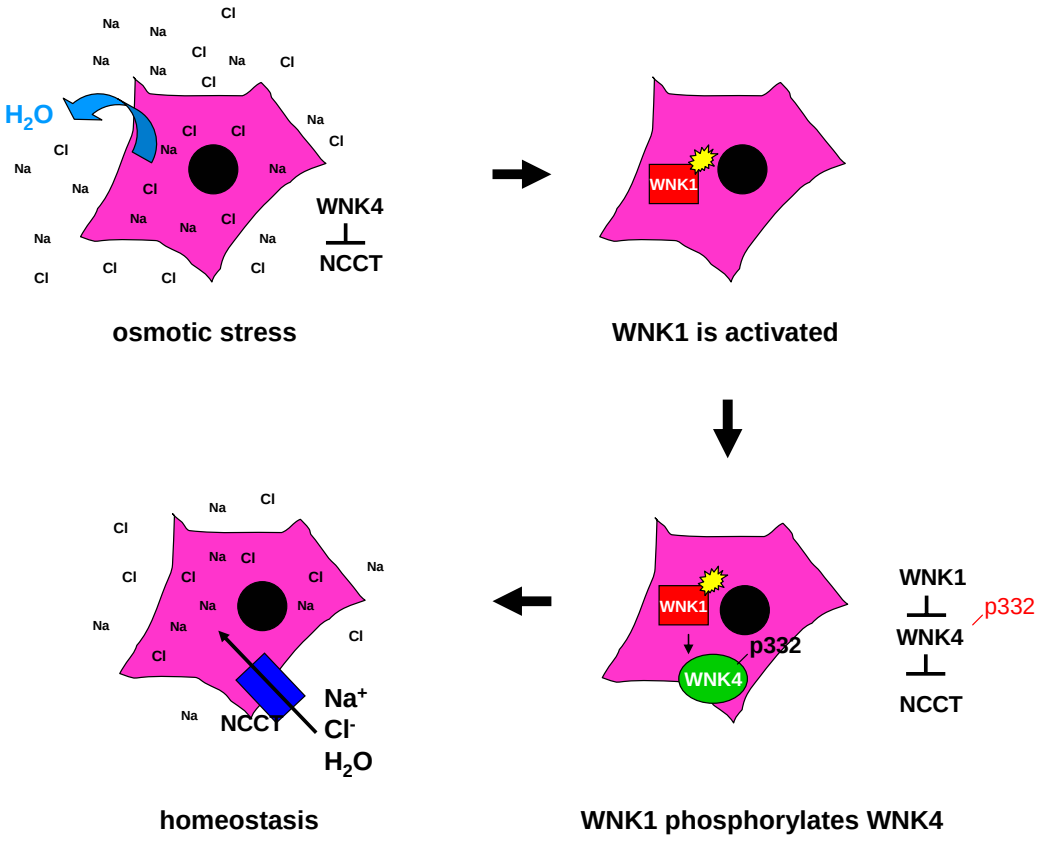

Fig. 10: Model of how WNK1 and WNK4 may regulate ion balance through NCCT. Under normal circumstances WNK4 inhibits the surface expression and activity of NCCT. Upon osmotic shock, significant amounts of water are lost and WNK1 is activated. WNK1 then phosphorylates WNK4 on S332, relieving the WNK4-mediated inhibition of NCCT. Activated NCCT then promotes the uptake of sodium, chloride, and water to normalize the cell's ion balance.

Chapter 3

WNK1 & PAK1

Introduction

P21-activated kinases (PAKs) are serine/threonine protein kinases that modulate multiple cellular processes. They influence cell migration via the turnover of focal adhesions and actin stress fibers and regulate cell survival pathways and transcription through the activation of MAPK cascades. Specifically, PAK1 phosphorylates and activates Lin-11, Isl-1 and Mec-3 (LIM kinase), which inactivates the actin-depolymerizing protein cofilin to influence cell motility, and PAK1 phosphorylates Raf1 and MEK1 to regulate MAPK signaling pathways (reviewed in Zhao and Manser 2005; reviewed in Parrini *et al.* 2005).

The PAK kinases are divided into two major groups, group A (PAK1, PAK2, and PAK3) and group B (PAK4, PAK5, and PAK6) (reviewed in Jaffer and Chernoff 2002). The group A PAKs, which are the more highly studied PAKs, are activated by Cdc42 and Rac1, members of the Ras-related Rho family of GTPases. The regulation of their kinase activities is highly complex and is influenced by adaptor proteins and their phosphorylation state. PAKs are activated by growth factors including platelet-derived growth factor (PDGF) to regulate the activity of ERK1/2, c-Jun N-terminal kinase (JNK), and p38 MAPK (Zhang *et al.* 1995; Frost *et al.* 1996; Besser *et al.* 2005; Dechert *et al.* 2001).

The group A PAKs contain an N-terminal autoinhibitory domain and a C-terminal catalytic domain. In their inactive states, the autoinhibitory domain of

one PAK binds to the kinase domain of another PAK. Upon activation, GTP-bound Cdc42 or Rac1 binds to the Cdc42/Rac1 interaction and binding domain (CRIB), preventing the autoinhibitory domain from binding to the catalytic domain. PAK1 then autophosphorylates within its kinase domain and becomes fully activated. See figure 1 for a schematic of the architecture of PAK1 (reviewed in Zhao and Manser 2005).

The N-terminal regulatory domain is not only important for regulating PAK kinase activity but also for modulating its localization and interactions with binding partners. The N-terminal domain of PAK1 directly interacts with the adaptors Nck and Grb2, which have been hypothesized to bring PAK1 to activated tyrosine kinase receptors, and it acts as a scaffold by binding to the Cdc42/Rac1 guanine nucleotide exchange factors PAK-interacting exchange factors alpha and beta (PIXα/β) at focal adhesion sites (reviewed in Li *et al.* 2000; reviewed in Zhao and Manser 2005; reviewed in Parrini *et al.* 2005).

PAK1 is the most highly studied PAK, and importantly its expression has been implicated in promoting the proliferation of breast cancer and melanoma cells (Vadlamudi *et al.* 2000; Wang *et al.* 2006; Pavey *et al.* 2006). PAK1 transgenic mice expressing kinase active PAK1 under the control of the ovine beta lactoglobulin (BLG) promoter exhibit increased cyclin D expression and nuclear accumulation in the mammary gland (Balasenthil *et al.* 2004), and the breast cancer drug Iressa, which targets the epidermal growth factor receptor

(EGFR), has been shown to inhibit PAK1 activity in cancer cells (Yang *et al.* 2004). In addition, PAK1 has also been shown to phosphorylate estrogen receptor (ER) and its over-expression increases ER-mediated transcription (Wang *et al.* 2002).

I determined that three of the WNK family members, WNK1, WNK2 and WNK4, phosphorylate PAK1 within its N-terminus after using PAK1 as a negative control in another assay. I pursued this finding because we had reported that the WNK1 interacting protein OSR1 phosphorylates PAK1 in its regulatory domain at T84 (Chen *et al.* 2003) and I anticipated that WNK1, PAK1, and OSR1 may belong to a ternary signaling complex. I have used mass spectrometry to identity the residues phosphorylated on PAK1 by WNK1 and WNK4 and have hypothesized WNK1 regulates PAK1 kinase activity.

Methods

Cell Culture and Harvesting- HEK293, HT-29, SW480, MDA-MB-231 and MCF7 were cultured in DMEM with 10% fetal bovine serum and 1% L-glutamine at 37 °C under 5% CO_2. DCT cells were cultured as above except with 110 mg/L sodium pyruvate under 10% CO_2. Confluent cells were harvested in buffer containing 50 mM HEPES (pH 7.5), 150 mM NaCl, 1.5 mM $MgCl_2$, 1 mM EGTA, 10% glycerol, 100 mM NaF, 0.2 mM Na_3VO_4, 50 mM β-glycerophosphate, 1 mM dithiothreitol, 1 mM benzamidine hydrochloride, 10

mg/L leupeptin, 0.5 mg/L pepstatin A, 1.5 mg/L aprotinin and with or without Triton X-100. The cells were vortexed for 30 s, incubated on ice for 10 min, and centrifuged for 15 min at 14,000 rpm to remove insoluble material.

Constructs- Myc-PAK1/CMV5 and GST-PAK1 K298A/pGEX-KG were provided by Wei Chen. PAK1 75-190/pGEX-KG and PAK1 190-254/pGEX-KG were generated by performing polymerase chain reactions of PAK1 cDNA and subcloning the fragments into pGEX-KG at the BamHI and EcoRI sites. PAK1 75-190 T146A/pGEX-KG, PAK1 190-254 T213A/pGEX-KG, PAK1 T146A K298A/pGEX-KG, PAK1 T213A K298A/pGEX-KG, and PAK1 T146A T213A K293A/pGEX-KG were generated by site-directed mutagenesis.

Antibodies and Proteins- The anti-PAK1 antibody N-20 was purchased from Santa Cruz Biotechnology (cat. no. sc-882), the anti-WNK1 antibody Q256 was previously described (Xu *et al.* 2000), and anti-myc monoclonal antibody was prepared from the cell line Myc 1-9E10.2 (American Type Culture Collection).

GST-tagged full-length PAK1 and GST-tagged $Rac1^{V12}$ were provided by Jeff Frost (MD Anderson Cancer Center) and previously described (Wang *et al.* 1999), GST-PAK1 1-231 T84E was provided by Wei Chen, and GST-WNK1 1-491 was provided by Charles Heise. GST-tagged PAK1 75-190, PAK1 75-190 T146A, PAK1 190-254, PAK1 190-254 T213A, PAK1 K298A, PAK1 T146A K298A, PAK1 T213A K298A, PAK1 T146A T213A K298A, and GST-MEK1

insert were purified as follows with the only difference due to variable amounts of protease inhibitors. BL-21 cultures were treated for 12-24 h with 20-200 μM isopropyl β-D-1-thiogalactopyranoside (IPTG). The bacteria were washed with buffer A (50 mM Tris pH 8.0, 10 mM EDTA, 25% sucrose, 10 mM benzamidine hydrochloride, 10 mM dithiothreitol, 100 mg/L leupeptin, 15 mg/L aprotinin, 100 mg/L pepstatin A), resuspended in lysis buffer (50 mM Tris pH 7.4, 150 mM NaCl, 5% glycerol, 5 mg/L pepstatin A, 15 mg/L aprotinin, 20 mg/L leupeptin, 1 mM dithiothreitol, 2 mM benzamidine hydrochloride, 0.05% Triton X-100, 2 mM EDTA), sonicated, and added to a column containing glutationine-agarose beads. The beads were washed with wash buffer 1 (50 mM Tris pH 7.4, 10 mM EDTA, 25% sucrose, 5 mg/L pepstatin A, 15 mg/L aprotinin, 20 mg/L leupeptin, 2 mM benzamidine hydrochloride, 1 mM dithiothreitol, 0.05% Triton X-100, 2 mM EDTA) and wash buffer 2 (wash buffer 1 without Triton X-100 and EDTA), and eluted with elution buffer (50 mM Tris pH 7.4, 10 mM EDTA, 25% sucrose, 0.5 mg/L pepstatin A, 1.5 mg/L aprotinin, 2 mg/L leupeptin, 1 mM benzamidine hydrochloride, 1 mM dithiothreitol, 10 mM glutathione).

In Vitro Kinase Assay- In the kinase assays to show WNKs phosphorylate PAK1, the kinase domains of WNK1, WNK2 or WNK4 (described in Chapter 2) were incubated with increasing amounts of GST-PAK1 1-231 T84E at 30°C for 30 min in kinase buffer (10 mM HEPES (pH 8.0), 5 mM $MgCl_2$, 25 μM ATP (~5000 cpm/pmol [γ-^{32}P]ATP), 0.5 mM benzamidine hydrochloride, 0.5 mM

dithiothreitol). The samples were then subjected to SDS-PAGE, the gels were dried and exposed to film to generate autoradiograms, and the PAK1 bands were excised. The bands were counted with a scintillation counter and the moles of incorporated phosphate per moles of substrate were calculated.

In the *in vitro* coupled kinase assays, GST-PAK1 full-length was pre-incubated with either WNK1 1-491 or $Rac1^{V12}$ in kinase buffer with 200 μg/mL BSA and 25 μM ATP (~5000 cpm/pmol [γ-^{32}P]ATP) at 30°C for 5-15 min. After the first reaction, the MEK1 insert was added and incubated for an additional 5-15 min, the proteins were separated on 13% polyacrylamide gels in SDS, and an autoradiogram was generated.

Mass Spectometry- GST-PAK1 1-231 T84E (0.5 μg) was incubated with the kinase domains of WNK1 or WNK4 in kinase buffer (10 mM HEPES (pH 8.0), 5 mM $MgCl_2$, 0.5 mM benzamidine hydrochloride, 0.5 mM dithiothreitol) with ~5000 cpm/pmol [γ-^{32}P]ATP at 30°C for 2 h. PAK1 was incubated with either 4.8 μg WNK1, 800 μM ATP, and 200 μg/mL BSA or with 2.5 μg WNK4 and 400 μM ATP. The proteins were separated on 8% polyacrylamide gels in SDS, the gels were stained in colloidal coomassie blue, and PAK1 was excised. Hongjun Sun and Yingming Zhao in the Department of Biochemistry digested PAK1 with trypsin and performed mass spectrometry to identify the peptides and residues that were phosphorylated.

Western Blotting- Western blots were generally performed as follows. Proteins from cell lysates were resolved on 7.5% polyacrylamide gels in SDS and transferred to nitrocellulose membranes at 200 mA overnight. The membranes were blocked in 5% nonfat dry milk, incubated with 1:1000 primary antibody and 1:5000 secondary antibody, and visualized by enhanced chemiluminescence.

Co-immunoprecipitation- HEK293 cells were transfected with Myc-PAK1/CMV5 using Fugene and harvested approximately 12 h later without or with 1% Triton X-100. The lysates were incubated with Q256 or Q256 preimmune serum for 1 h and protein A Sepharose beads for an additional 1 h. The beads were washed 3X with 0.1-1.0 M NaCl in Tris buffer, and the immunoprecipitates were subjected to SDS-PAGE and immunoblotted with the anti-Myc antibody to detect PAK1.

Results

WNK Kinases Phosphorylate PAK1- The N-terminal half of PAK1 was used as a negative control in experiments to test if the WNK1 autoinhibitory domain inhibits the kinase activity of WNK2 and WNK4 (Chapter 2, Figure 9). In these assays, increasing amounts of the WNK1 autoinhibitory domain or PAK1 1-231 T84E were incubated with the kinase domains of WNK1, WNK2 or WNK4. Interestingly, WNK1, WNK2 and WNK4 all strongly phosphorylated PAK1 1-231 (Figure 2).

Because it appeared that a relatively large amount of phosphate was incorporated into PAK1, the stoichiometry of phosphorylation for these reactions was calculated. For example, in one experiment 0.2 mol P_i was incorporated per mol of PAK1 in the presence of WNK1. Since no attempt was made in these experiments to obtain a high stoichiometry of phosphorylation, I concluded that PAK1 may be a reasonable substrate of WNK kinases and decided to further pursue this finding.

Attempts to Co-immunoprecipitate WNK1 and PAK1- Co-immunoprecipitation experiments were performed to determine whether WNK1 and PAK1 interact. PAK1 cDNA was transfected into HEK293 cells, endogenous WNK1 was immunoprecipitated with Q256, and the precipitates were immunoblotted for PAK1. I did not observe an association between WNK1 and PAK1 (data not shown), but this negative result does not definitively show that they do not bind to one another. Yeast-two-hybrid, *in vitro* binding assays and further co-immunoprecipitation experiments may be employed to determine whether WNK1 and PAK1 interact.

WNK1 Phosphorylates Rat PAK1 at T146 and T213 and WNK4 Phosphorylate PAK1 T213- To identify the residues in PAK1 that WNK1 and WNK4 phosphorylate, mass spectrometry was performed in collaboration with Hongjun Sun (Alliance for Cellular Signaling) and later with Yingming Zhao. The stoichiometry of phosphorylation was first optimized by varying the amount

of ATP. I obtained a stoichiometry of 0.33 mol P_i/mol PAK1 with WNK1 and a stoichiometry of 1.4 mol P_i/mol PAK1 with WNK4. PAK1 1-231 T84E was then phosphorylated by the kinase domains of WNK1 and WNK4 for site analysis. Hongjun Sun identified the following PAK1 phosphopeptides phosphorylated by WNK1: residues 142-162 (1 site), 198-214 (2 sites), and 203-214 (1 site), and the following phosphorylated by WNK4: residues 163-197 (1 site), 203-214 (1 site), and 215-231 (1 site) (Figure 3).

Yingming Zhao also performed mass spectrometry and determined that WNK1 phosphorylates rat PAK1 T146 and T213 and that WNK4 phosphorylates T213 (Figures 4 and 5). Rat T146 is equivalent to human T146 and rat T213 is equivalent to human T214.

To date, there is no information available about phosphorylation of T146 or T214. However, nearby threonine and serine residues have been found to be phosphorylated. There is one report that shows two autophosphorylation sites, S144 and S149, contribute to the activation of PAK1, and there have been reports that T212 is phosphorylated by Cdk5 (Chong *et al.* 2001; Rashid *et al.* 2001; Banerjee *et al.* 2002).

Efforts to Confirm the PAK1 Phosphorylation Sites- To provide *in vitro* confirmation of the phosphorylation sites identified by mass spectrometry, I performed *in vitro* kinase assays with recombinant mutated proteins. The following GST-tagged proteins were tested in these experiments: PAK1 75-190,

PAK1 75-190 T146A, PAK1 190-254, and PAK1 190-254 T213A. Unfortunately, these two mutant proteins did not exhibit decreased phosphorylation by WNK1 in comparison to their wild-type counterpart. To ensure protein folding of the fragments was not affecting its phosphorylation by WNK1, full-length kinase-inactive PAK1 was tested in these assays. PAK1 K298A, PAK1 T146A/ K298A, PAK1 T213A/K298A, and PAK1 T146A/T213A/K298A were phosphorylated by WNK1, but as with the N-terminal fragments, the mutant proteins were phosphorylated to the same extent as PAK1 K293A. Further investigation is required to determine or confirm the sites WNK1 phosphorylates on PAK1.

Tests of Function- Because there is evidence that WNK1 phosphorylates PAK1 within a region that is autophosphorylated to influence its kinase activity, I hypothesized that WNK1 increases the activity of PAK1. To test this idea, *in vitro* coupled kinase assays with WNK1, PAK1, and the PAK1 substrate MEK1 (a fragment of MEK1 that encompasses a unique proline-rich insert) were performed (Frost *et al.* 1997). In these assays, PAK1 was pre-phosphorylated with WNK1 before the MEK1 insert was added to be phosphorylated by PAK1. Unfortunately, the results from these studies were inconclusive. There was no increase in PAK1 activity when it was pre-phosphorylated by WNK1, but there was also no increase in activity when PAK1 was incubated with its activator, Rac^{V12}. It is possible that the activity of PAK1 is too high to observe any increases in its activity. It has been previously reported that GST-tagged PAK1 is

constitutively active *in vitro* (Knaus *et al.* 1995). I increased the amount of substrate that was added and decreased the reaction time in efforts to lower the basal amount of phosphate incorporated into the MEK1 insert, but these modifications still yielded inconclusive results.

As an alternative approach to the *in vitro* coupled kinase assay, I tested whether PAK1 is also activated by hypertonic stress with the anticipation of being able to test the idea WNK1 influences the activation of PAK1 by this stimulus. Before conducting these experiments, I performed a PAK1 Western blot to confirm that cell lines of interest express the protein. PAK1 is expressed in the epithelial-derived cell lines DCT, MCF7, MDA-MB-231, HT-29, and SW480 (Figure 6). As a next step, I attempted to immunoprecipitate endogenous PAK1 from MCF7 and MDA-MB-231 cells but was unable to detect any immunoprecipitated protein. As an alternative strategy, PAK1 was transfected into HEK293, HeLa and COS cells and the cells were treated with 0.5 M NaCl. Western blots showing electrophoretic mobility shifts in PAK1 and *in vitro* kinase assays were performed to support the idea that PAK1 is activated by hypertonic stress within 15-20 minutes (Figure 7 and data not shown).

Discussion

These studies show that at least three of the WNK family members, WNK1, WNK2 and WNK4, phosphoryate the N-terminal half of PAK1, PAK1 is

expressed in the epithelial-derived cell lines DCT, MCF7, MDA-MB-231, HT-29 and SW480, and PAK1 is activated by hypertonic stress. Mass spectrometry was used to determine that WNK1 phosphorylates rat PAK1 T146 and T213 and that WNK4 phosphorylates T213. To determine the consequence of these phosphorylation events, I hypothesized that WNK1 influences PAK1 kinase activity and pursued this idea using several approaches.

To test the idea that WNK1 mediates PAK1 activation by hypertonic stress, the following experiments should be conducted: knock down WNK1 expression by RNAi and determine whether the activation of PAK1 by hypertonic stress is decreased; determine if PAK1 T146A/T213A is less active than wild-type PAK1 in response to NaCl treatment; and determine if PAK1 exhibits less activity in response to hypertonic stress in WNK1 heterozygous and homozygous deleted mouse embryonic fibroblasts (MEF).

Determining if WNK1 activates PAK1 would be a significant finding because it could help link WNK1 signaling to multiple downstream outputs including cell motility, focal adhesion turnover, and proliferation. Because WNK1 is linked to modulating the surface expression of several plasma membrane proteins, it is conceivable that one mechanism of action may be through regulating the cytoskeletal network. The cytoskeleton rearranges during endocytosis to promote the internalization of newly formed vesicles, and therefore

this rearrangement in actin and tubulin is critical for the proper intracellular trafficking of plasma membrane proteins.

Connecting WNK kinases to PAK1 would also provide further information about WNK signaling, an area that is largely unexplored and not well understood. If the hypothesis is correct that WNK1 increases PAK1 kinase activity, it would be interesting to test whether WNK1 is involved in the regulation of PAK1-mediated functions including cell motility via LIM kinase and cofilin or cell proliferation through activation of MAPK cascades. To test these possibilities, mutations in the PAK1 residues that are phosphorylated by WNK1 should be generated and used in cell-based motility and proliferation assays, or alternatively, WNK1 expression should be knocked down via RNAi and tested for function. Information from these studies will help in determining whether WNK1 performs functions in addition to regulating the cell surface presentation of ion transporters and channels.

Additionally, the idea that WNK1, OSR1 and PAK1 belong to a signaling complex is attractive because several studies linking these proteins together have been reported. As discussed previously, WNK1 interacts with and phosphorylates OSR1, and OSR1 phosphorylates T84 in PAK1. It would be interesting to identify the function of these events and to test the idea that these interactions are involved in the regulation of NKCC, the cotransporter that is activated by OSR1. This avenue of study merits further investigation.

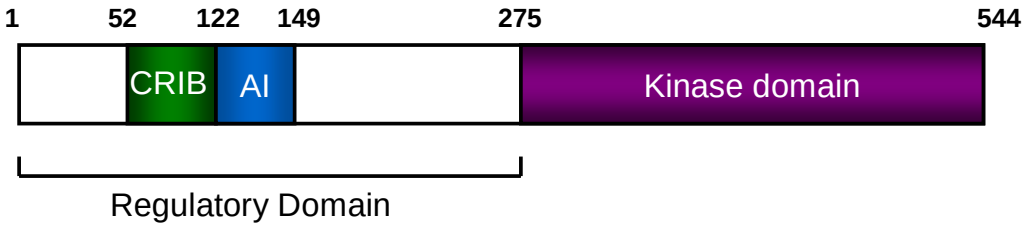

Fig. 1: Architecture of PAK1. CRIB: Cdc42/Rac1 interaction and binding; AI: autoinhibitory.

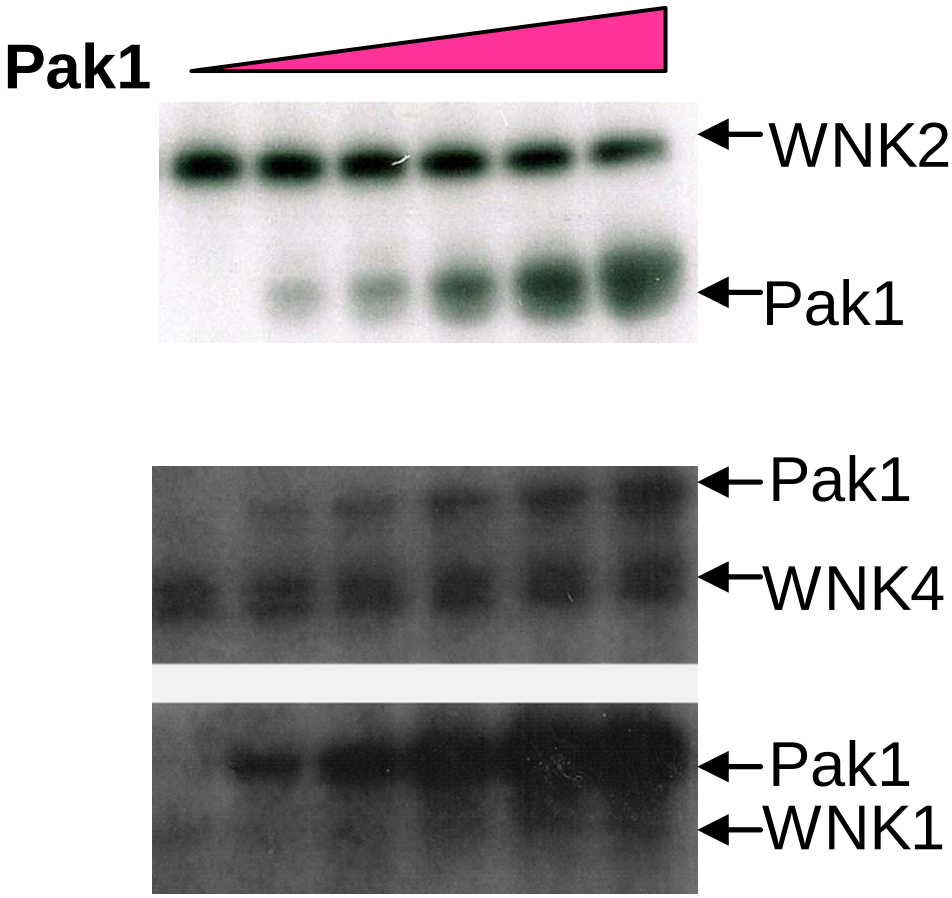

Fig. 2: WNK1, WNK2 and WNK4 phosphorylate PAK1 1-231. The kinase domains of WNK1, WNK2 and WNK4 were incubated with increasing amounts of PAK1 1-231 T84E in *in vitro* kinase assays.

WNK1 with PAK1

SVIEPLPVTPTR (203-214,1 phos)
YMSFTDKSAEDYNSSNTLNVK (142-162, 1 phos)
SVYTRSVIEPLPVTPTR (198-214, 2 phos)

WNK4 with PAK1

SVIEPLPVTPTR (203-214,1 phos)
DVATSPISPTENNTTPP (215-231, 1 phos)
TVSETPAVPPVSEDEDDDDDATPPPVIAPRPEHTK (163-197,1 phos)

Fig. 3: Phosphopeptides detected in PAK1 after phosphorylation by WNK1 and WNK4. The kinase domains of WNK1 and WNK4 were incubated with GST-tagged PAK1 1-231 T84E, the proteins were separated on a polyacrylamide gel in SDS, and PAK1 was excised. Hongjun Sun then used mass spectrometry to identify phosphorylated peptides.

A

```
  1 MSPILGYWK I K GLVQPTRLL LEYLEEKYEE HLYERDEGDK WR NK KFELGL
 51 EFPNLPYYID GDVKLTQSMA IIRYIADKHN MLGGCPKERA EISMLEGAVL
101 DIRYGVSRIA YSKDFETLKV DFLSKLPEML KMFEDRLCHK TYLNGDHVTH
151 PDFMLYDALD VVLYMDPMCL DAFPK LVCFK KRIEAIPQID KYLKSSKYIA
201 WPLQGWQATF GGGDHPPKSD LVPRGSPGIS GGGGGIPMSN NGLDVQDKPP
251 APPMRNTSTM IGAGSKDPGT LNHGSKPLPP NPEEKKKKDR FYRSILAGDK
301 TNKKK EKERP EISLPSDFEH TIHVGFDAVT GEFTGMPEQW AR LLQTSNIT
351 KSEQKKNPQA VLDVLEFYNS KKTSNSQKYM SFTDKSAEDY NSSNTLNVK T
401 VSETPAVPPV SEDEDDDDDA TPPPVIAPRP EHTK SVYTRS VIEPLPVTPT
451 RDVATSPISP TENNTTPP
```

B

372-385	KTSNSQKYMSFpTDK (T146)
440-451	SVIEPLPVTPpTR (T213)

Fig. 4: WNK1 phosphorylates PAK1 on T146 and T213. The kinase domain of WNK1 was incubated with GST-tagged PAK1 1-231 T84E, the proteins were separated on a polyacrylamide gel in SDS, and PAK1 was excised. Yingming Zhao then used mass spectrometry to identify peptides and residues that were phosphorylated on PAK1. ***A,*** Sequence of GST fused to PAK1 1-231 where the peptides detected by the instrument are underlined. ***B,*** The two phosphorylated peptides and residues detected in PAK1.

A

```
  1 MSPILGYWKI KGLVQPTRLL LEYLEEKYEE HLYERDEGDK WRNKKFELGL
 51 EFPNLPYYID GDVKLTQSMA IIRYIADKHN MLGGCPKERA EISMLEGAVL
101 DIRYGVSRIA YSKDFETLKV DFLSKLPEML KMFEDRLCHK TYLNGDHVTH
151 PDFMLYDALD VVLYMDPMCL DAFPK LVCFK K RIEAIPQID K YLKSSK YIA
201 WPLQGWQATF GGGDHPPKSD LVPRGSPGIS GGGGGIPMSN NGLDVQDKPP
251 APPMRNTSTM IGAGSKDPGT LNHGSKPLPP NPEEKK KK DR FYRSILAGDK
301 TNKKK EKERP EISLPSDFEH TIHVGFDAVT GEFTGMPEQW AR LLQTSNIT
351 KSEQKKNPQA VLDVLEFYNS KKTSNSQKYM SFTDKSAEDY NSSNTLNVK T
401 VSETPAVPPV SEDEDDDDDA TPPPVIAPRP EHTK SVYTRS VIEPLPVTPT
451 RDVATSPISP TENNTTPP
```

B

440-451 SVIEPLPVTPpTR (T213)

Fig. 5: WNK4 phosphorylates PAK1 on T213. The kinase domain of WNK1 was incubated with GST-tagged PAK1 1-231 T84E, the proteins were separated on a polyacrylamide gel in SDS, and PAK1 was excised. Yingming Zhao then used mass spectrometry to identify peptides and residues that were phosphorylated on PAK1. ***A,*** Sequence of GST fused to PAK1 1-231 where the peptides detected by the instrument are underlined. ***B,*** The phosphorylated peptide and residue detected in PAK1.

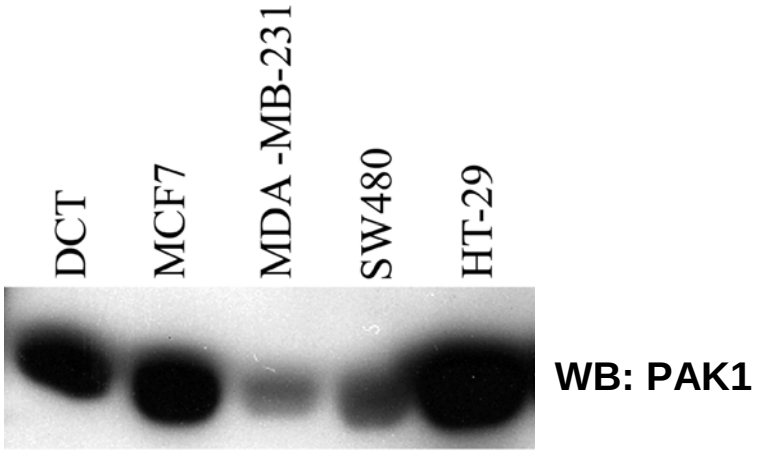

Fig. 6: PAK1 is expressed in epithelial-derived cell lines. Equal amounts of total protein were separated on a poly-acrylamide gel in SDS and Western blotted with an anti-PAK1 antibody. This experiment was performed once.

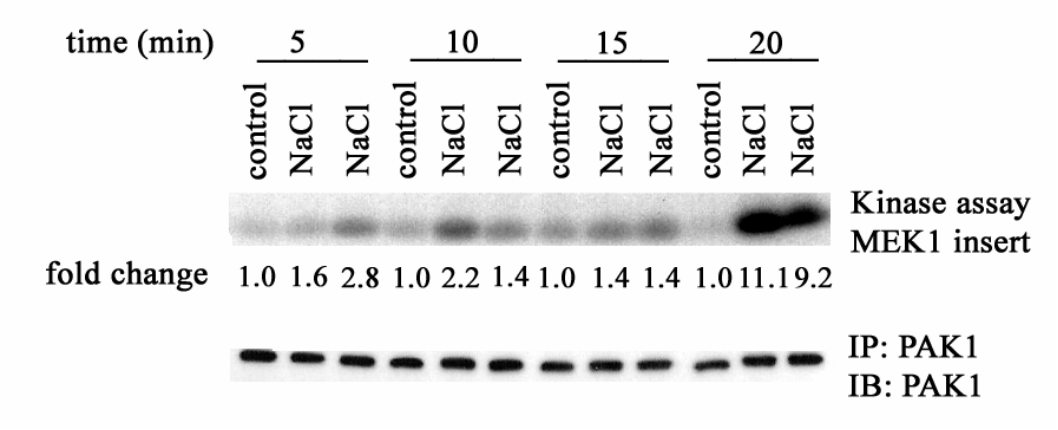

Fig. 7: PAK1 is activated by hypertonic stress. HEK293 cells were transfected with full-length PAK1, treated with 0.5 M NaCl, and harvested. PAK1 was immunoprecipitated with an anti-PAK1 antibody and used in an *in vitro* kinase assay with recombinant GST-tagged MEK1 insert (top). As a loading control, the immunoprecipitates were Western blotted with the anti-PAK1 antibody (bottom).

Chapter 4

The Interaction of WNK1 with VPS4a

Introduction

Vacuolar protein sorting 4 (VPS4) is considered a vital component of trafficking through recycling and late endosomes. The transport of proteins to and from these endosomes is critical for numerous fundamental processes such as the cell surface presentation of receptors, the down-regulation of signals arising from the plasma membrane, and the biosynthesis of proteins. Recycled plasma membrane receptors are returned to the cell surface via transport through recycling endosomes, while plasma membrane receptors destined for degradation are transported to multivesciular bodies (MVB) and ultimately lysosomes. In addition, some trans-Golgi network (TGN) proteins are recycled between the golgi and the cell surface via recycling and sorting endosomes (reviewed in Katzmann *et al.* 2002).

VPS4 is a member of the class E VPS proteins, which were first characterized in yeast in efforts to identify endosomal trafficking mutants. Mutant class E proteins all cause the formation of an aberrant endosomal structure known as the class E compartment. In yeast, this structure appears to be prevacuolar-like and is adjacent to vacuoles. As an essential step in protein trafficking, VPS4 binds to and releases other class E VPS proteins from the endosomal membranes, allowing those class E VPS proteins to participate in additional rounds of sorting (reviewed in Katzmann *et al.* 2002).

There are two mammalian VPS4 homologs, VPS4a and VPS4b (also known as suppressor of K^+ transport growth defect 1 (SKD1)), and one homolog in yeast. VPS4 is an ATPases associated with diverse cellular activities (AAA-ATPase), a family of proteins that catalyze the dissociation of large protein complexes. Other AAA-ATPases include Pex1 and Pex6 which are involved in peroxisome biogenesis, Sec18/NSF (N-ethylmaleimide-sensitive factor) which also plays a role in vesicular transport, and the cell cycle control protein Cdc48/p97. These proteins are characterized by their ~240 amino acid ATPase domain and a microtubule interacting trafficking domain (MIT) that has been shown to be important for localizing the ATPases to their sites of action (reviewed in Lupas and Martin 2002; reviewed in Hurley and Emr 2006). See Figure 1 for a schematic of the architecture of VPS4a.

VPS4a is 437 amino acids, VPS4b is 444 amino acids, and the two mammalian homologs share 80% sequence identity (Figure 2). Investigators use VPS4a and VPS4b interchangeably because they appear to perform redundant functions (Scheurine *et al.* 2001). Expression studies have shown that VPS4a mRNA is expressed in the heart, brain and testes, and that VPS4b mRNA is expressed in the liver and kidney (Beyer *et al.* 2003). VPS4 is a monomer or dimer in solution and oligomerizes with itself when bound to ATP (Scott *et al.* 2005). It is presumed that VPS4 oligomerizes on the membrane of the late

endosome or MVB and is monomeric or dimeric after it hydrolyzes ATP and is released from the MVB (Figure 3).

The mechanisms of MVB maturation are not well understood, but a series of events have been characterized. During MVB formation, the protein complexes known as endosomal sorting complex required for transport (ESCRT) associate with the membrane of a maturing MVB. The ESCRT complexes are divided into three subclasses: ESCRT-I, ESCRT-II, and ESCRT-III. ESCRT-I consists of VPS23 (also known as TSG101), VPS28, and VPS37. ESCRT-II consists of VPS22 (EAP30), VPS25 (EAP20), and VPS36 (EAP45), and ESCRT-III consists of VPS2 (CHMP2), VPS20 (CHMP6), VPS24 (CHMP3/NEDF), and VPS32 (CHMP4). VPS4 binds to ESCRT-III proteins, and upon the hydrolysis of ATP by VPS4, the ESCRT complexes dissociate from the endosome and the membrane invaginations form a mature vesicle (reviewed in Katzmann *et al.* 2002; reviewed in Hurley and Emr 2006).

When the ATP hydrolysis mutants of VPS4 are over-expressed in cell lines the intracellular trafficking of proteins is greatly affected. One of the best characterized phenotypes of cells expressing mutant VPS4 is that lysosomal-mediated degradation of surface receptors is slowed. Investigators have used Western blotting of total EGFR to show mutant VPS4 decreases the rate of EGF-mediated EGFR degradation, while others have used immunofluorescence to

show EGFR becomes trapped in intracellular compartments (Yoshimori *et al.* 2000; Fujita *et al.* 2003; Hislop *et al.* 2004).

Besides promoting the degradation of surface proteins, VPS4 is also involved in transporting proteins from the TGN to vacuoles (the yeast equivalent of lysosomes) and to the cell surface. Specifically, yeast expressing temperature-sensitive Vps4 or *vps4Δ* yeast are defective at transporting newly synthesized carboxy-peptidase Y (CPY) from the TGN to the vacuole, and the transport of the TGN protein TGN38 to the cell surface is abrogated in cells over-expressing a VPS4a mutant that is unable to hydrolyze ATP (Babst *et al.* 1997; Fujita *et al.* 2003).

Interestingly, the VPS machinery is highjacked during infection to promote the budding of viruses from the cell. VPS4 ATP hydrolysis mutants have been shown to inhibit the budding of several viruses including human immunodeficiency virus type 1 (HIV-1), Hepatitis B, prototypic foamy virus (PFV), paramyxovirus, and Ebola virus (Garrus *et al.* 2001; Licata *et al.* 2003; Patton *et al.* 2005; Schmitt *et al.* 2005; Kian Chua *et al.* 2006). The topology of viral budding is the same as the invagination of late endosomes to form MVBs. As with MVB maturation, ESCRT-I, ESCRT-II, ESCRT-III, and VPS4 are involved in this process. During viral budding, the late (L) domain of the virus associates with a member of the ESCRT complex through a specific motif. These L domains shown to be critical for viral budding include P(T/S)AP, found in the

HIV-1 Gag p6 domain, and $YP(X)_nL$, found in the p9 domain of the EIAV Gag protein. After associating with an ESCRT protein, the L-domain-containing proteins are sorted into a developing plasma membrane bud, and, as during MVB formation, VPS4 hydrolyzes ATP and the maturing bud pinches off (reviewed in Morita and Sundquist 2004).

I identified VPS4a as a WNK1 interacting protein in a yeast-two-hybrid screen. This is a potentially important finding because the evidence to support the idea that WNKs regulate the surface expression of several ion transporters and channels has been accumulating (reviewed in Xie *et al.* 2006; reviewed in Chapter 1). As discussed in the introduction, the mechanisms by which WNKs function to regulate these proteins are beginning to be defined but only for a few channels and transporters. It is possible that WNK1 may interact with VPS4a to regulate the intracellular trafficking of specific plasma membrane proteins, thereby modulating their surface expression and activity.

During these studies, I confirmed the interaction of WNK1 with VPS4a using multiple techniques, mapped the region in VPS4a to which WNK1 binds, and determined VPS4a is not a WNK1 substrate. I also discovered that expression of mutant VPS4a in HEK293 and HeLa cells causes WNK1 to localize to aberrant VPS4a E228Q-positive compartments, possibly through a vesicle fusion event. Finally, I tested the idea that VPS4a modulates the activity of

ROMK, the potassium channel that is regulated by WNK kinases (reviewed in Chapter 1).

Methods

Cell Culture and Harvesting- HEK293, HeLa, and HT-29 were cultured in DMEM with 10% fetal bovine serum and 1% L-glutamine at 37 °C under 5% CO_2. Confluent cells were harvested in buffer containing 0.1-1% Triton X-100, 50 mM HEPES (pH 7.5), 150 mM NaCl, 1.5 mM $MgCl_2$, 1 mM EGTA, 10% glycerol, 100 mM NaF, 0.2 mM Na_3VO_4, 50 mM β-glycerophosphate, 1 mM dithiothreitol, 1 mM benzamidine hydrochloride, 10 mg/L leupeptin, 0.5 mg/L pepstatin A, and 1.5 mg/L aprotinin. The cells were vortexed for 30 s, incubated on ice for 10 min, and centrifuged for 15 min at 14,000 rpm to remove insoluble material.

Antibodies and Proteins- Two WNK1 antibodies were used: Q256 and anti-WNK1 purchased from Cell Signaling (cat. no. 4979). Anti-myc monoclonal antibody was prepared from the cell line Myc 1-9E10.2 (American Type Culture Collection), polyclonal anti-hemaglutinin (HA) was purchased from Santa Cruz Biotechnology (cat. no. sc-805), and the Alexa fluorophore-conjugated secondary antibodies were purchased from Molecular Probes. Anti-SKD1 was a gift from Scott Emr (University of California San Diego) and Markus Babst (University of Utah).

The WNK1 kinase domain (residues 194-483) was provided by Xiaoshan Min and full-length GST-WNK1 was provided by Steve Stippec. To generate purified VPS4a, VPS4a was subcloned into pGEX-KG, the plasmid was transformed into BL21 *E. coli*, and an IPTG induction test was conducted to identify the optimal conditions for expressing the protein. For the purification, the bacteria were cultured overnight at 30°C but IPTG was not added because the expression was leaky enough to promote protein synthesis and IPTG treatment resulted in protein degradation. The bacteria were washed with buffer A (50 mM Tris-Cl (pH 8.0), 10 mM EDTA, 25% sucrose, 1 mM benzamidine hydrochloride, 1 mM dithiothreitol, 10 mg/L leupeptin, 1.5 mg/L aprotinin, 0.5 mg/L pepstatin A), resuspended in lysis buffer (150 mM NaCl, 1.5 mM $MgCl_2$, 1 mM EGTA, 10% glycerol, 50 mM HEPES (pH 7.5), 100 mM NaF, 0.2 mM Na_3VO_4, 50 mM β-glycerophosphate, 2 mM EDTA, 0.5% Triton X-100, 1 mM dithiothreitol, 2 mM benzamidine hydrochloride, 20 mg/L leupeptin, 5 mg/L pepstatin A, and 15 mg/L aprotinin), sonicated, and added to a column containing glutationine-agarose beads. The beads were washed with wash buffer 1 (50 mM Tris-Cl (pH 7.4), 150 mM NaCl, 5% glycerol, 0.5% Triton X-100, 2 mM EDTA, 5 mg/L pepstatin A, 15 mg/L aprotinin, 20 mg/L leupeptin, 2 mM benzamidine hydrochloride, 1 mM dithiothreitol) and with wash buffer 2 (50 mM Tri-Cl (pH 7.4), 150 mM NaCl, 5% glycerol, 5 mg/L pepstatin A, 15 mg/L aprotinin, 20 mg/L leupeptin, 2 mM benzamidine hydrochloride, 1 mM dithiothreitol), and the

protein was eluted with elution buffer at pH 7.4 (50 mM Tris-Cl, 150 mM NaCl, 5% glycerol, 0.5 mg/L pepstatin A, 0.5 mg/L pepstatin A, 10 mg/L leupeptin, 1 mM benzamidine hydrochloride, 1 mM dithiothreitol, 10 mM glutathione).

Yeast-Two-Hybrid Screen- The LexA DNA binding domain (bait) and GAL4 activation domain (prey) system was utilized for the yeast-two-hybrid screen. A neonatal mouse brain cDNA library in the plasmid pGADGH was provided by Mark Henkemeyer (UT Southwestern, Center of Developmental Biology) and Wei Chen, and the bait construct, WNK1 1311-1542/pVJLII, was provided and tested for autoactivation by Byung-Hoon Lee. For the large scale transformation, the *S. cerevisiae* strain L40 was transformed using lithium acetate with 110 μg library DNA and 2 mg salmon sperm DNA as carrier, and the yeast were streaked onto complete supplemental medium (BIO 101, Inc.) lacking Leu, Trp, and His to obtain potential positive WNK1 interactors. Colonies on the -Leu -Trp -His medium were streaked onto dropout plates lacking Leu and onto plates lacking Trp to select for yeast containing only the pGADGH construct from the library and not the WNK1 bait construct. The colonies had to be re-streaked several times onto -Leu plates to get rid of the bait plasmid. Once the prey plasmids were subjected to selection they were isolated using Zymogen's yeast plasmid minipreparation kit and sequenced using a pGADGH-specific primer.

In Vitro Kinase Assay- GST-tagged VPS4a was incubated with either the kinase domain of WNK1 (residues 194-483), WNK1 immunoprecipitated from

DCT cells treated with 0.5 M NaCl, or GST-tagged full-length WNK1. For the experiment shown in Figure 5, 0.2 μg GST-tagged full-length WNK1 was incubated with 2 μg GST-VPS4a in kinase buffer (10 mM HEPES (pH 8.0), 10 mM $MgCl_2$, 25 μM ATP, 1 mM benzamidine hydrochloride, 1 mM dithiothreitol) and ~5000 cpm/pmol [γ-^{32}P]ATP at 30°C for 20 min. The samples were subjected to SDS-PAGE, the gel was dried, and an autoradiogram was generated.

Pairwise Yeast-Two-Hybrid Tests- The yeast LexA/Gal4 system was also utilized for these experiments. Bait genes were subcloned into the plasmid pVJL II and prey genes were subcloned into the plasmid pGADGH. CHMP1b cDNA was a gift from Wesley Sundquist (University of Utah), and CHMP4b cDNA and CHMP6 cDNA were gifts from Masatoshi Maki (Nagoya University, Japan). The constructs were transformed into competent L40 cells using the Zymogen EZ Transformation Kit and transformed cells were selected on complete supplemental medium without Leu and Trp. Colonies were then streaked onto plates lacking Leu, Trp, and His and scored based on growth. Generally, 20 or 40 ng of each plasmid was used for each pairwise test.

Co-immunoprecipitation of WNK1 and VPS4a- The following plasmids were constructed for these experiments. Flag-tagged VPS4a was generated by subcloning VPS4a into pCMV7, and GFP-tagged VPS4a was generated by subcloning VPS4a into Myc-GFP/CMV5, with the Myc tag fused to the N-terminus of VPS4a and GFP fused to the C-terminus. Myc-VPS4a E228Q-

GFP/CMV5 was constructed by site-directed mutagensis of Myc-VPS4a-GFP/CMV5.

For the experiment shown in Figure 7, Myc-VPS4a E228Q-GFP/CMV5 was transfected into HEK293 cells, and approximately 18 h post-transfection, the cells were scraped in lysis buffer containing 0.1% Triton X-100. The lysates were pooled to have the same amount of over-expressed VPS4a E228Q in each sample. The lysates were incubated with Q256, Q256 preimmune serum, or anti-HA antibody at 4°C for 1 h and protein A Sepharose beads were added and incubated for an additional hour. The beads were washed 3 X with IP buffer (20 mM Tris-Cl (pH 7.4), 0.1 M NaCl, 0.1% Triton X-100) and sample buffer was added. Next, the proteins were separated on a 7.5% polyacrylamide gel in SDS, transferred to a nitrocellulose membrane, and immunoblotted with anti-Myc antibody.

Localization of VPS4a and WNK1- For the localization analysis of over-expressed proteins, GFP- and HA-tagged VPS4a and full-length WNK1 were expressed in HEK293 or HeLa cells. The HA-tagged VPS4a constructs were generated by subcloning wild-type VPS4a and VPS4a E228Q into CMV5-HA (Clontech). Myc-WNK1/CMV5 was provided by Bing-e Xu. Generally, cells were plated onto 35 mm^2 Matex dishes that contained an uncoated cover slip in the center, and 1 μg of DNA was transfected into ~50-80% confluent cultures using a 3:1 Lipofectamine^{TM} 2000 to DNA ratio. Twelve to 24 h later, either live cells were transported to the imaging facility or they were fixed, permeabilized,

and stained with antibodies. Images were captured with a Zeiss Deltavision deconvolution microscope.

For the fixed samples, the plates were washed 1X with TBS and fixed for 10 min at room temperature in 4% paraformaldehyde in PBS. The plates were washed 3X for 5 min with TBS and permeabilized with 0.5% Triton X-100 in TBS at room temperature for 10 min. The samples were then washed 2X for 5 min with TBS, washed 1X for 5 min with TBST, and blocked in 1% BSA in TBST for 30 min. They were then incubated for 1h with 1:200 primary antibodies in block solution, quickly washed 2X with TBST, and washed 3X for 5 min with TBST. The samples were then incubated with 1:10,000 Alexa secondary antibodies in block for 1 h, quickly washed 2X with TBST, washed 3X for 5 min with TBST, and stored at 4°C in TBST.

Endogenous WNK1 was stained with either Q256 or anti-WNK1 from Cell Signaling that was diluted 1:200. For experiments that included the antigenic peptide mixed with the antibody as a negative control, the antibody and peptide were generally pre-incubated for 5 min in a 1:1 ratio before adding the mixture to the fixed cells. For the WNK1 antibody from Cell Signaling, the 1:1 ratio corresponds to 1 μg antibody to 1 μg peptide. For Q256, the 1:1 ratio indicates 1 μl of serum was pre-incubated with 1 μg peptide.

The three-dimensional models were constructed with the Imaris® software from the z-stack Deltavision files with the help of Kate Luby-Phelps and Abhijit Bugde.

Transmission Electron Microscopy- GFP-VPS4a/CMV5 and GFP-VPS4a E228Q/CMV5 were transfected into HEK293 using Lipofectamine™ 2000. Twenty-four hours post-transfection, the cells were fixed with 2.5% gluteraldehyde, post-fixed with 1% osmium, dehydrated with a series of alcohol washes, and embedded in Embed 812. The samples were then stained with uranyl acetate, sliced, and mounted on grids by Tom Januszewski in the UT Southwestern electron microscopy core facility.

Live Cell Imaging with LysoTracker®- LysoTracker® red fluorescent acidotropic probe labels acidic compartments such as lysosomes (Molecular Probes). HEK293 cells were cultured on uncoated 35mm^2 Matex dishes and transfected with 0.5 μg GFP-VPS4a E228Q. Eighteen hours post-transfection, 5 nM LysoTracker® Red was added to the culture medium, the cells were incubated with the marker for 20 min, and the medium was changed. The live cells were then imaged with a Zeiss Deltavision deconvolution microscope that has a CO_2 chamber and a temperature regulator to maintain the cells at 37°C.

EGFR Degradation Assay- One microgram Myc-VPS4a-GFP/CMV5, Myc-VPS4a E228Q-GFP/CMV5, and Flag-WNK1 1311-1542 were transfected with Fugene into HeLa cells growing on 60 mm^2 dishes. Twelve to 24 h post-

transfection the cells were treated with 10 ng/mL EGF and harvested at the indicated times. Cell lysates were prepared, and the samples were separated on 7.5% polyacrylamide gels in SDS, transferred to nitrocellulose membranes, and Western blotted with the anti-EGFR monoclonal antibody 15E11 (gift from Nita Maihle and Jill Reiter, Yale University).

Whole-Cell Patch-Clamp Recording of ROMK Channels- HEK293 cells were co-transfected with cDNAs encoding GFP-ROMK (0.5 μg), VPS4a wild-type (1.5 μg), VPS4a E228Q (1.5 μg) or VPS4a/b siRNA (200 ng). In each experiment, the total amount of DNA per transfection was balanced by using empty vectors or scrambled RNA oligo nucleotides. Approximately 36-48 h post-transfection, whole-cell currents were recorded by using an Axopatch 200B amplifier as described previously (Xu *et al.* 2005a; Yeh *et al.* 2003). Transfected cells were identified by using epifluorescent microscopy. The bath and pipette solution contained 145 mM KCl, 2 mM $MgCl_2$, 2 mM $CaCl_2$, 10 mM Hepes (pH 7.4) and 145 mM KCl, 2 mM EDTA, 10 mM Hepes (pH 7.4), respectively. Capacitance and access resistance were monitored and 75% compensated. The voltage protocol consists of 0 mV holding potential and 400 ms steps from -100 to 100 mV in 20-mV increments. Statistical comparisons were made by using the unpaired Student's t-test.

Results

A Proline-rich Region of WNK1 Interacts with VPS4a- There are relatively few WNK1 interacting proteins that have been identified. Previous yeast-two-hybrid screens from our laboratory identified SGK1, Munc18c, and SytII as WNK1 binding partners using N-terminal WNK1 fragments as baits. I chose to search for proteins that bind to the unique C-terminal proline-rich area of WNK1 by also conducting a yeast-two-hybrid screen.

I used rat WNK1 1311-1542 as bait and obtained 11 colonies. I anticipated obtaining more hits because WNK1 1311-1542 contains 10 PxxP motifs, which potentially bind to SH3 domain-containing proteins (Figure 4). Six colonies encoded ATP synthase, three encoded heat shock 70 kDa protein, and two encoded full-length VPS4a. ATP synthase and heat shock 70 kDa are known to be common yeast-two-hybrid false positives. To reconfirm the interaction between WNK1 1311-1542 and VPS4a, I subcloned the VPS4a plasmid obtained from the screen into pGADGH and eliminated the small 5' untranslated region present in the original clone. This was then used in direct yeast-two-hybrid tests with WNK1 and the negative controls OSR1 and lamin to show the VPS4a untranslated region was not mediating its binding with WNK1 and that VPS4a has selectivity in its binding partners.

WNK1 Does Not Phosphorylate VPS4a- One of the first experiments I performed after identifying VPS4a as a WNK1 substrate was an *in vitro* kinase

assay to test whether VPS4a is a WNK1 substrate. To date, it is not known if VPS4a is phosphorylated. I performed these assays using the purified kinase domain of WNK1, WNK1 immunoprecipitated from mouse DCT cells treated with 0.5M NaCl to obtain active kinase, and full-length GST-WNK1. In each of these experiments no detectable phosphate was incorporated into VPS4a (Figure 5). The results in Figure 5 show that WNK1 autophosphorylation is lower when VPS4a was added, but I do not think this is representative or significant since I only observed this one time. These data suggest that any direct action of WNK1 on VPS4a is kinase-independent.

WNK1 1311-1542 Interacts with the N-terminal Half of VPS4a- I performed pairwise yeast-two-hybrid interaction tests to determine where WNK1 interacts with VPS4a. Identifying the site of interaction between WNK1 and VPS4a may provide information about how to test the function of their association. For example, if WNK1 binds to the VPS4a MIT domain it may influence its protein localization, or if it binds to the ATPase domain it may regulate its catalytic activity.

I conducted several pairwise interaction tests and concluded with confidence that WNK1 1311-1542 but not other fragments of WNK1 interacts with the N-terminal half of VPS4a (Table 1). As discussed previously, the N-terminus of VPS4a contains the MIT domain which is important for protein localization (Figure 1). Mutation of the residues critical for VPS4a ATPase

hydrolytic activity does not impact the binding of VPS4a and WNK1 because WNK1 strongly binds to VPS4a K173Q, E228Q, and the double mutant K173Q/E228Q (Table 1).

There were several interactions tested that produced results that I could not interpret with confidence because the VPS4a fragments also interacted with lamin, a protein that is considered sticky and is often used as a negative control in yeast-two-hybrid experiments (Table 2). These fragments included VPS4a 1-397, 1-353, 1-337, 1-317, 1-297, 1-277, and 50-243. Nonetheless, I consistently observed that WNK1 1311-1542 interacted with VPS4a 1-243 while the negative controls lamin, OSR1 and TAO2 1-320 D169A did not.

To determine what residues at the N-terminus were important for binding to WNK1, I constructed the fragments VPS4a 20-437, 40-437, 60-437, 80-437, and 100-437 to use in pairwise two-hybrid tests with WNK1 1311-1542. Unfortunately, I did not observe growth on selection medium for any of these fragments. Overall, although some of the interaction tests produced results that were not interpretable, I can conclude with confidence that WNK1 1311-1542 interacts with the N-terminal half of VPS4a.

A Mutation in the MIT Domain of VPS4a Abolishes its Binding to WNK1- Like several of the VPS proteins, CHMP1b binds to VPS4a. The binding of CHMP1b to VPS4a is dependent upon the VPS4a surface exposed residue L64 located in the MIT domain. Importantly, it was reported that mutation of this site

to alanine does not induce a conformational change (Scott *et al.* 2005b). Because I had evidence that WNK1 1311-1542 binds to the N-terminal half of VPS4a, the same region to which CHMP1b binds, I tested whether mutation of VPS4a L64A would abolish its interaction with WNK1. VPS4a L64A/pGADGH was generated by site-directed mutagenesis and used in pairwise yeast-two-hybrid tests (Table 3). Both CHMP1b and WNK1 1311-1542 interact with full-length VPS4a, VPS4a 1-243, and VPS4a 1-160 but they do not interact with VPS4a L64A. As a control, CHMP6 interacts with both wild-type and L64A VPS4a (Yeo *et al.* 2003). The identification of leucine 64 as an important residue in the binding of WNK1 to VPS4a potentially provides a tool to assess the function of the interaction between WNK1 and VPS4a.

WNK1 May or May Not Interact With VPS4b- In addition to mapping the region of VPS4a that binds WNK1, I tested whether WNK1 is also capable of binding to VPS4b. VPS4a and VPS4b share a high percent sequence identity and their functions appear to be redundant (Scheurine *et al.* 2001). I obtained full-length VPS4b DNA from ATCC and subcloned it into pGADGH. I did not observe an interaction with WNK1, but this result in inconclusive since I also did not observe any binding with the positive control CHMP6 (Table 4). The CHMP6 yeast homolog, VPS20, is known to bind to yeast VPS4 (Yeo *et al.* 2003).

Smaller WNK1 Fragments Do Not Interact With VPS4a- In further interaction studies, I attempted to identify a smaller fragment within WNK1 1311-

1542 that binds with VPS4a (Table 4). I subcloned WNK1 1340-1399 and WNK1 1400-1542 into pVJL II and co-transformed them with VPS4a/pGADGH into L40 to test whether they associate. I did not observe any growth on selection medium with these combinations, and consequently the results were inconclusive.

I also subcloned the proline-rich region of WNK4 (residues 776-1020) into pVJL II in attempts to determine whether it also interacts with VPS4a but unfortunately that fragment is a strong autoactivator. This was determined by streaking WNK4-transformed L40 onto complete supplemental medium lacking Trp and His but containing 3-aminotriazole (3-AT). WNK4 776-1020 grew on plates containing a high concentration of 3-AT (20 mM) and therefore produced too much background to be able to use in pairwise interaction tests.

WNK1 and VPS4a Co-Immuniprecipitate- To further support the idea that WNK1 and VPS4a interact, the two proteins were co-immunoprecipitated. I used several approaches to show convincingly that VPS4a associates with WNK1. I first attempted to co-immunoprecipitate Flag-tagged wild-type VPS4a with endogenous WNK1 from HEK293 cells. WNK1 was immunoprecipitated from HEK293 cells over-expressing Flag-VPS4a with the antibody Q256 and the precipitates were Western blotted with an anti-Flag antibody. Unfortunately Flag-VPS4a migrated close to the heavy chain IgG band on an SDS-PAGE gel and therefore the results were difficult to interpret. Conversely, I attempted to immunoprecipitate Flag-VPS4a with an anti-Flag antibody and Western blot the

precipitates with Q256. I used several negative controls including Flag-RGS2 and Flag-MEK5b but they all appeared to pull down endogenous WNK1.

To avoid the problem of VPS4a migrating with the heavy chain IgG band and the seemingly non-specificity of the Flag antibody, I added a GFP tag to VPS4a. Other groups had generated similar constructs to avoid the migration problem. This construct was transfected into HEK293 cells, lysates were prepared, and WNK1 was immunoprecipitated with Q256. Q256 preimmune serum, the ERK2 antibody Y691, and Myc-GFP were used as negative controls. Q256 did not immunoprecipitate Myc-GFP and it did pull down more VPS4a than the negative control antibodies.

Many groups have used the VPS4a ATP hydrolysis mutants to show VPS4 interacts with members of the ESCRT complexes. The premise is that if VPS4a is trapped on a late endosome/MVB it is more likely to interact with ESCRT proteins. To potentially obtain cleaner results, VPS4a E228Q was co-immunoprecipitated with endogenous WNK1 (Figure 7). More VPS4a E228Q was immunoprecipitated with Q256 than with the negative controls Q256 preimmune serum and anti-HA antibody. This approach produced the most convincing data showing endogenous WNK1 and over-expressed VPS4a associate and it helped validate the yeast-two-hybrid results.

VPS4a E228Q Localizes to Large Spherical Structures in HEK293 Cells- To show if and where WNK1 and VPS4a co-localize in cells,

immunofluorescence was employed. Prior to performing the WNK1/VPS4a co-localization studies, the localization of each protein was examined separately. The localization of VPS4a E228Q was analyzed in both HEK293 and HeLa cells and the localization of WNK1 was analyzed in HEK293, HeLa, and HT-29 cells.

VPS4a E228Q expressed in HEK293 cells localizes around large and small ring-like structures (Figures 8-16), while wild-type GFP-tagged VPS4a appears diffusely cytoplasmic (Figure 17). Figures 8, 10, 14 and 17 are z-stacks of HEK293 cells in which the top left image is a stack near the bottom of the cell and the image at the bottom right is a stack near the top of the cell. It should be noted that HA-tagged VPS4a and GFP-fused VPS4a E228Q expressed in HEK293 cells appear to exhibit similar localization patterns. Figure 16 shows compressed z-stacks of cells stained for HA-tagged E228Q.

The large VPS4a E228Q-positive spherical structures found in HEK293 have also been reportedly found in other cell lines including normal rat kidney (NRK) and African green monkey kidney (COS7), but some of the structures I observed are larger than those shown in the literature (Yoshimiri *et al.* 2000; Howard *et al.* 2001; Fujita *et al.* 2003). Fujita *et al.* described the VPS4 ATP hydrolysis mutant-positive organelles as “hybrid organelles” of the late endocytic pathway while Yoshimiri *et al.* described the VPS4-positive structures in NRK cells as “aberrant vacuoles”. Because the VPS4a E228Q-positive spheres in

HEK293 cells are unusually large, I wanted to study these structures in more detail. Data from these studies will be discussed later.

Some of the VPS4a E228Q expressed in HEK293 cells appears to be within the ring-like structures (see arrows on Figure 11) while the majority of it is located around the spheres. Three-dimensional models were created using the Imaris® software to better visualize the localization pattern (Figures 12-13). These models show that VPS4a E228Q often surrounds the structure but in some cases it may reside within it.

VPS4a E228Q Also Localizes to Aberrant Structures in HeLa Cells- VPS4a E228Q expressed in HeLa cells also localizes to the circular structures (Figure 18), whereas wild-type VPS4a appears diffusely cytoplasmic (data not shown). These two different localization patterns observed between VPS4a wild-type and E228Q may be explained by the following. Because VPS4a E228Q cannot hydrolyze ATP, the ESCRT complexes and VPS4a itself get trapped on the late endosome/MVB, causing VPS4a E228Q to accumulate on aberrant MVBs that keep accepting cargo from the plasma membrane but do not properly form the internal buds. Conversely, wild-type VPS4a is able to localize to the MVB and then dissociate itself from it, consequently appearing mostly diffusely cytoplasmic.

WNK1 Exhibits a Punctate Localization Pattern- Data showing WNK1 and VPS4a interact and the increasing evidence that WNKs may regulate the

vesicular trafficking of ion transporters and channels prompted me to test the idea that WNK1 is localized on vesicles. Previous data from our laboratory showed that WNK1 in HEK293 cells is diffusely cytoplasmic, but I wanted to analyze its localization more in more detail.

The localization of over-expressed WNK1 was studied in HEK293 and HeLa cells, and the localization of endogenous protein was analyzed in HEK293, HeLa, and HT-29 using the two different anti-WNK1 antibodies. HEK293 were chosen because they had been used in several other assays pertaining to VPS4a and WNK1, and HT-29 cells were studied because they express a large amount of WNK1 in comparison to other epithelial-derived lines (Chapter 2, Figure 2). WNK1 localization was analyzed in HeLa to determine whether its localization would be similar in a different cell type. In addition, HeLa express a relatively lower amount of WNK1 in comparison to other lines (data not shown) and therefore any structural components to its localization pattern may be easier to visualize at the fluorescence microscopy level.

Immunofluorescence of over-expressed and endogenous WNK1 shows that the kinase displays a punctate pattern in the cytoplasm (Figures 19-25). Figures 20, 22 and 25 are three-dimensional models that clearly show WNK1 is not in the nucleus. The WNK1 localization pattern is reminiscent of that for early endosome antigen 1 (EEA1), a hydrophilic peripheral membrane protein that

localizes to early endosomes but not to late endosomes (Mu *et al.* 2005). This will be discussed further.

VPS4a E228Q and WNK1 Co-Localize- Over-expressed WNK1 and VPS4a E228Q strongly co-localize with one another in HEK293 cells (Figures 26-31). Single z-stacks with the green image (VPS4a E228Q), red image (WNK1), and merged images are shown in Figures 26 and 29. Figures 27 and 30 are three-dimensional models that were constructed with the Imaris® program from the z-stack data generated with the Deltavision deconvolution microscope. Areas where both VPS4a E228Q and WNK1 are present are white. To analyze their association more carefully, highly detailed three-dimensional models were generated to show that WNK1 and VPS4a E228Q are localized on the same large spherical structures (Figures 28 and 31).

In the three-dimensional models in panel D of Figures 28 and 31 where the green, red, and yellow are depicted, it is sometimes difficult to visualize the yellow where WNK1 and VPS4a E228Q are co-localized. Because these images are three-dimensional, the co-localized areas may be masked by either VPS4a or WNK1 exclusive areas. Because of this, higher magnification pictures of the models were generated as shown in Figures 28 E-G and Figure 31 E-G. These images show that yellow is often masked behind either red or green, and it therefore provides a more accurate assessment of the localization of WNK1 and VPS4a E228Q.

In contrast, WNK1 and VPS4a E228Q do not appear to co-localize as strongly in HeLa cells as in HEK293 cells but they do exhibit overlapping localization as shown by detailed three-dimensional models of over-expressed and endogenous WNK1 with VPS4a E228Q (Figure 32-33). From these models a potentially important finding was discovered. It seems that WNK1-positive areas interface with VPS4a E228Q-positive structures. If the WNK1 and VPS4a-positive structures are indeed vesicles, the two proteins appear to not be located on the same vesicle but on vesicles that interact with each other. It is possible that WNK1-containing vesicles may be either docking or budding from VPS4a-containing vesicles.

Wild-type VPS4a and WNK1 Exhibit Overlapping Localization- To determine whether VPS4a has to be mutated to visualize co-localization with WNK1, immunofluorescence was employed. As shown in Figure 34, over-expressed WNK1 and wild-type VPS4a do co-localize in HeLa cells but they may not to the same extent as WNK1 with VPS4a E228Q.

Testing the Idea That Over-expression of VPS4a E228Q in HEK293 Cells Promotes Autophagy- I further examined the abnormal VPS4a E228Q-positive spherical structures present in HEK293 cells. Others have conducted studies to show mammalian cells over-expressing the VPS4 ATP hydrolysis mutant and *S. cerevisiae* containing temperature-sensitive VPS4 incubated at a non-permissive temperature display a morphological alteration in their endosomal components

termed the class E compartment (Babst *et al.* 1997; Fujita *et al.* 2003; Figure 36). To gain a better understanding about the morphology of the VPS4a E228Q-positive large and small ring-like structures found in HEK293 cells, I performed transmission electron microscopy of cells transfected with VPS4a E228Q.

Because some of the VPS4a E228Q-positive ring structures in HEK293 cells are unusually massive, it was hypothesized that those structures are autophagosomes or autolysosomes. Autophagosomes and autolysosomes are formed in response to nutrient starvation and infection by some viruses and bacteria in order for the cells to digest their intracellular material. After initiation of the autophagy pathway, a flat membrane sack wraps around a part of the cytoplasm and closes, forming an autophagosome. Next, endosomes deliver lysosomal enzymes to the autophagosome, and finally, the autophagosome fuses with late endosomes, MVBs, or lysosomes. At this final step the autophagosome is termed an autolysosome (reviewed in Landes Bioscience). See Figure 37 for a schematic.

Transmission electron microscopy was performed to observe the morphological changes that are caused by mutant VPS4a (Figure 36). I originally conducted this experiment to determine the consequences of over-expressing VPS4a L64A, the point mutant that does not bind to CHMP1b or to WNK1 1311-1542 (Table 3). I hypothesized that VPS4a L64A has reduced function and over-expression of it would result in the formation of the class E compartment. After

analyzing the images, however, it became apparent that positively identifying the class E compartment would be difficult because the morphology of some of the subcellular structures did not resemble the reported class E compartments (Babst *et al.* 1997; Fujita *et al.* 2003; Figure 35).

I did not conclude anything about the L64A mutation, but did initially conclude from this preliminary experiment that expression of VPS4a E228Q may promote the formation of autophagosomes or autolysosomes. The size of the large rings observed by fluorescence microscopy correlated with the size of the structures that resembled autophagosomes. I examined the same electron microscopy samples later and quantified the number of autophagosome-looking compartments in the cells transfected with wild-type verses VPS4a E228Q. My expectation that the VPS4a E228Q cells would have more autophagosomes than the VPS4a wild-type cells appeared to be false. A pitfall of the experiment was that I did not know which cells expressed exogenous VPS4a. Electron immunogold staining will be required to confirm this. Because I initially hypothesized though that mutant VPS4a promotes autophagy, I did attempt to determine whether VPS4a E228Q co-localizes with an autophagosome marker.

Some of the VPS4a E228Q-Positive Structures in HEK293 Cells Localize with LC3- Microtubule-associated protein (MAP) light chain 3 (LC3) is important for the formation of autophagosomes and is used by many as an autophagosome marker (reviewed in Tanida *et al.* 2004). I tested whether GFP-tagged LC3 (gift

from Beth Levine, UT Southwestern) localizes with HA-tagged VPS4a E228Q. Some of the LC3 localized with VPS4a E228Q in HEK293 cells but much of it did not (Figure 38). It is possible that not all autophagosomes or autolysosomes would be LC3-positive and that some of the VPS4a E228Q would not localize to autophagosomes but to abnormally large and aberrant late endosomes and MVBs. These preliminary data do suggest that at least some VPS4a E228Q in HEK293 cells is present on autophagosomes. Based on the electron microscopy experiment it appears that mutant VPS4a does not cause autophagy, but it is possible that the aberrant VPS4a-positive late endosomes/MVBs may become engulfed during the formation of autophagosomes.

WNK1 and LC3 Do Not Appear to Co-Localize- WNK1 and LC3 were over-expressed in HeLa cells, and it appears that they do not exhibit overlapping localization (Figure 39). This is not surprising because preliminary results show that VPS4a E228Q also does not appear to co-localize with LC3 in this cell type (data not shown).

VPS4a E228Q Does Not Largely Overlap With LysoTracker®- LysoTracker® was used to determine whether mutant VPS4a localizes to acidic compartments, but GFP-VPS4a E228Q and LysoTracker® Red did not appear to significantly overlap (Figure 40). There were a few acidic structures surrounded by VPS4a E228Q (Figure 41), but the VPS4a-positive rings were largely not acidic. These data suggest that if some of the VPS4a E228Q-positive structures

are components of the autophagy pathway, they are early in the pathway before the autophagosomes become acidified, and similarly, if they are aberrant MVBs, they have likely not been fused with lysosomes.

I also tested whether GFP-tagged WNK1 overlaps with LysoTracker® Red in HEK293 cells. GFP was inserted into Myc-WNK1/CMV5 between the Myc tag and WNK1. Data from this experiment was inconclusive because N-terminally tagged WNK1 exhibited a different localization pattern than over-expressed Myc-WNK1 or endogenous WNK1. I am currently fusing GFP to the C-terminus of WNK1 and will assess its localization to determine whether it may be used for live cell imaging.

Tests of Function- To help identity the purpose of the WNK1-VPS4a interaction, I attempted to determine whether over-expression of WNK1 1311-1542 (the fragment that binds to VPS4a) modulates EGFR degradation and/or the activity of ROMK. As discussed previously, over-expression of the VPS4 ATPase mutants slows EGF-mediated EGFR degradation (Yoshimori *et al.* 2000; Fujita *et al.* 2003; Hislop *et al.* 2004). I first attempted to confirm the previous findings by treating HeLa cells that were transfected with either GFP, VPS4a wild-type, or VPS4a E228Q with EGF and Western blotting the total amount of receptor remaining over a time course. Unfortunately I did not observe any differences in the rates of degradation between GFP, wild-type VPS4a, and mutant VPS4a as had been previously reported. I conducted the same experiment

once with over-expressed WNK1 1311-1542 alone and may have observed less EGFR degradation in the presence of this fragment (data not shown). This experiment is currently being repeated. If this result can be validated, it may imply that WNK1 helps facilitate VPS4a-mediated movement of cargo through the lysosomal pathway.

In collaboration with Hao-Ran Wang and Chou-Long Huang from the Department of Internal Medicine, we tested whether VPS4 or WNK1 1311-1542 impacts the activity of ROMK, the potassium channel that has been shown to be negatively regulated by WNK1, WNK3 and WNK4 (reviewed in Chapter 1). VPS4a wild-type, VPS4a E288Q, WNK1 1311-1542, and VPS4a/b siRNA were co-transfected into HEK293 cells with ROMK, and whole-cell patch-clamp recordings were performed. Unfortunately we did not observe any reproducible differences in ROMK current when VPS4a and WNK1 1311-1542 were over-expressed or when VPS4a/b siRNA oligo nucleotides were co-transfected (data not shown). It remains unclear if the interaction of WNK1 with VPS4a modulates the activity of ROMK or other ion channels or transporters.

Discussion

These studies show that WNK1 interacts with the N-terminus of VPS4a, a critical component of trafficking through recycling and late endosomes. This finding is significant because it may connect WNK1 to the regulation of ion

channels and transporters via intracellular sorting. The current understanding of how WNK1 regulates the activity of membrane proteins is limited and lacks mechanistic information. Thus, this study provides a starting point for deciphering the actions of WNK1.

WNK1 positively regulates ENaC, NCCT and NKCC, but negatively regulates TRPV4 and ROMK. As discussed in Chapter 1, there is some information available about how ENaC, NCCT and NKCC are modulated by WNK1, but there is significantly less known about the regulation of TRPV4 and ROMK. ENaC is up-regulated via the WNK1 N-terminus, which activates SGK-1 to inhibit the E3 ubiquitin ligase Nedd4-2. WNK1 increases NKCC activity by phosphorylating OSR1, and it increases NCCT activity by relieving WNK4-mediated inhibition of the co-transporter. In contrast, the role of WNK1 in the negative regulation of ROMK and TRPV4 has been less well characterized.

I theorize that WNK1 facilitates the delivery of ROMK and TRPV4-containing vesicles to late endosomes and MVBs through its interaction with VPS4a. Although this is speculative, the following data may support this idea. Endogenous and over-expressed WNK1 exhibits a punctate localization pattern in the cytoplasm that is reminiscent of endosomal staining. At least in HeLa cells, three-dimensional models of WNK1 and VPS4a E228Q co-localization suggest that WNK1 and VPS4a interact at the interface of two structures. Therefore, WNK1-positive vesicles may be associating with VPS4a-positive vesicles to

deliver cargo from the plasma membrane. The EGFR degradation result with WNK1 1311-1542 would further support this idea if confirmed. When WNK1 1311-1542 is over-expressed, it likely blocks the endogenous interaction of WNK1 and VPS4a and possibly the association of two different vesicles. If the interaction of WNK1 with VPS4a is blocked, the cargo being delivered by WNK1 will not reach the later stages of endosomal sorting.

This research warrants further investigation, and to help support the hypothesis that WNK1 delivers cargo to late endosomes and MVBs via its interaction with VPS4a the following should be done: 1) show WNK1 localizes to early endosomes, and 2) show that disrupting the interaction of WNK1 with VPS4a slows the degradation of plasma membrane proteins. I am currently testing whether endogenous WNK1 in HeLa cells co-localizes with the early endosomal markers early endosome antigen 1 (EEA1), phosphatidyl inositol-3-phosphate (PI(3)P), and internalized transferrin. Preliminary results from the WNK1 and EEA1 co-localization analyses show that a portion of WNK1 overlaps with EEA1. I am also repeating the EGFR degradation assay to determine whether saturating VPS4a with WNK1 1311-1542 and therefore preventing its binding to endogenous WNK1 slows the degradation of the receptor.

To better address some of the questions that were discussed, the following modifications or additional experiments may be helpful. As an example, when mapping the region in VPS4a that WNK1 binds, generating the VPS4a fragments

for pairwise yeast-two-hybrid interaction tests should be approached differently. For many of my interaction tests, I sequentially deleted 20 amino acids from either the N-terminus or the C-terminus or made random deletions within the gene. Using a secondary structure prediction program to determine where the various helices and sheets begin and end may help avoid creating proteins that fold poorly. Improper protein folding may explain why some of the VPS4a fragments I tested for interaction with WNK1 1311-1542 produced inconclusive results.

As another example, in order to definitively show WNK1 and VPS4a co-localize, electron immunogold labeling would be valuable. I have three-dimensional models that suggest WNK1 and VPS4a are expressed on different structures in HeLa cells but overlap at their interface. Electron immunogold labeling would determine whether WNK1 and VPS4a are indeed localized on different vesicles because the resolution is significantly higher than that for fluorescence microscopy. I attempted electron immunogold labeling with over-expressed Myc-WNK1 in HEK293 cells, but unfortunately the transfection efficiency was low, and therefore the staining pattern with WNK1 appeared similar to the pattern observed with the vector only control.

In addition, to determine whether disrupting the interaction of WNK1 with VPS4a modulates the amount of other ion transporters and channels on the plasma membrane, other channels besides ROMK should be pursued. Surface biotinylation assays for the other proteins known to be regulated by WNK1

should be performed to determine whether the WNK1-VPS4a interaction regulates their surface expression.

Despite the remaining questions concerning the relationship between WNK1 and VPS4a, these studies show that WNK1 physically interacts with a critical component of the lysosomal degradation pathway. This is a significant finding in the WNK field because it has been speculated that WNK1 regulates trafficking to influence the activity of various cell surface proteins, and its interaction with VPS4a potentially links it to this process.

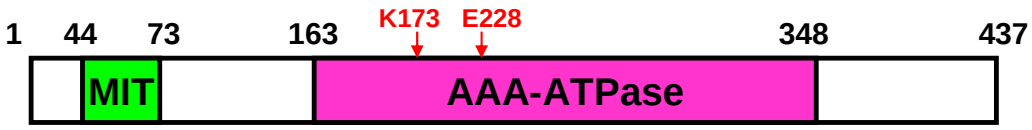

Fig. 1: Architecture of VPS4a. VPS4a contains a ~200 residue ATPase domain and an N-terminal MIT domain. Mutations in K173 or E228 render the protein non-functional. MIT: microtubule interacting trafficking; AAA: ATPases associated with diverse cellular activities.

Fig. 2: VPS4a and VPS4b share a high sequence similarity. Mouse VPS4a and VPS4b were aligned using the program BioEdit. They share 80% sequence identity.

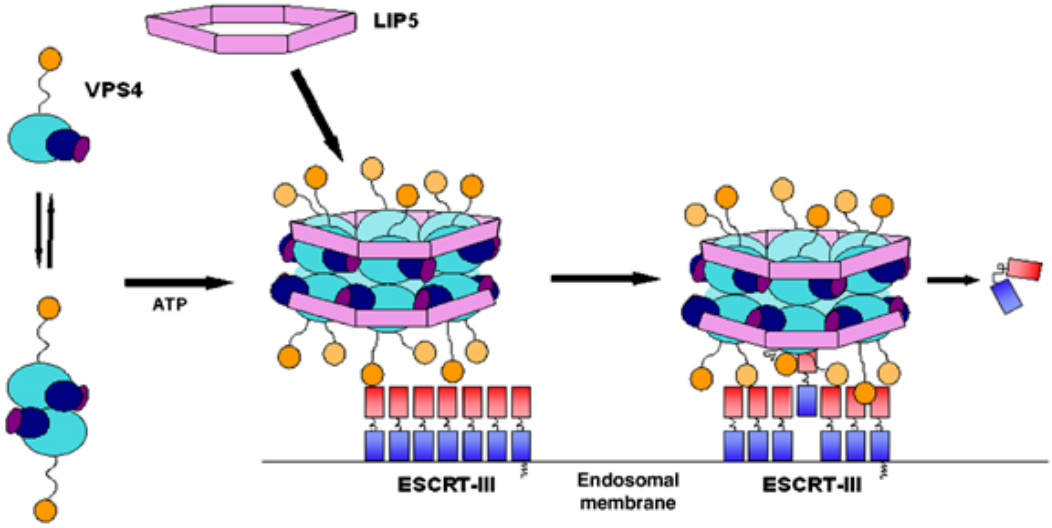

Fig. 3: Schematic of VPS4 binding to the ESCRT-III complex on the endosomal membrane. VPS4 is either a monomer or dimer in the cytoplasm but is a homo-oligomer at the endosomal membrane. The N-terminal portion of VPS4 (yellow), which contains the MIT domain, binds to some of the ESCRT-III complex members. It has been hypothesized that upon ATP hydrolysis the ESCRT-III proteins translocate through the VPS4 pore. LIP5 is a known VPS4 interacting protein. This schematic is from Scott *et al.* 2005a and is being used with permission.

1311

PLVISSAIASTPVLPQPAVPTSTPL
LPQVPNIPPLVQPVANVPAVQQTLI
HSQPQPALLPNQPHTHCPEMDADTQ
SKAPGIDDIKTLEEKLRSLFSEHSS
SGTQHASVSLETPLVVETVTPGIPT
TAVAPSKLMTSTTSTCLPPTNLPLG
TAGMPVMPVGTPGQVSTPGTHASAP
ASTATGAKPGTTPPKPSLTKTVVPP
VGTELSAGTVPCEQLPPFPGPSLIQ
TQQPLE[1542]

Fig 4: WNK1 1311-1542 contains 10 PxxP motifs. Amino acid sequence of the WNK1 bait used in the yeast-two-hybrid screen.

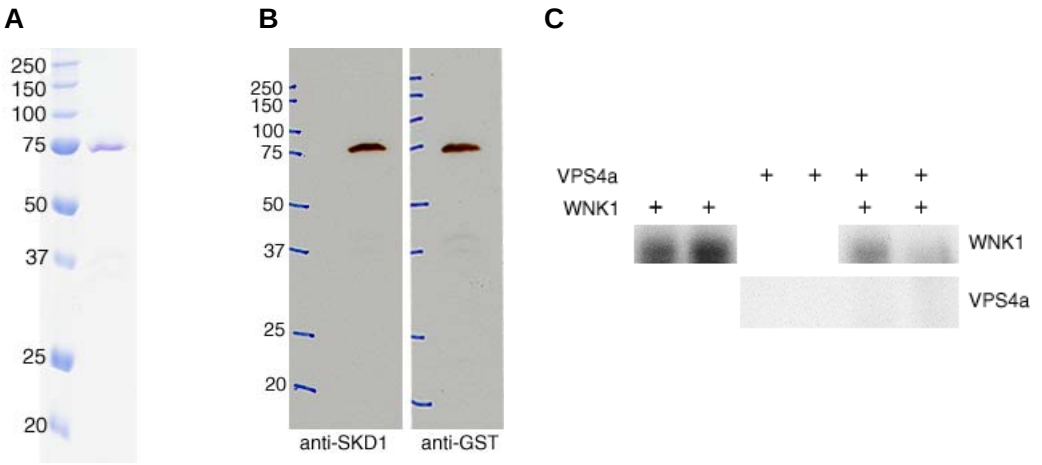

Fig. 5: WNK1 does not phosphorylate VPS4a. ***A,*** Coomaisse blue stained acrylamide gel of purified GST-VPS4a. ***B,*** Western blot of purified GST-VPS4a using an anti-SKD1 (VPS4b) antibody (left) and an anti-GST antibody (right). ***C,*** *In vitro* kinase assay of purified GST-WNK1 full-length with purified GST-VPS4a.

pVJL (bait)	pGADGH (prey)	Interaction
WNK1 1311-1542	VPS4a FL	+++++
WNK1 1311-1542	VPS4a K173Q	+++++
WNK1 1311-1542	VPS4a E228Q	+++++
WNK1 1311-1542	VPS4a K173Q,E228Q	+++++
WNK1 1311-1542	VPS4a 1-243	++
WNK1 1311-1542	VPS4a 241-437	-
WNK1 1311-1542	CHMP6	-
CHMP1b	VPS4a	+++++
CHMP6	VPS4a	+
OSR1	VPS4a	-
Lamin	VPS4a	-
TAO2	VPS4a	-
WNK1 1-222	VPS4a	-
WNK1 217-494	VPS4a	-
WNK1 220-940	VPS4a	-
WNK1 1541-1812	VPS4a	-
WNK1 1811-1910	VPS4a	-

Table 1: The proline-rich region of WNK1 binds to the N-terminal half of VPS4a. Pairwise yeast-two-hybrid results of WNK1 1311-1542 with VPS4a. CHMP6 and CHMP1b are other VPS proteins. The interactions were scored based on the ability of the yeast to grow on selection medium.

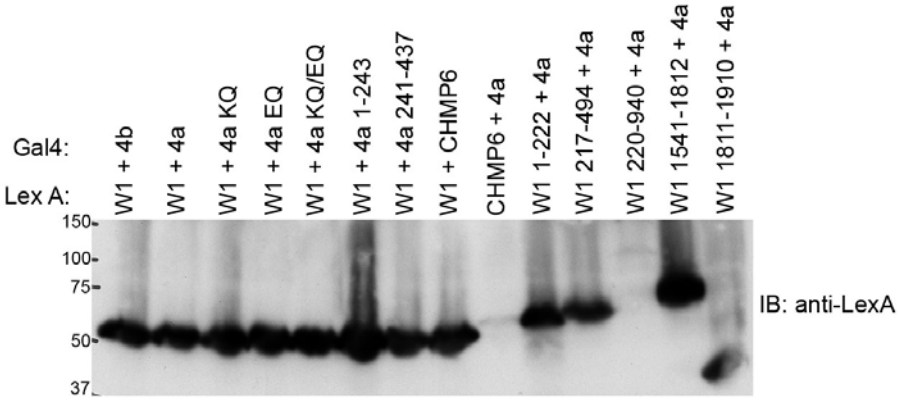

Fig 6: Expression of bait proteins in pairwise yeast-two-hybrid tests. Anti-LexA Western blot of some of the bait proteins listed in the above table. W1: WNK1; 4b: VPS4b; 4a: VPS4a.

Prey	WNK1 1311-1542	Lamin	TAO2 1-320 D169A
VPS4b FL	-	-	-
VPS4a FL	+++++	-	-
VPS4a FL K173Q	+++++	-	-
VPS4a FL E228Q	+++++	-	-
VPS4a FL KQ/EQ	+++++	-	-
VPS4a 1-417	++++	-	-
VPS4a 1-397	+	+	-
VPS4a 1-377	-	-	-
VPS4a 1-357	-	-	-
VPS4a 1-353	++	+	-
VPS4a 1-337	+	+	-
VPS4a 1-317	+	+	-
VPS4a 1-297	+	+	-
VPS4a 1-277	+	+	-
VPS4a 1-257	-	-	-
VPS4a 1-243	+	-	-
VPS4a 50-243	-	++	-
VPS4a 100-243	-	-	-
VPS4a 150-243	-	-	-
VPS4a 150-353	-	-	-
VPS4a 241-437	-	-	-
VPS4a 1-100	-	-	-
VPS4a 1-50	-	-	-
VPS4a 20-437	-	-	-
VPS4a 40-437	-	-	-
VPS4a 60-437	-	-	-
VPS4a 80-437	-	-	-
VPS4a 100-437	-	-	-
CHMP4b	-	-	-
CHMP6	-	-	-
LIP5	-	-	-

Table 2: Pairwise yeast-two-hybrid tests of VPS4a fragments with WNK1, lamin, and TAO2. This is an expansion of Table 1 and includes the negative controls lamin and TAO2 1-320 D169A. The interactions were scored based on the ability of the yeast to grow on selection medium. This assay was conducted once with the help of Colleen Vanderbilt, and many of the pairwise interactions were tested further in other experiments.

	CHMP1b	WNK1 1311-1542	CHMP6
VPS4a FL	++++	++++	+
VPS4a L64A	-	-	+
VPS4a 1-243	++++	+	-
VPS4a 1-160	++++	½ +	-
VPS4a 1-100	++	-	-
VPS4a 241-437	-	-	-

Table 3: CHMP6 but not WNK1 or CHMP1b interact with VPS4a L64A. Pairwise yeast-two-hybrid interactions that were scored based on the ability of the yeast to grow on selection medium.

Bait (pVJL)	Prey (pGADGH)	Interaction
WNK1 1340-1399	VPS4a	-
WNK1 1340-1399	VPS4b	-
WNK1 1400-1542	VPS4a	-
WNK1 1400-1542	VPS4b	-
WNK4 776-1020	VPS4a	AA
WNK4 776-1020	VPS4b	AA
CHMP4b	VPS4a	unsure
CHMP4b	VPS4b	-
CHMP6	VPS4a	+
CHMP6	VPS4b	-
LIP5	VPS4a	AA
LIP5	VPS4b	AA

Table 4: Additional pairwise interactions tested by yeast-two-hybrid. WNK4 776-1020 and LIP5 were both autoactivators and therefore no conclusions could be drawn about the interactions with these proteins. VPS4b did not bind to any of the tested proteins. CHMP4b and VPS4a displayed a small amount of growth on triple dropout medium but I am not confident if this indicates a protein-protein interaction. AA: autoactivator.

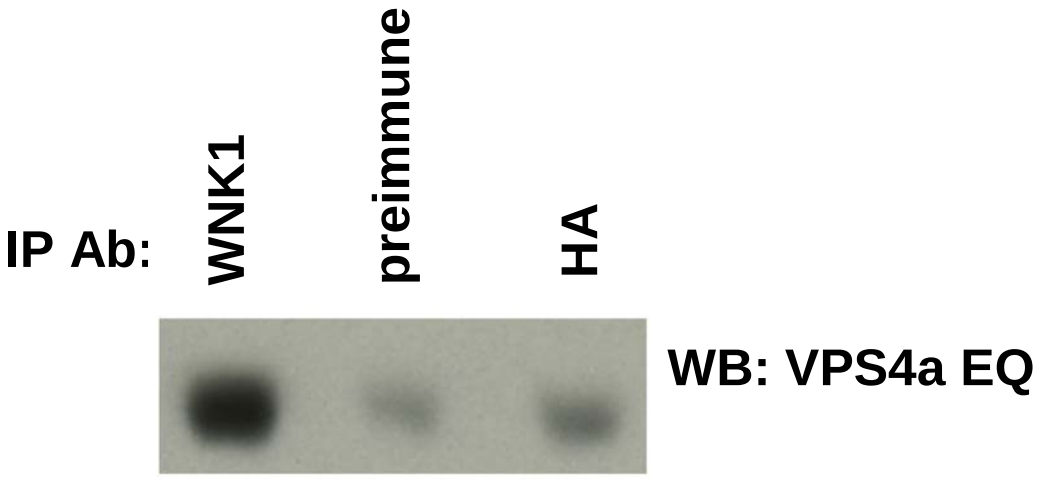

Fig 7: Endogenous WNK1 and over-expressed VPS4a E228Q interact. Western blot of Myc-tagged VPS4a E228Q from HEK293 cells that was co-immunoprecipitated with WNK1 using the WNK1-specific antibody Q256 WNK1 preimmune serum and an anti-HA antibody were used as negative controls.

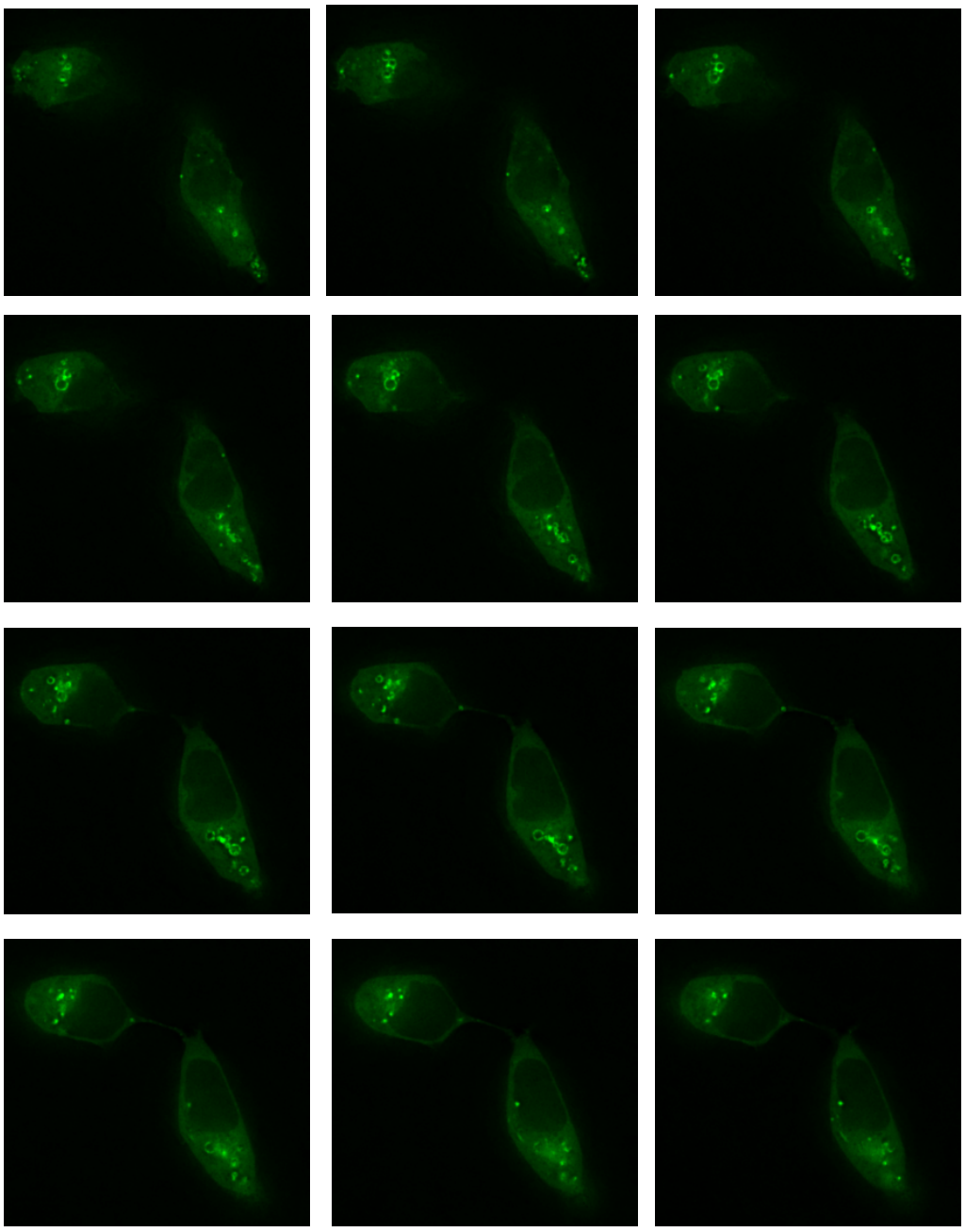

Fig. 8: GFP-tagged VPS4a E228Q localizes at ring-like structures. GFP-VPS4a E228Q was over-expressed in HEK293 and live cells were analyzed with the Zeiss Deltavision microscope. From the top left to the bottom right are z-stacks starting from the bottom portion of the cells. These images were deconvolved.

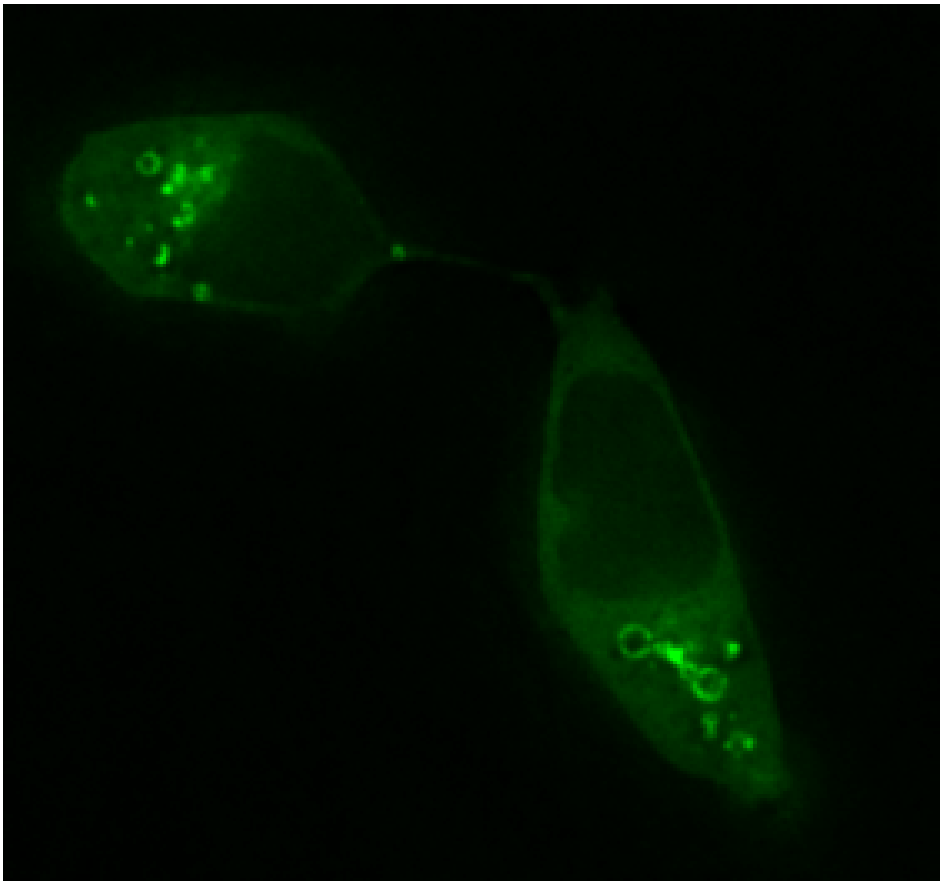

Fig. 9: Larger image of one GFP-VPS4a E228Q stack shown in Figure 8.

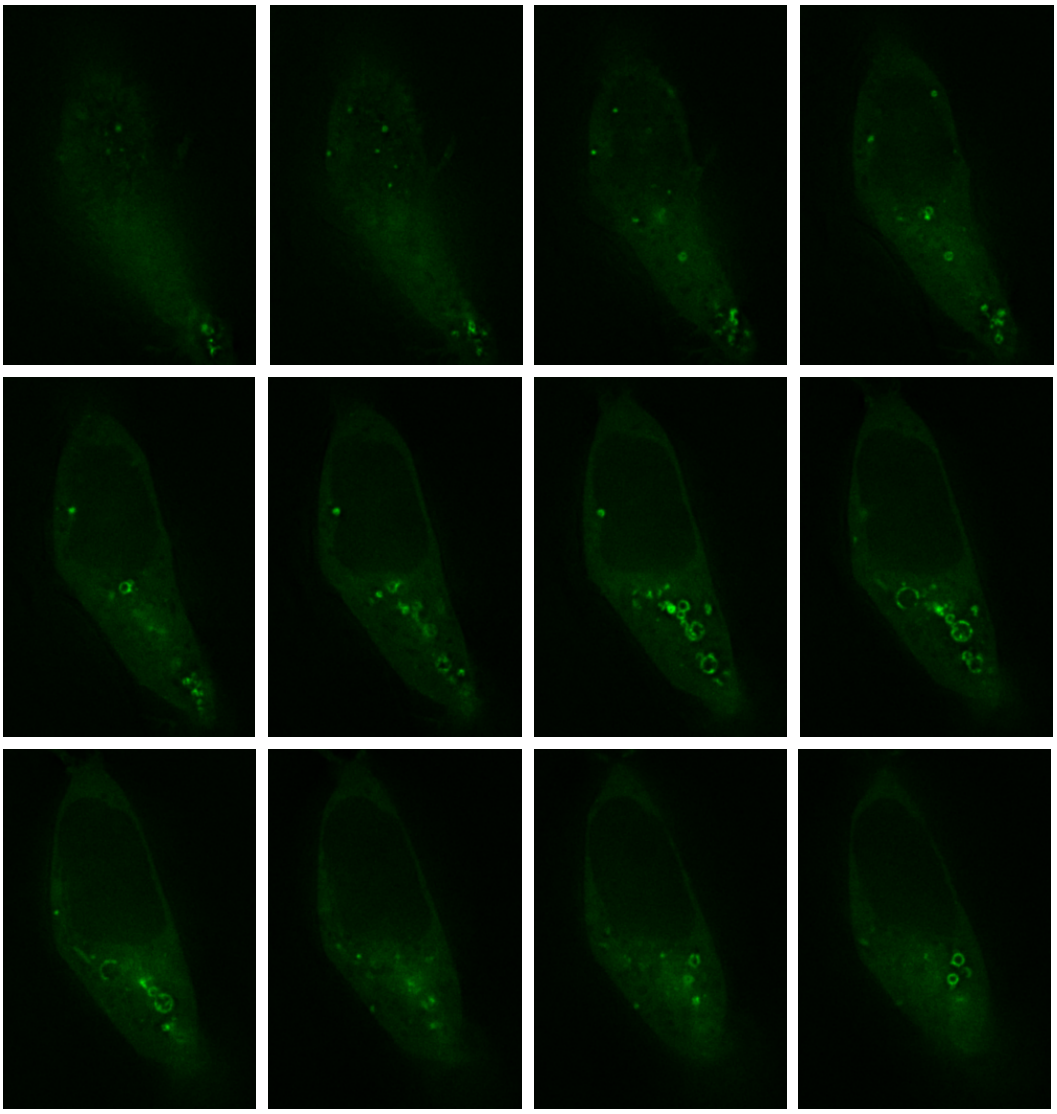

Fig. 10: Localization of GFP-tagged VPS4a E228Q. GFP-VPS4a E228Q was over-expressed in HEK293 and live cells were analyzed with a Zeiss Deltavision microscope. From the top left to the bottom right are z-stacks starting from the bottom portion of the cell. These images were deconvolved.

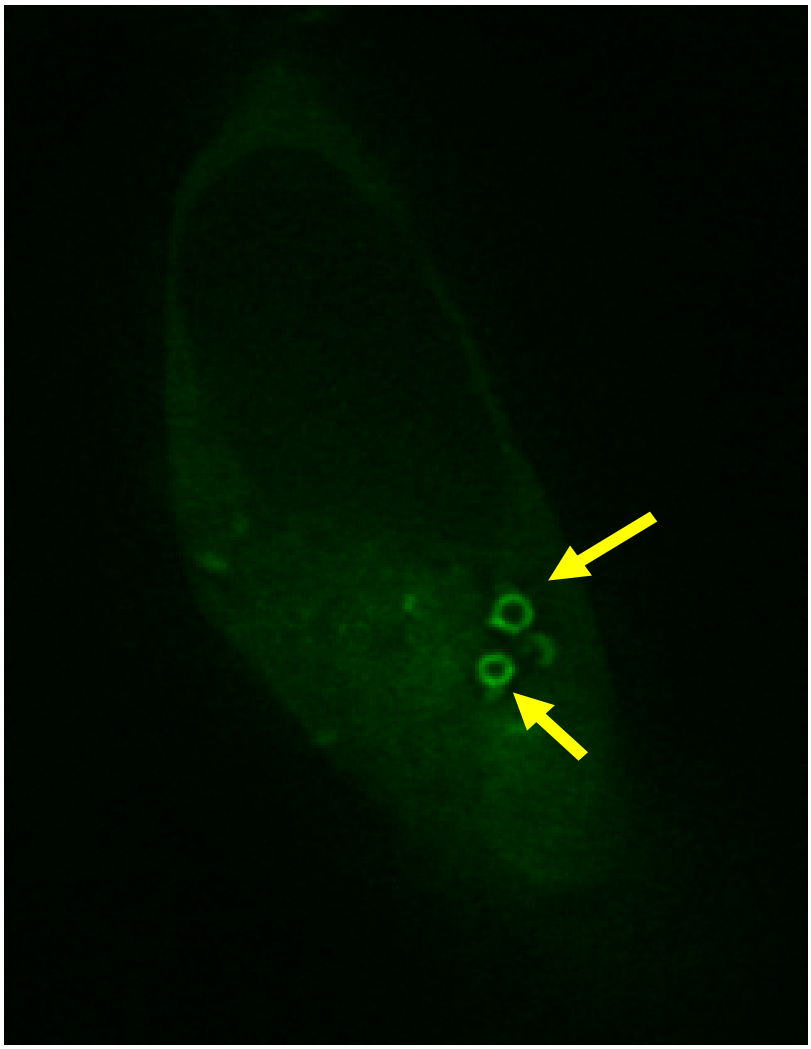

Fig. 11: Larger image of one stack shown in Figure 10. GFP-tagged VPS4a E228Q often localizes on large circular structures.

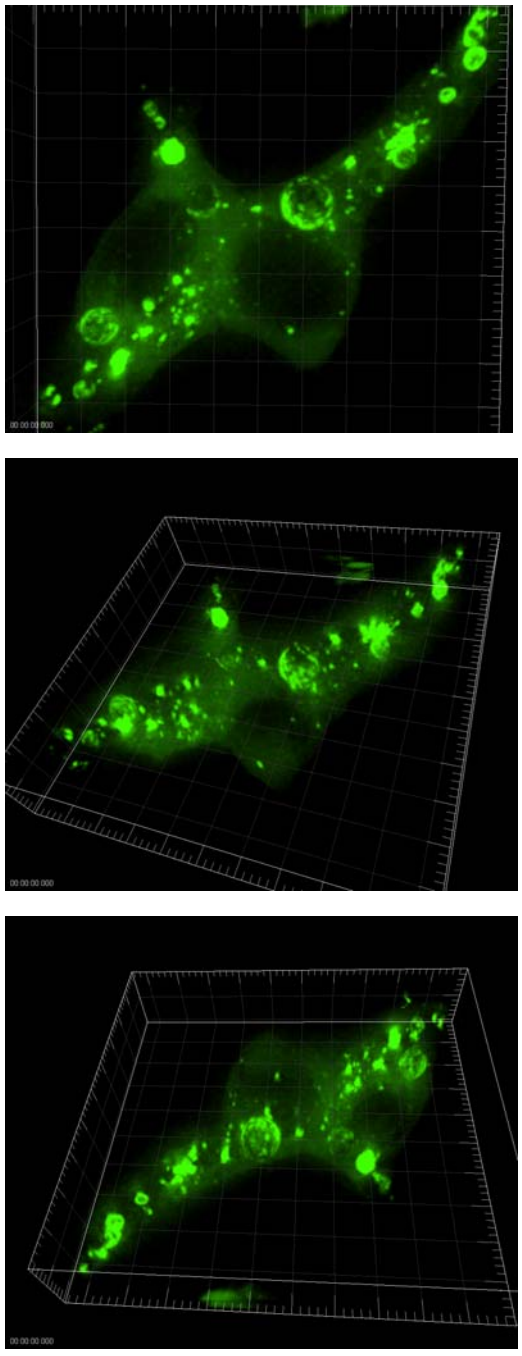

Fig. 12: Three-dimensional model of GFP-VPS4a E228Q in a HEK293 cell. Different angles of the same cell are shown. These models were constructed by Abhijit Bugde.

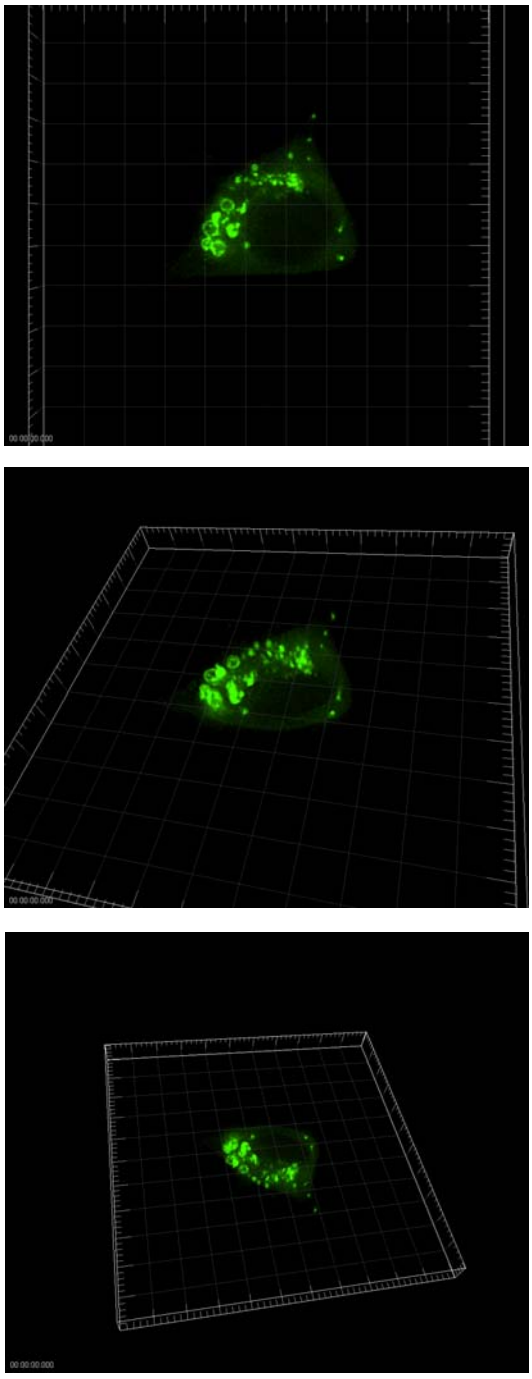

Fig. 13: Three-dimensional model of GFP-VPS4a E228Q in a HEK293 cell. Different angles of the same cell are shown. These models were constructed by Abhijit Bugde.

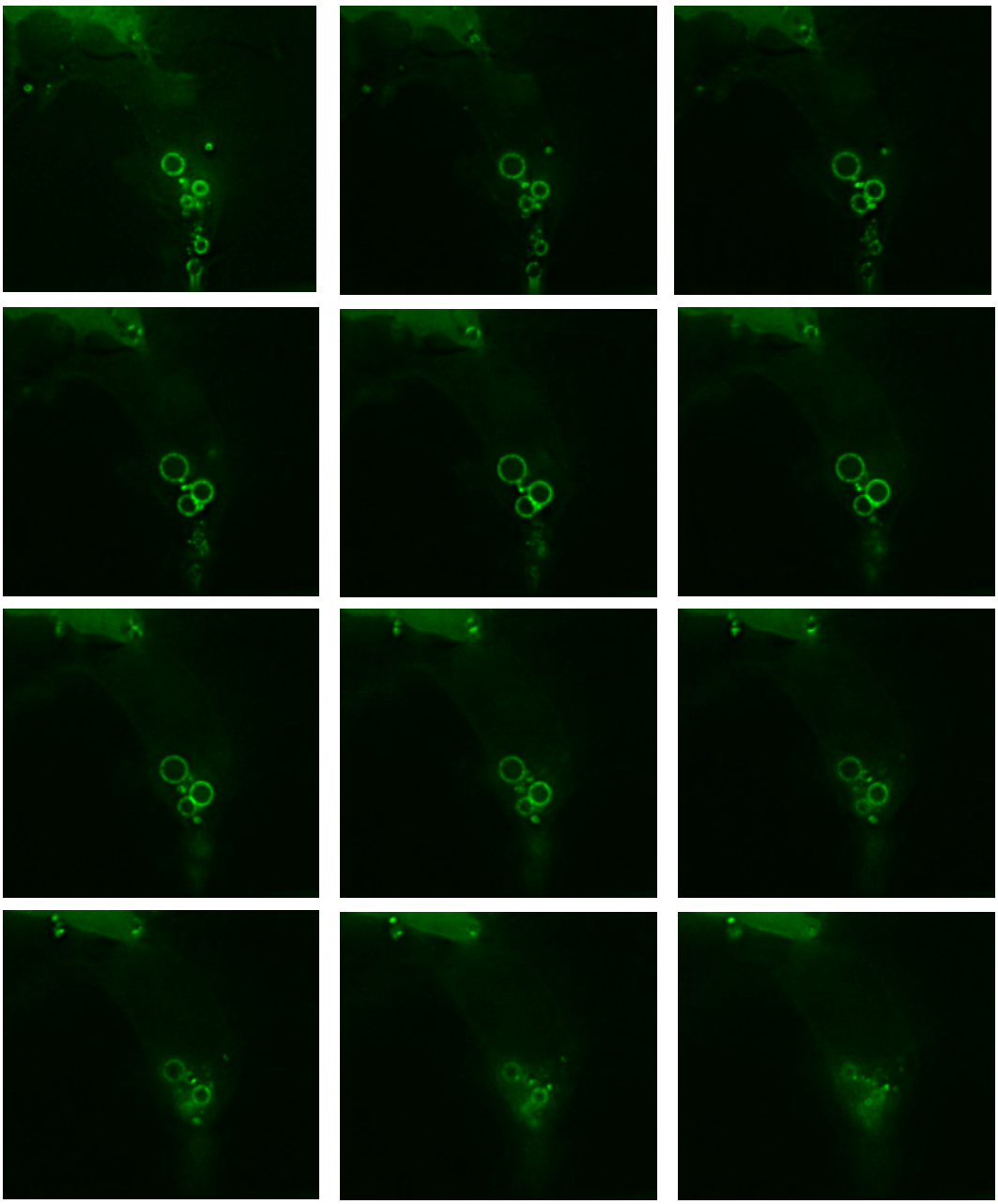

Fig. 14: Localization of HA-tagged VPS4a E228Q. HEK293 cells were transfected with HA-VPS4a E228Q, fixed, stained with anti-HA antibody, analyzed with a Zeiss Deltavision microscope, and deconvolved. From the top left to the bottom right are z-stacks starting from the bottom portion of the cell.

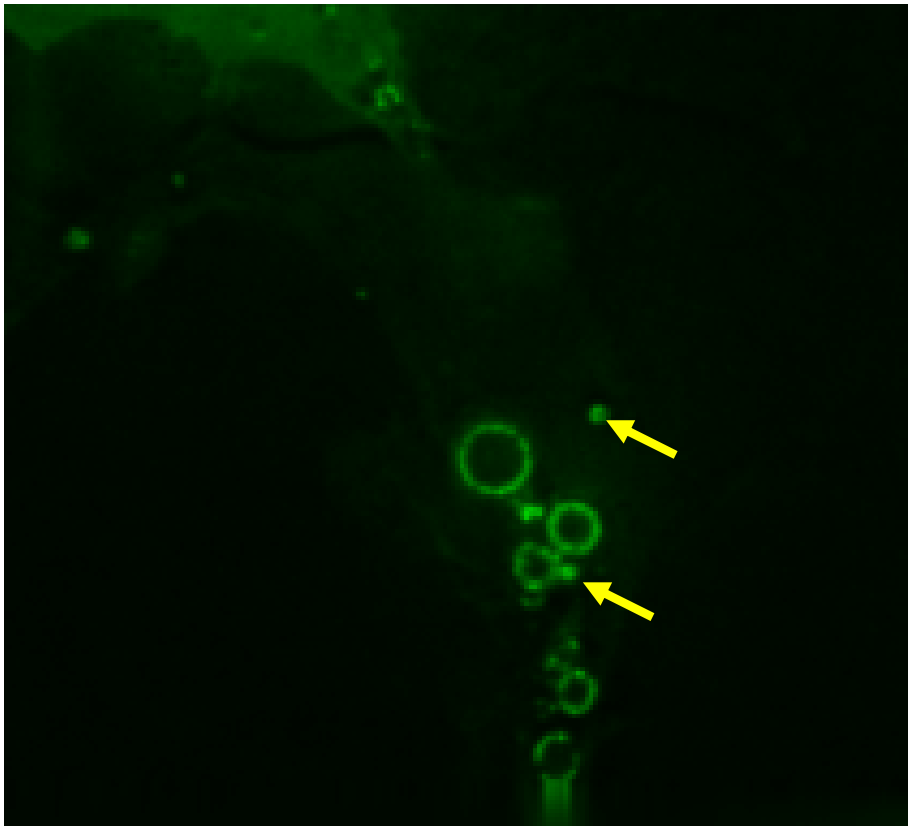

Fig. 15: Larger image of one stack shown in Figure 14. The majority of VPS4a E228Q is located on the outside of large ring-like structures while some of it appears to fill a small structure (see arrows).

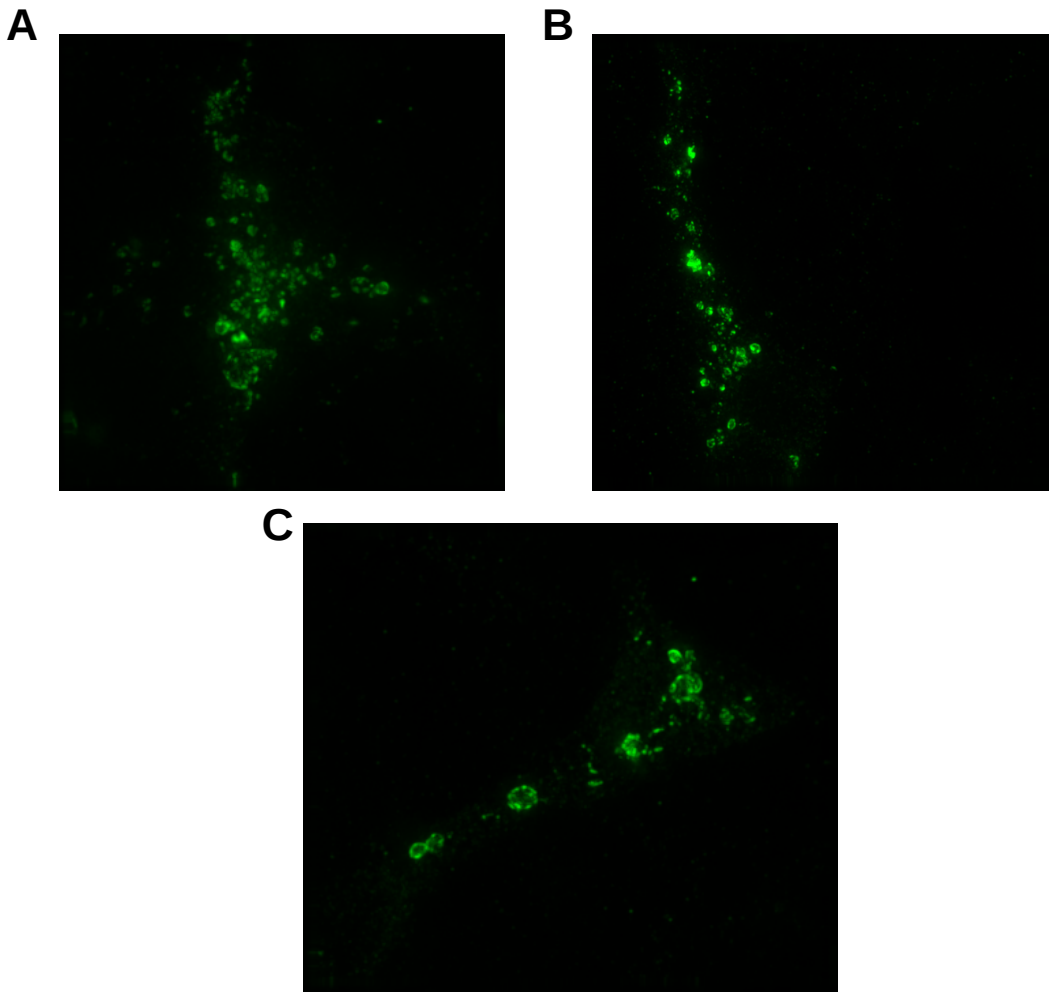

Fig. 16: Compressed z-stacks of HA-VPS4a E228Q. HEK293 cells were transfected with HA-VPS4a E228Q, fixed, stained with anti-HA antibody, analyzed with a Zeiss Deltavision microscope, and the images were deconvolved. The pictures shown above were created by projecting the z-stacks into one image.

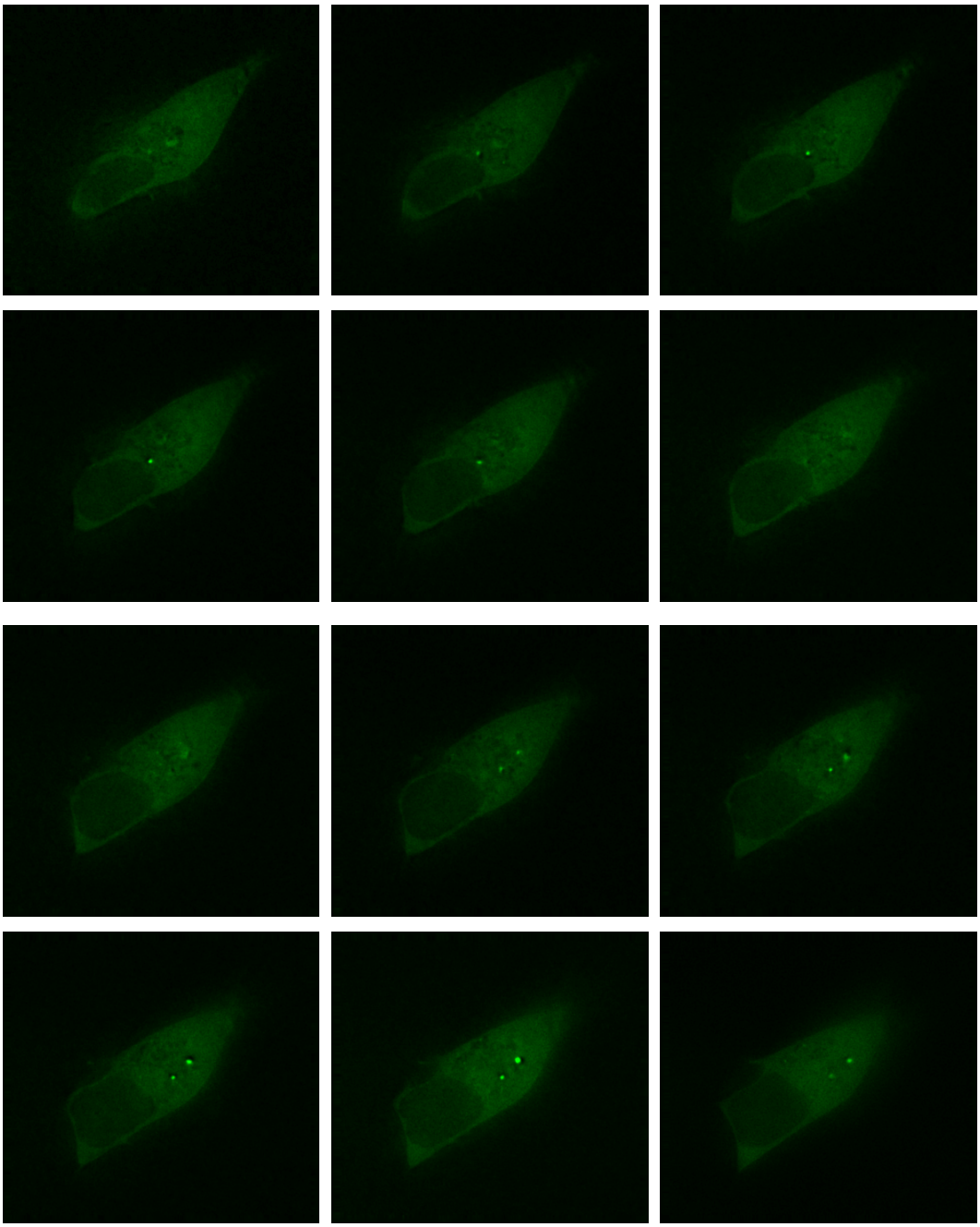

Fig. 17: GFP-tagged wild-type VPS4a is diffusely cytoplasmic. GFP-VPS4a wild-type was over-expressed in HEK293, live cells were analyzed with the Zeiss Deltavision microscope, and the images were deconvolved. From the top left to the bottom right are z-stacks starting from the bottom portion of the cell.

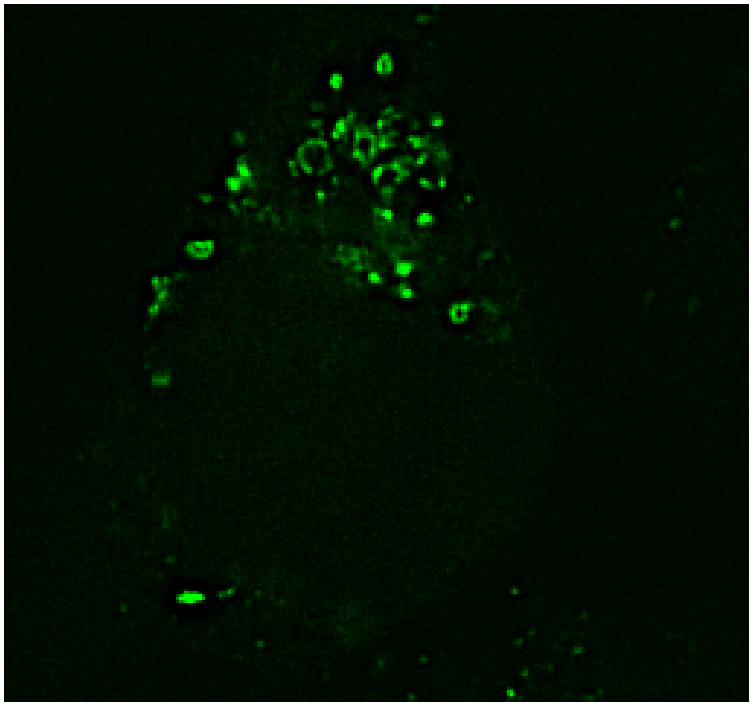

Fig. 18: VPS4a E228Q localization in HeLa. HeLa cells were transfected with GFP-tagged VPS4a E228Q, fixed and analyzed with a Zeiss Deltavision microscope. A single z-stack of one cell is shown.

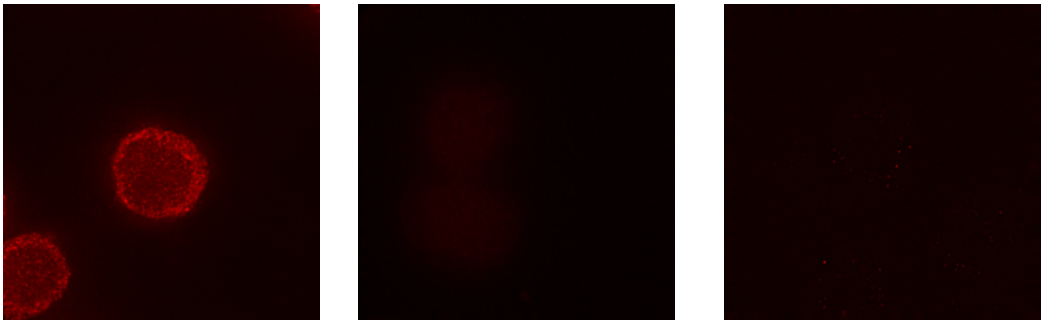

Fig. 19: Endogenous WNK1 in HT-29 cells displays a punctate pattern. HT-29 cells were stained with either the anti-WNK1 antibody Q256, Q256 that had been pre-incubated with the peptide used to generate the antibody, or secondary antibody only. The brightness and contrast of the three images were adjusted to the same levels using Image j.

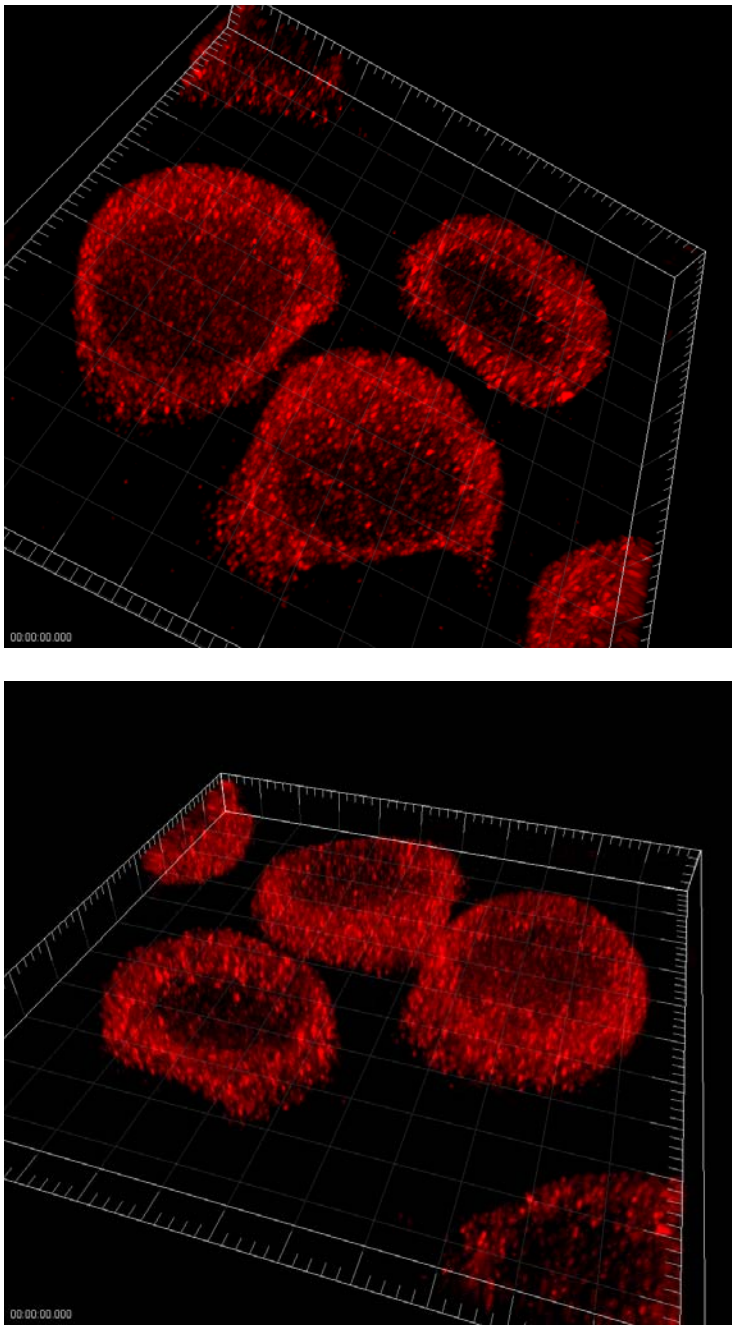

Fig. 20: Three-dimensional models of endogenous WNK1 in HT-29 cells. Different angles of the same cells stained with Q256 are shown. These models were constructed by Abhijit Bugde.

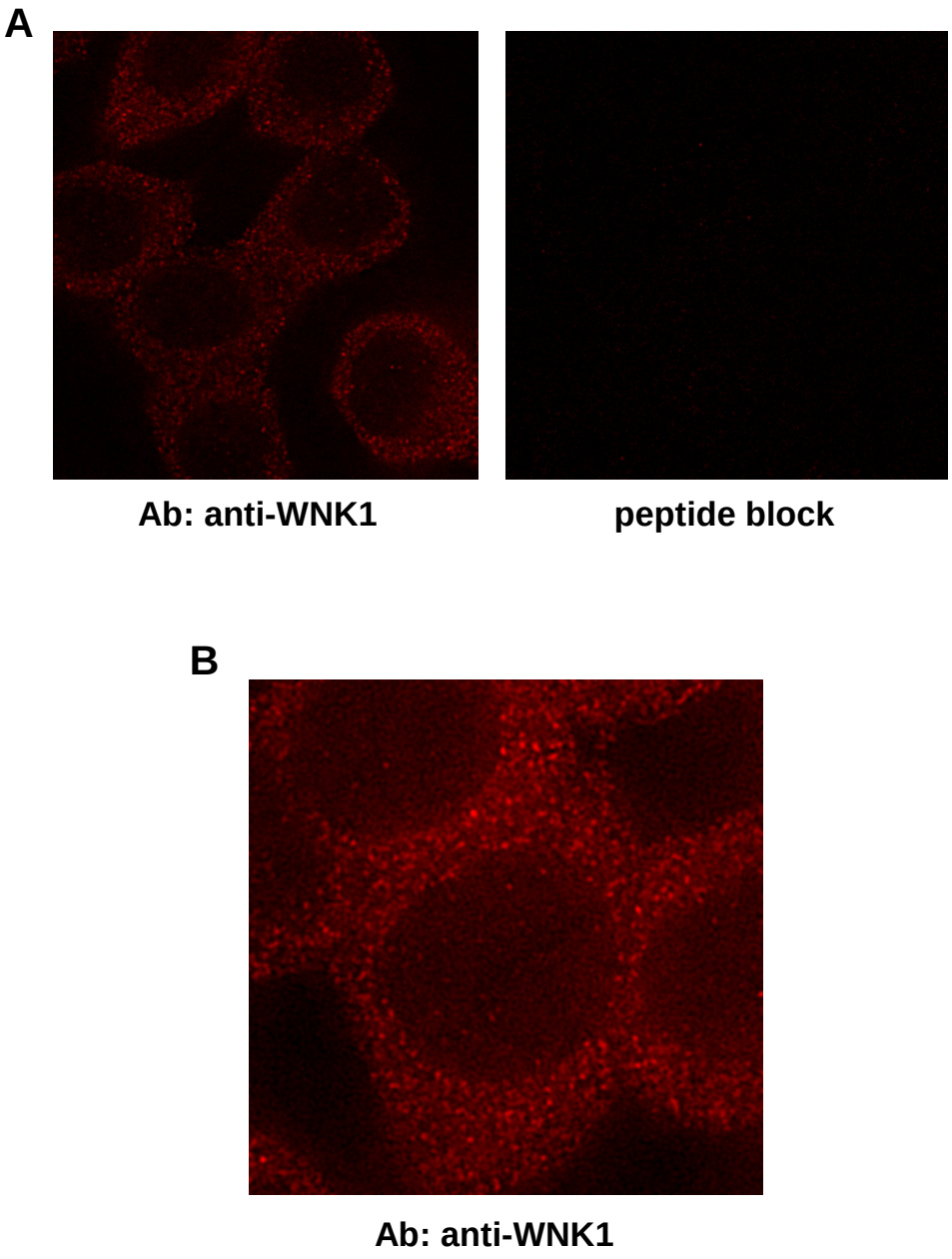

Fig. 21: Endogenous WNK1 in HT-29 cells displays a punctate pattern. HT-29 cells were stained with either the anti-WNK1 from Cell Signaling (left) or anti-WNK1 that had been pre-incubated with the peptide used to generate the antibody (right) and analyzed with a Zeiss Deltavision microscope. ***A,*** 60 X objective. ***B,*** 1000X objective.

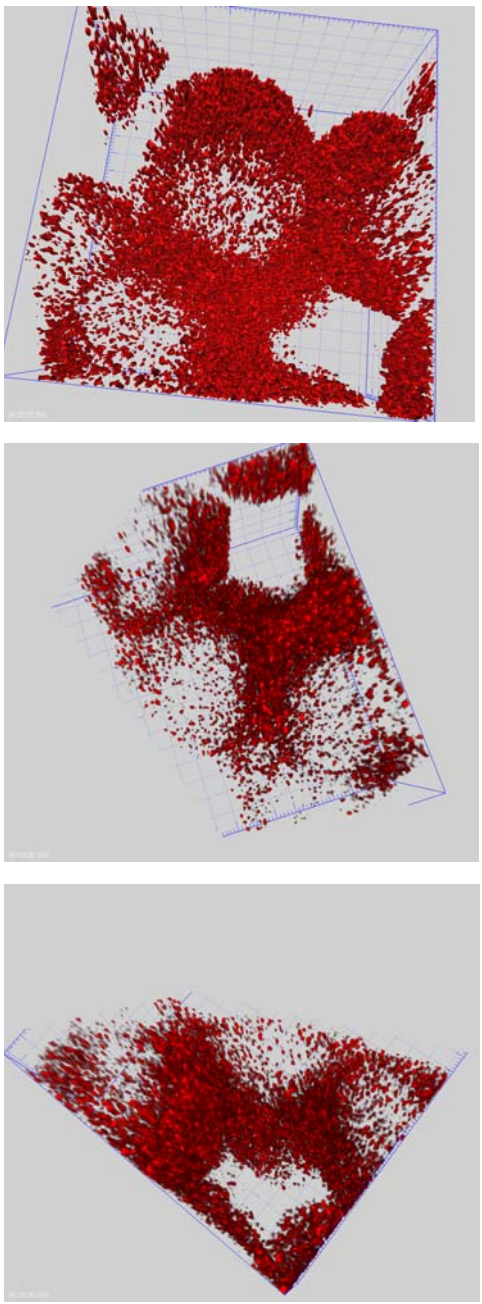

Fig. 22: Three-dimensional models of endogenous WNK1 in HT-29 cells. The cells used to construct these models were stained with the WNK1 antibody from Cell Signaling. These images show that WNK1 is excluded from the nucleus and exhibits a punctate pattern in the cytoplasm. These models were constructed by Abhijit Bugde from the data shown in Figure 21.

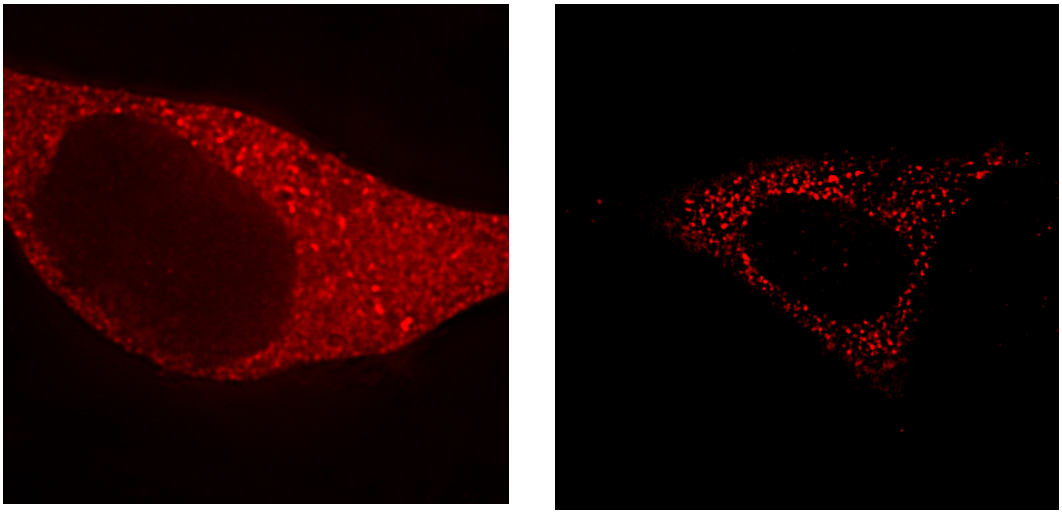

Fig. 23: Over-expressed WNK1 in HeLa cells displays a punctate pattern. HeLa cells were transfected with Myc-tagged WNK1, fixed, stained with an anti-Myc antibody, and analyzed with a Deltavision microscope. These images were deconvolved and processed with Image j by Szu-wei Tu.

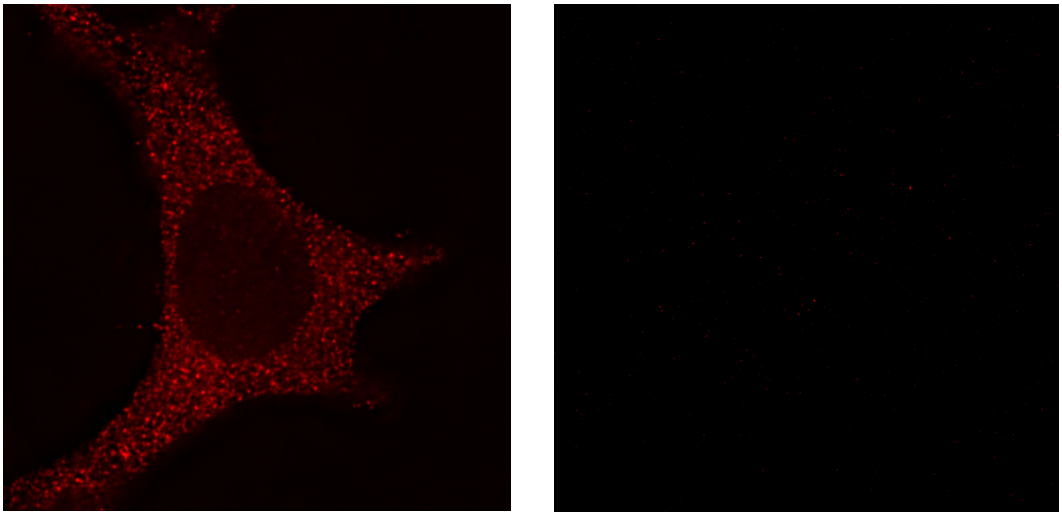

Fig. 24: Endogenous WNK1 in HeLa cells displays a punctate pattern. HeLa cells were stained with either anti-WNK1 from Cell Signaling or anti-WNK1 that had been pre-incubated with the peptide used to generate the antibody. The brightness and contrast of the two images were adjusted to the same levels.

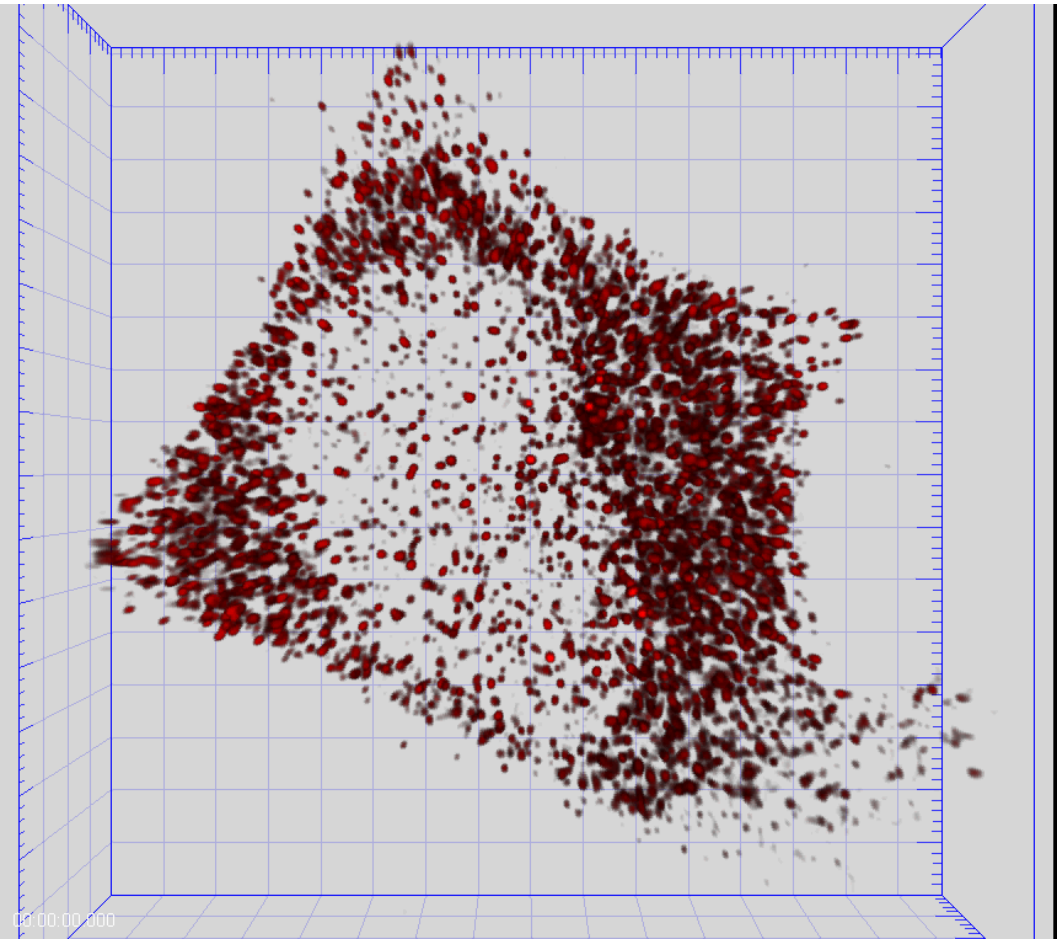

Fig. 25: Three-dimensional model of endogenous WNK1 in a HeLa cell. HeLa cells were fixed, stained with the anti-WNK1 antibody from Cell Signaling, analyzed with a Zeiss Deltavision microscope, and deconvolved. The Imaris® program was used to construct a three-dimensional model from the z-stack data. This model was generated by Abhijit Bugde.

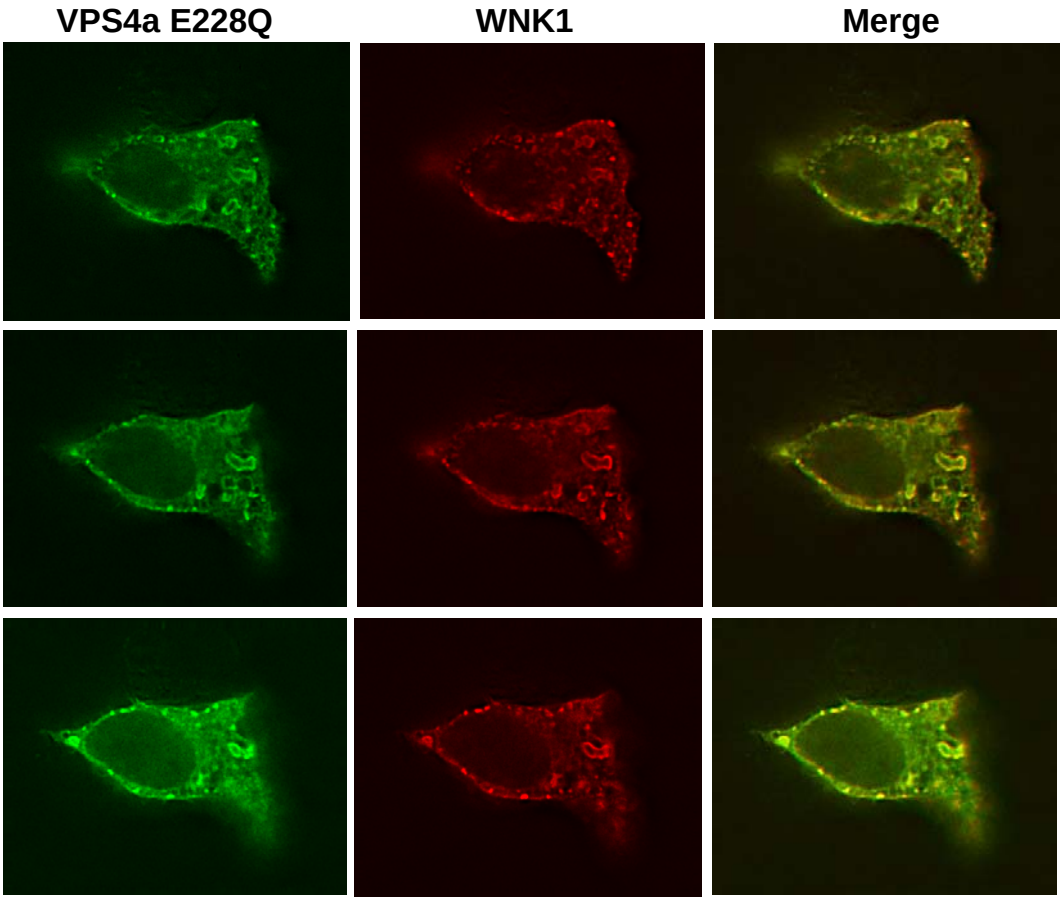

Fig. 26: Over-expressed WNK1 and VPS4a E228Q in HEK293 cells are found on large circular structures. HEK293 cells were co-transfected with Myc-WNK1 full-length and HA-VPS4a E228Q, fixed, stained with antibodies against Myc and HA, and analyzed with a Zeiss Deltavision microscope. Three representative deconvolved z-stacks are shown.

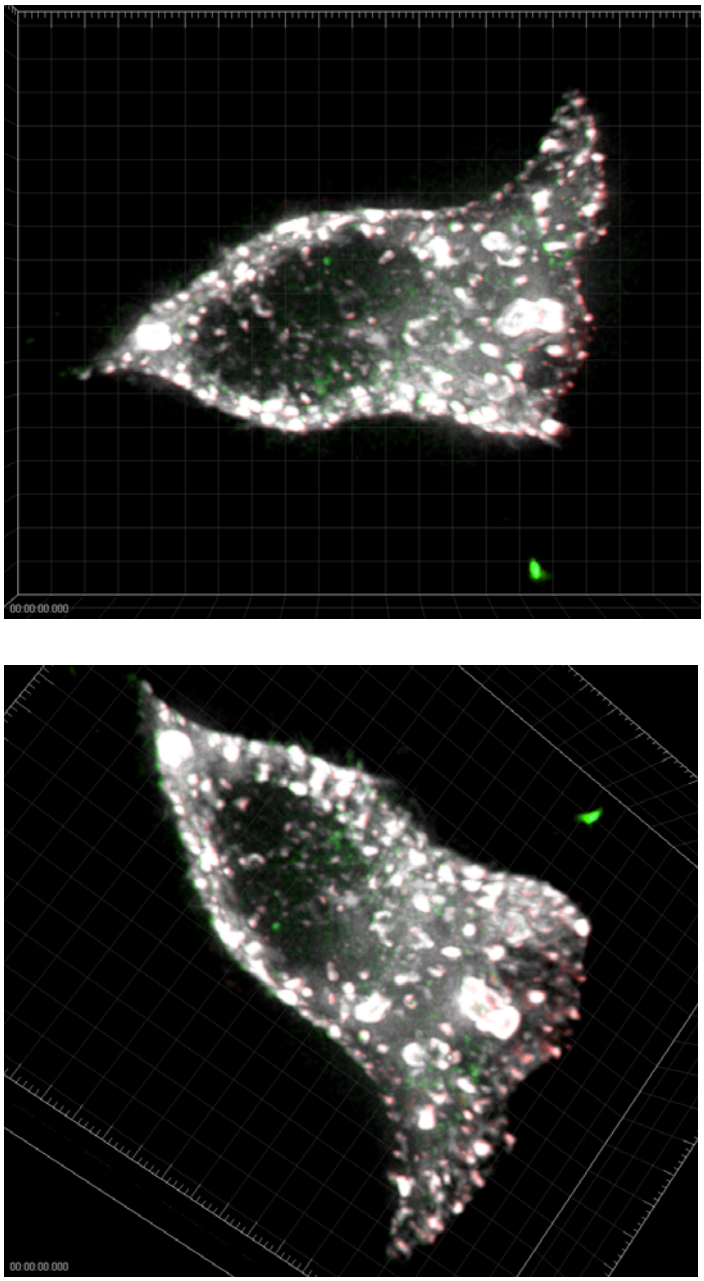

Fig. 27: Three-dimensional models of co-localized WNK1 and VPS4a E228Q in a HEK293 cell. The z-stacks from Figure 28 were analyzed and modeled by Abhijit Bugde using the Imaris® program. VPS4a E228Q is green, WNK1 is red, and the co-localized areas are white.

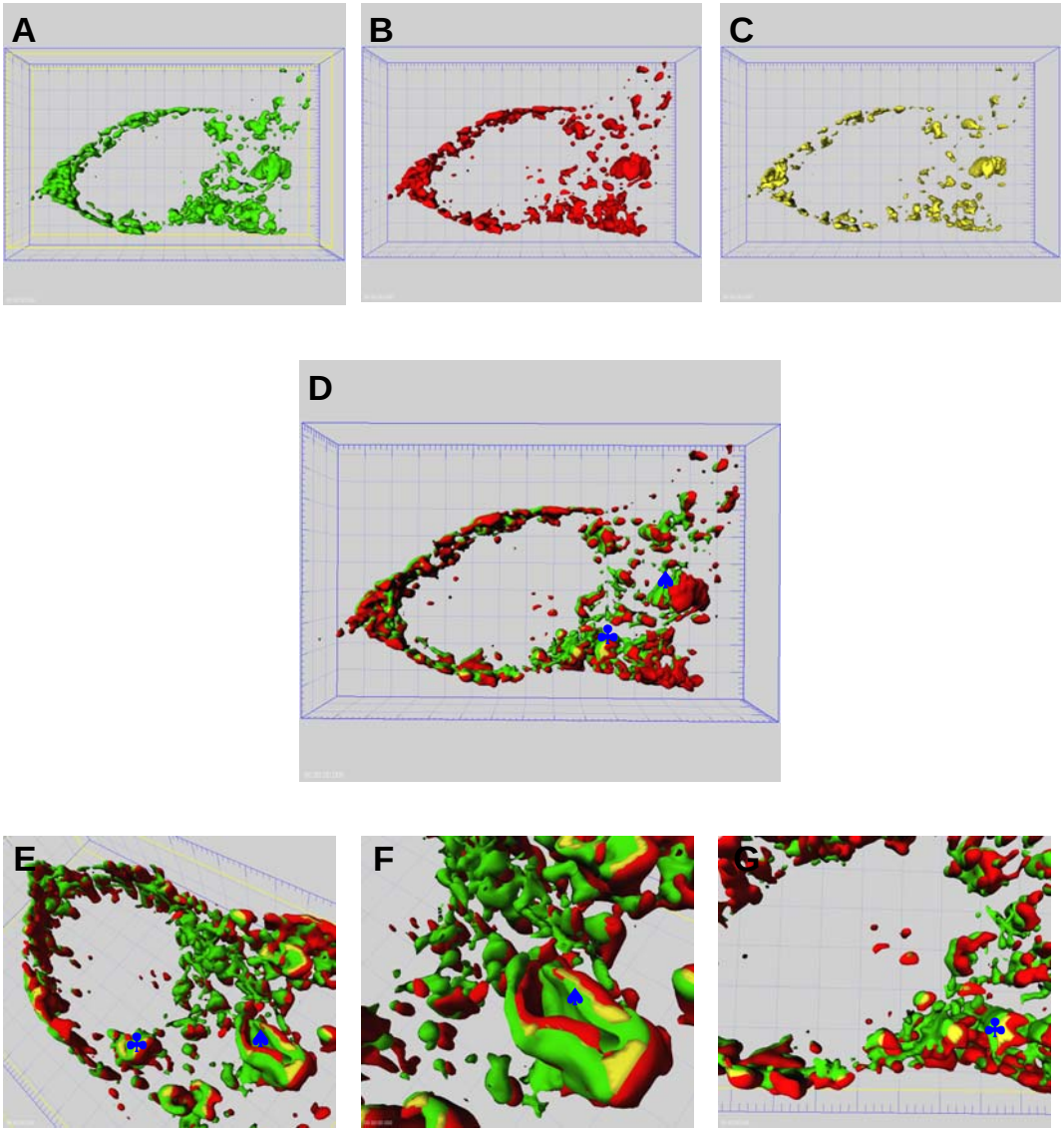

Fig. 28: Enlarged three-dimensional models of the WNK1/VPS4a E228Q co-localization data shown in Figure 28. These images show that WNK1 and VPS4a E228Q intercalate in HEK293 cells. ***A,*** Localization of VPS4a E228Q. ***B,*** Localization of WNK1. ***C,*** Areas where WNK1 and VPS4a E228Q co-localize. ***D,*** Panels A-C merged together. ***E-F,*** Panel D enlarged to show the WNK1/VPS4a E228Q co-localized structures in more detail. These models were created by Abhijit Bugde.

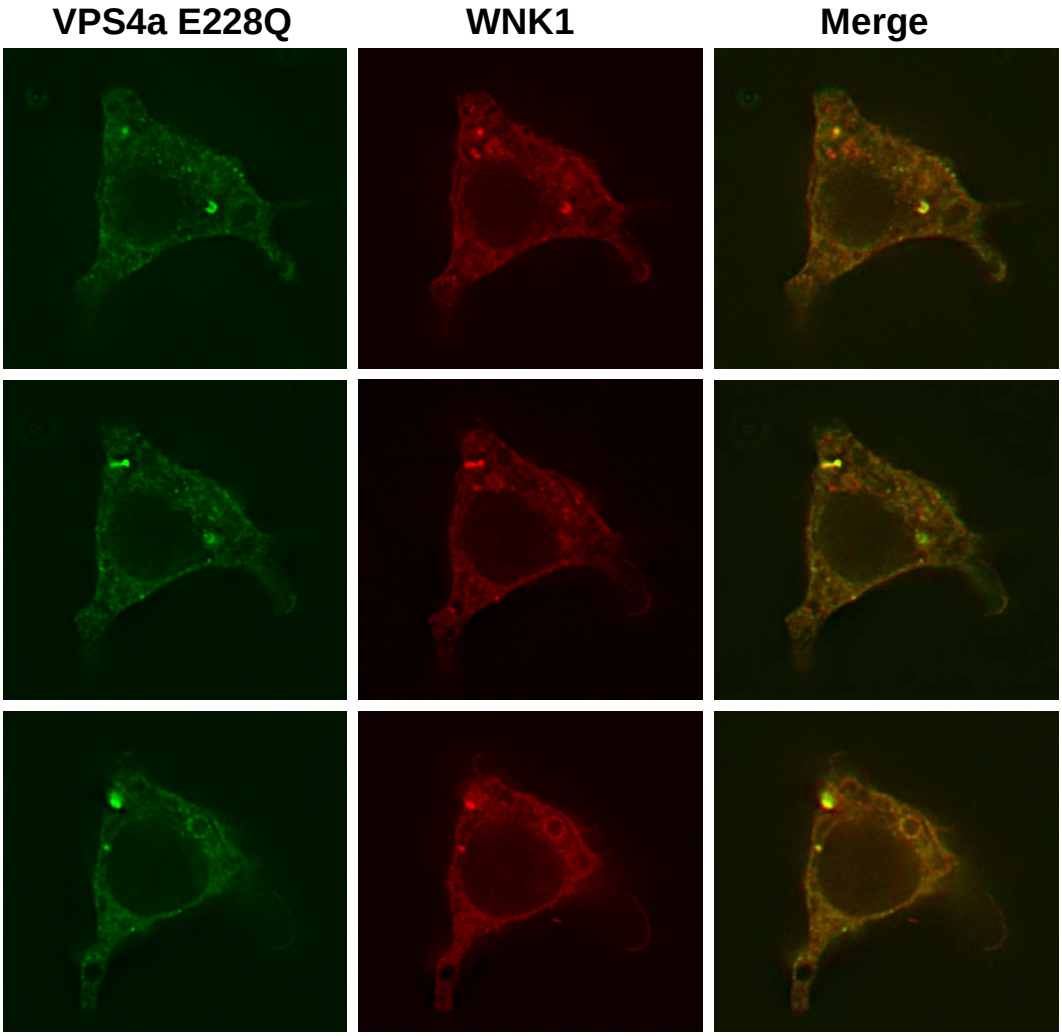

Fig. 29: Over-expressed WNK1 and VPS4a E228Q are found on large circular structures. HEK293 cells were co-transfected with Myc-WNK1 full-length and HA-VPS4a E228Q, fixed, stained with antibodies against Myc and HA, and analyzed with a Zeiss Deltavision microscope. Three representative deconvolved z-stacks are shown.

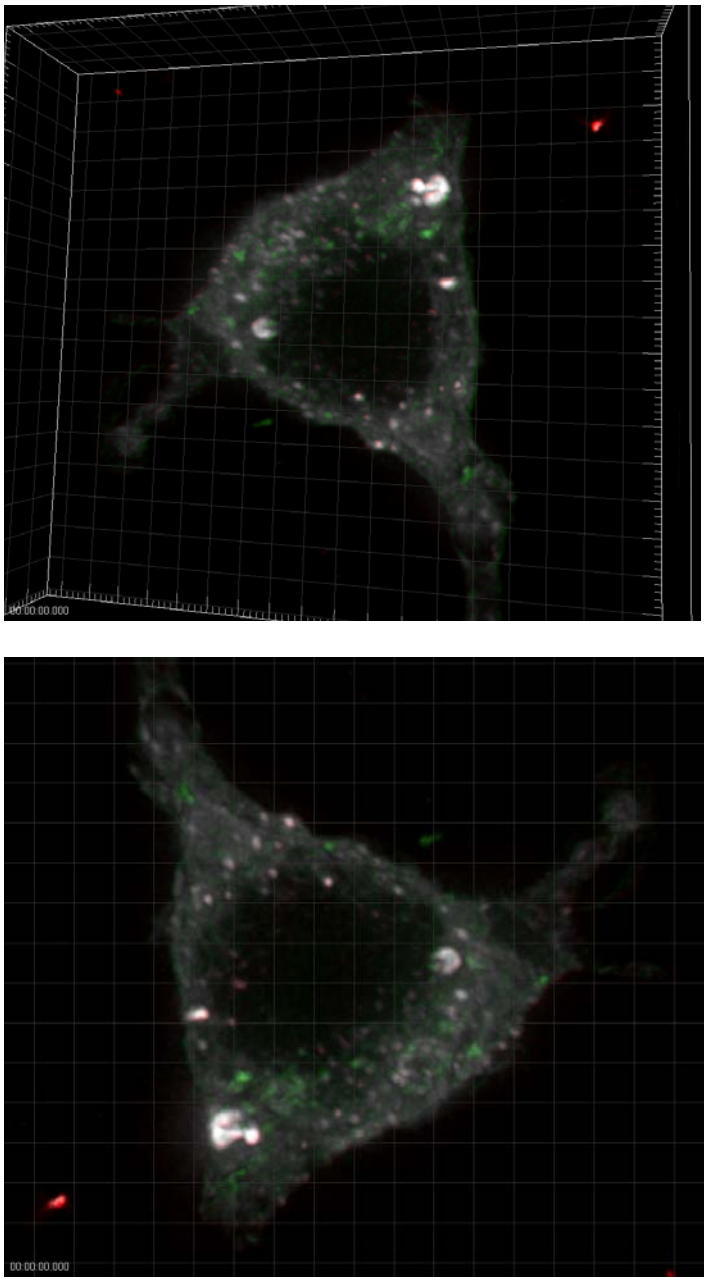

Fig. 30: Three-dimensional models of co-localized WNK1 and VPS4a E228Q in a HEK293 cell. The z-stacks from Figure 31 were analyzed and modeled by Abhijit Budge using the Imaris® program. VPS4a E228Q is green, WNK1 is red, and the co-localized areas are white.

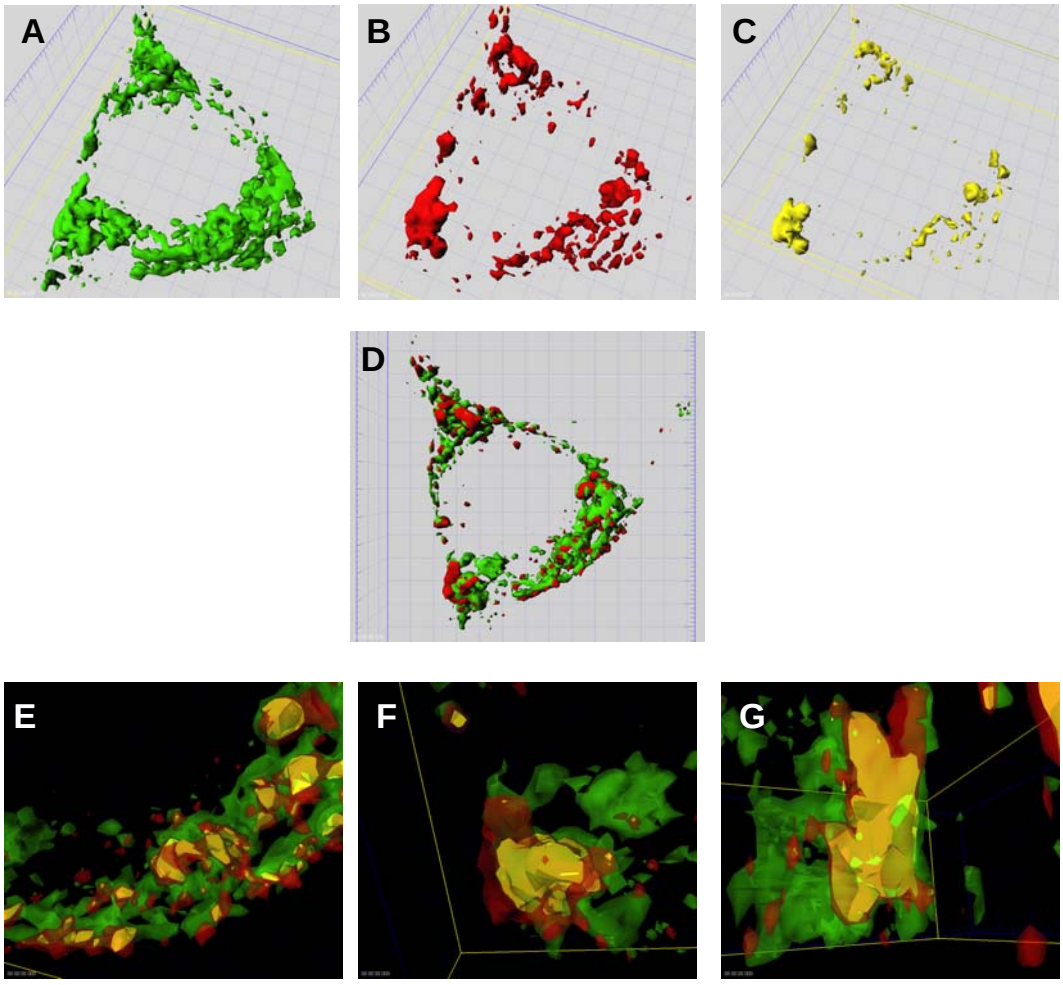

Fig. 31: Enlarged three-dimensional models of the WNK1/VPS4a E228Q co-localization data shown in Figure 31. These images show that WNK1 and VPS4a E228Q intercalate in HEK293 cells. ***A,*** Localization of VPS4a E228Q. ***B,*** Localization of WNK1. ***C,*** Areas where WNK1 and VPS4a E228Q co-localize. ***D,*** Panels A-C merged together. ***E-F,*** Panel D enlarged to show the WNK1/VPS4a E228Q co-localized structures in more detail. These models were created by Abhijit Bugde.

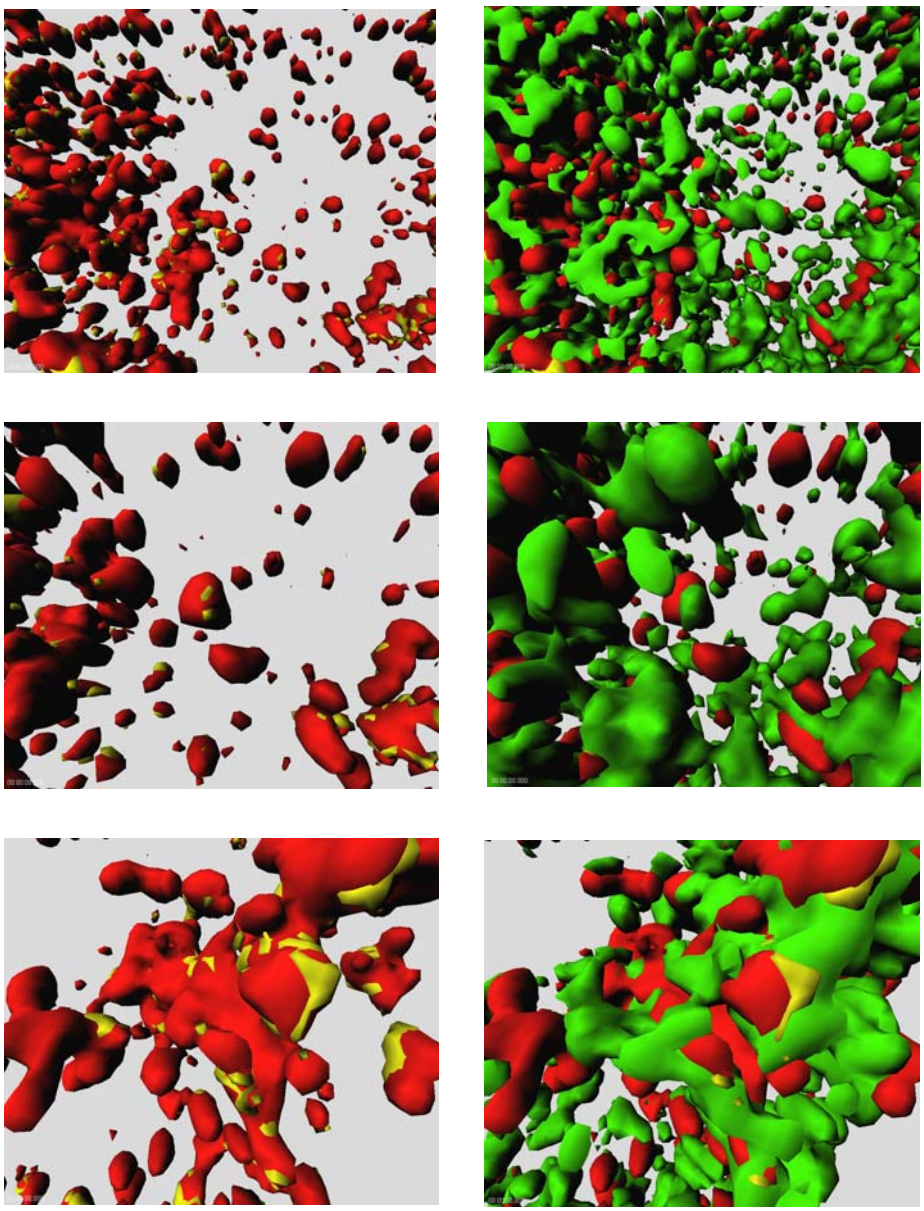

Fig. 32: Detailed three-dimensional models of WNK1 and VPS4a E228Q localization in HeLa cells. Full-length WNK1 and VPS4a E228Q were expressed in HeLa cells, the cells were fixed and stained, and z-stack images were taken with a Zeiss Deltavision microscope. A three-dimensional model was then constructed from the z-stack data using the Imaris® program. Red is WNK1, green is VPS4a E228Q, and yellow is where both proteins are present. The images on the left correspond to the images on the right. These data were generated with the help of Szu-wei Tu and Kate Luby-Phelps.

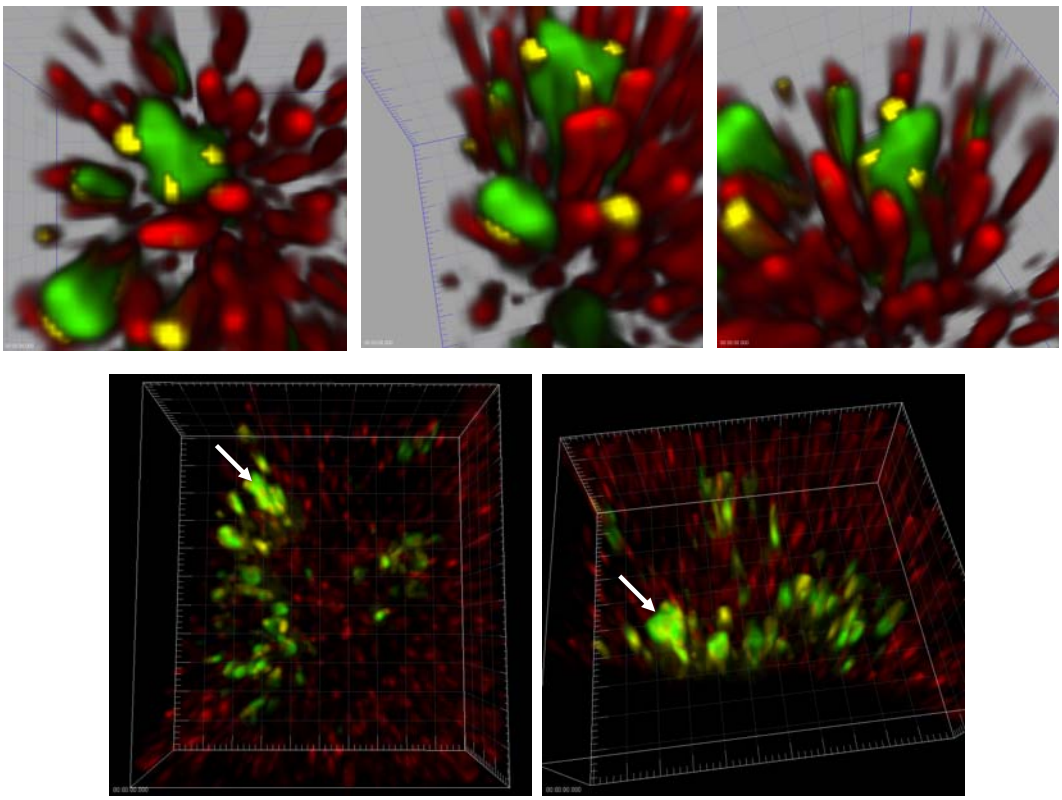

Fig. 33: Three-dimensional models of GFP-VPS4a E228Q and endogenous WNK1 co-localization in HeLa cells. VPS4a E228Q is green, WNK1 is red, and areas where both proteins are localized are yellow. Two VPS4a E228Q-positive structures are illustrated in the top images, where WNK1 resides on the outer surface of these compartments. The largest of the VPS4a-E228Q positive structure depicted in the top models is marked by arrows in the lower images. These data are representative of one experiment.

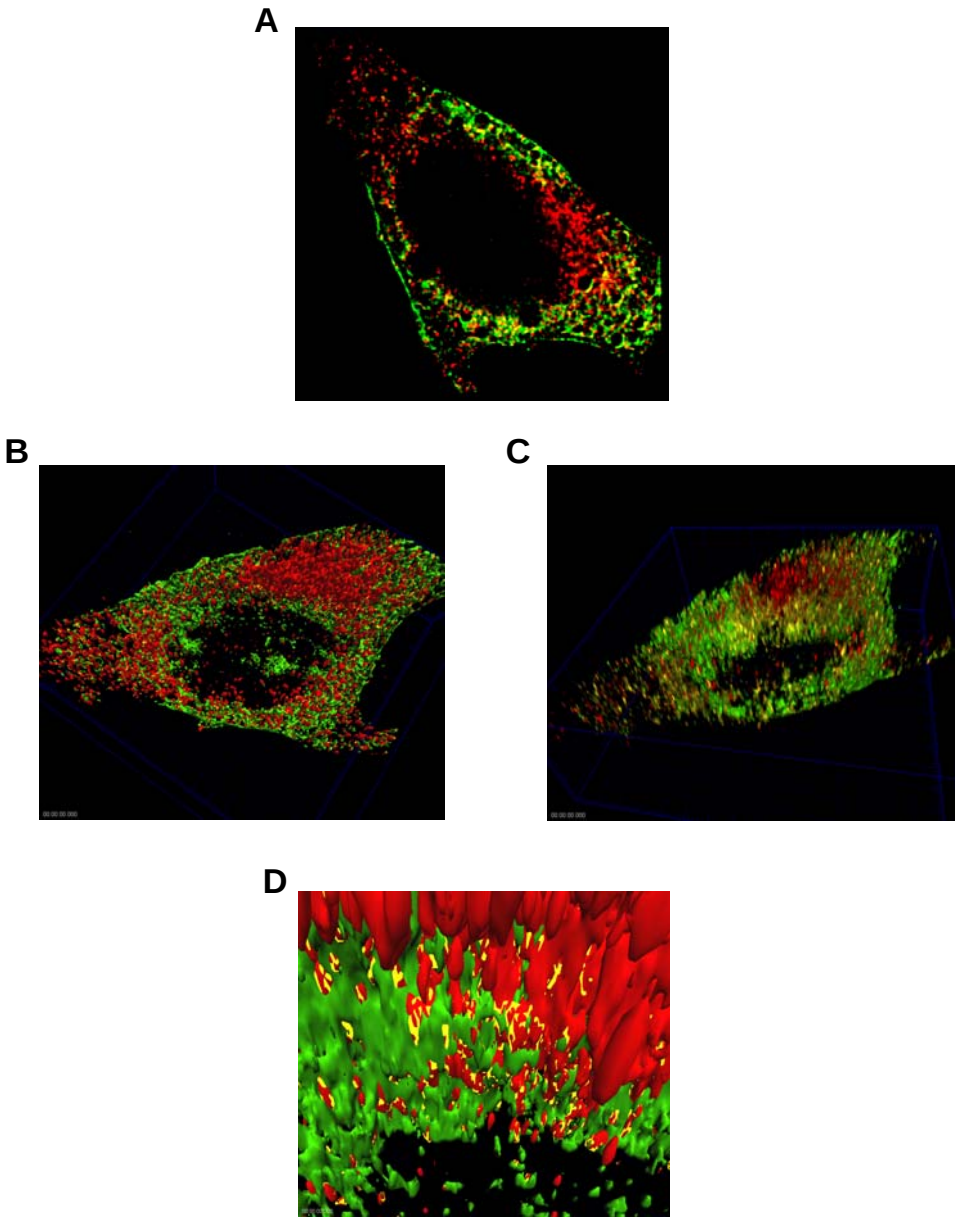

Fig. 34: WNK1 and wild-type VPS4a localization in HeLa cells. HeLa cells were transfected with Myc-WNK1 and HA-VPS4a, fixed, stained with anti-Myc and anti-HA antibodies, and analyzed with a Zeiss Deltavision microscope. ***A,*** Co-localization of WNK1 and VPS4a as analyzed with Image j. ***B-C,*** Three-dimensional model created with the Imaris® software. ***D,*** Magnified three-dimensional image shown in panels B and C. These data were generated by Abhijit Bugde and Szu-wei Tu and are representative of one experiment.

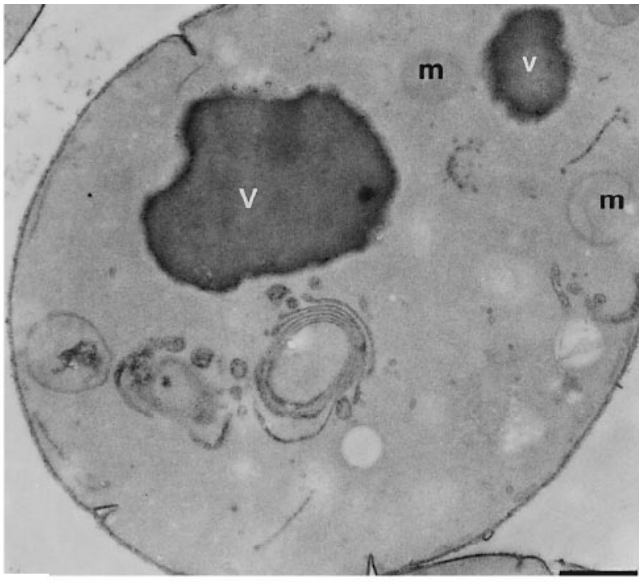

Fig. 35: Previously reported ultrastructural change caused by mutant VPS4. Electron microscope analysis of *vps4^{ts} S. cerevisiae* showing an aberrant stack located near the vacuole. This image is from Babst *et al.* 1997 and is being used with permission.

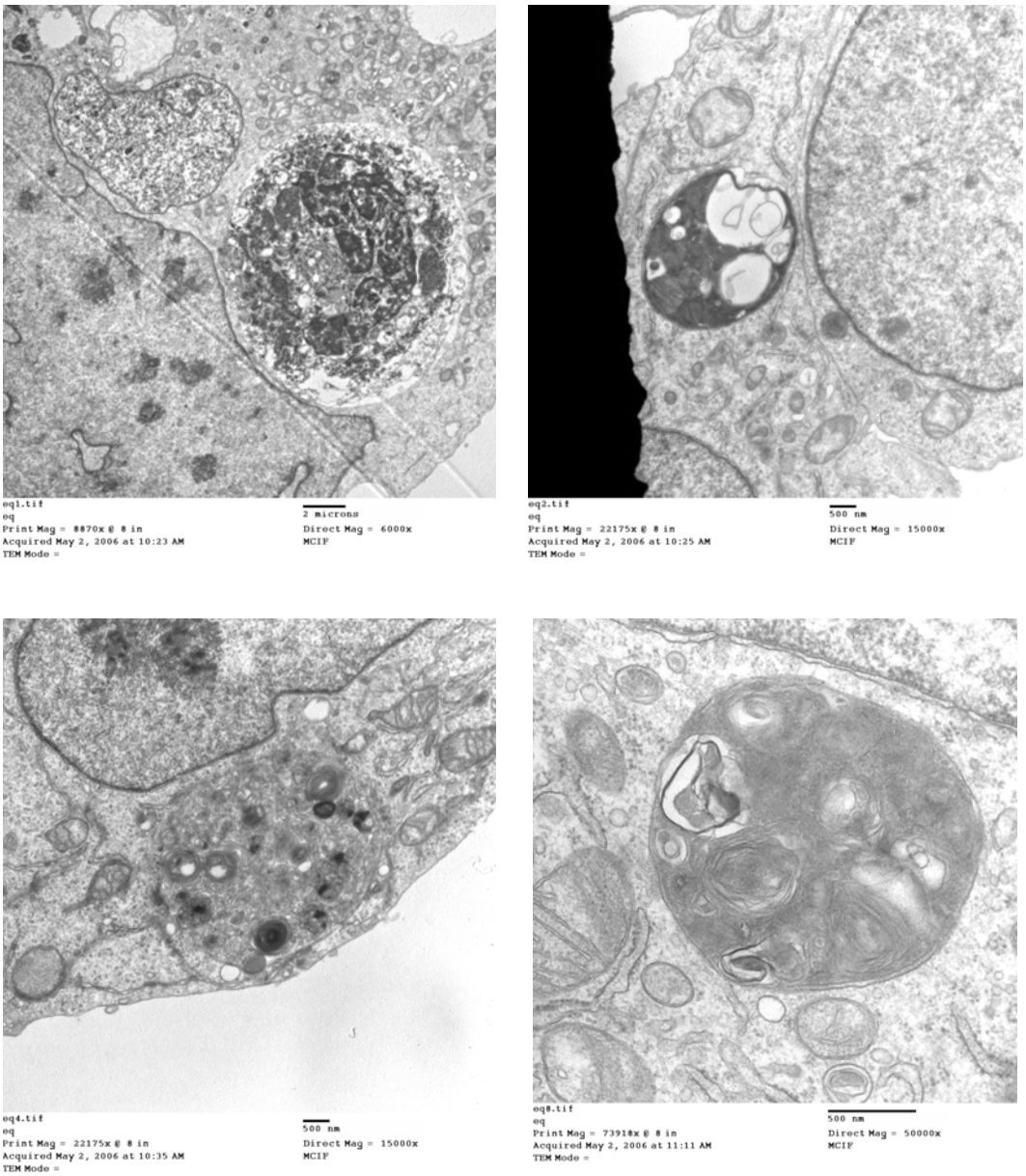

Fig. 36: TEM of HEK293 cells transfected with VPS4a E228Q. HEK293 cells were transfected with GFP-tagged VPS4a E228Q, fixed with glutaraldehyde, embedded in Embed, and sectioned. These particular images were taken by Chris Gilpin and are representative of one experiment.

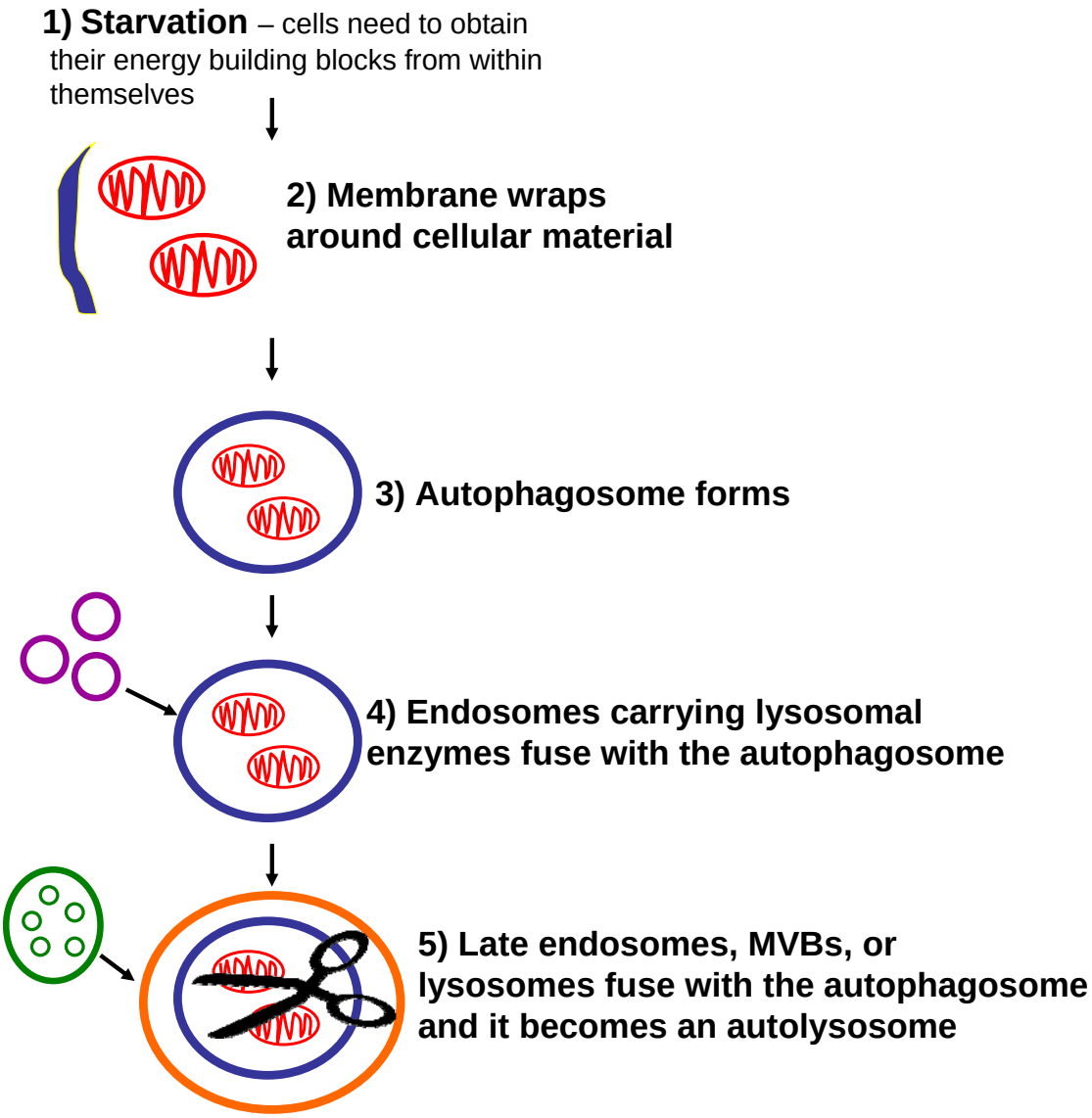

Fig. 37: Model of macroautophagic pathway in mammals.
Autophagosomes and autolysosomes are formed in response to nutrient starvation and infection by some viruses and bacteria. After initiation of the pathway (1), a flat membrane sack wraps around a part of the cytoplasm (2) and closes (3), forming an autophagosome. Next, endosomes deliver lysosomal enzymes to the autophagosome (4), and finally, the autophagosome fuses with late endosomes, MVBs, or lysosomes (5). At this final step the autophagosome is termed an autolysosome or degradative autophagic vacuole.

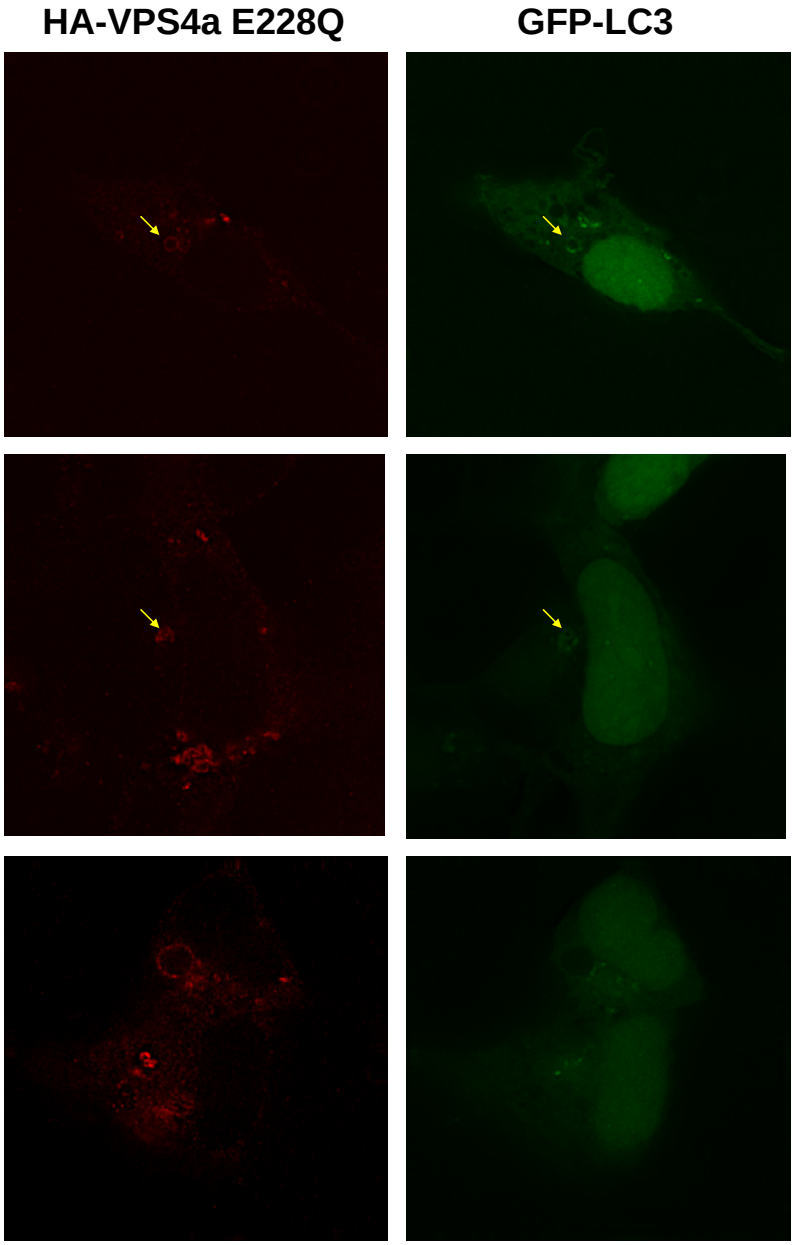

Fig. 38: A few of the VPS4a E228Q-positive structures in HEK293 co-localize with the autophagosome marker LC3. LC3 is GFP tagged. HA-tagged VPS4a E228Q was stained with an anti-HA antibody and an Alexa red secondary antibody. Structures where both LC3 and VPS4a E228Q are localized are marked with an arrow. These data are representative of one experiment.

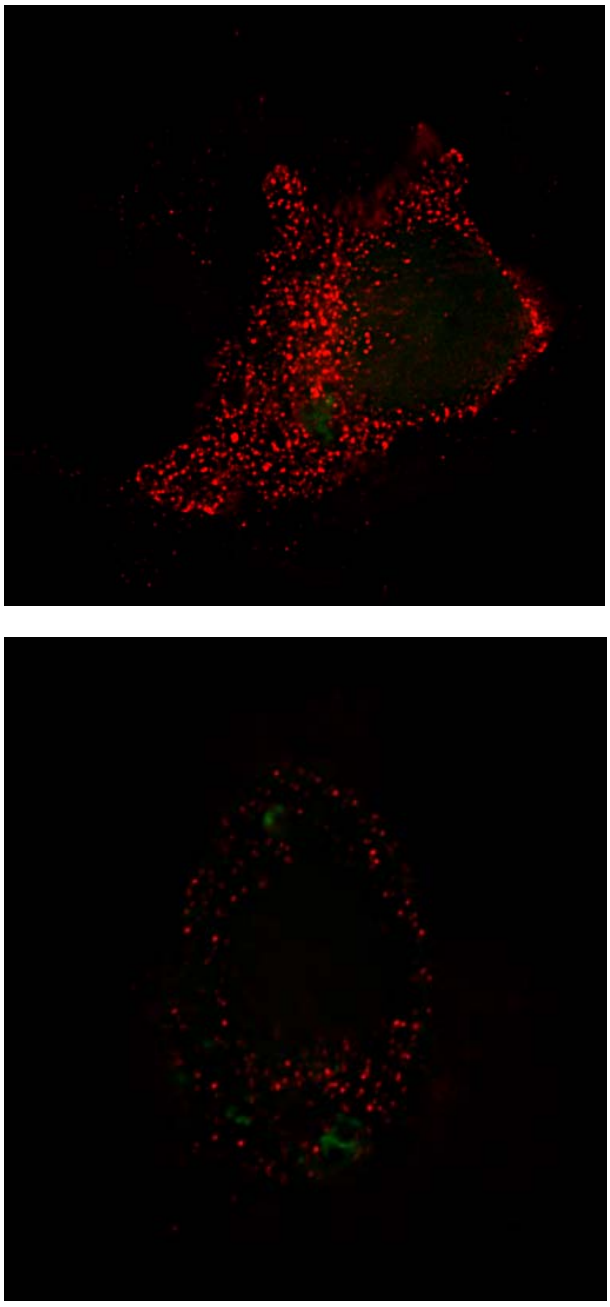

Fig. 39: WNK1 and LC3 do not overlap in HeLa cells. HeLa cells were transfected with Myc-WNK1 (red) and GFP-LC3 (green), fixed, stained with an anti-Myc antibody, analyzed with a Zeiss Deltavision microscope, and deconvolved. These data are representative of one experiment.

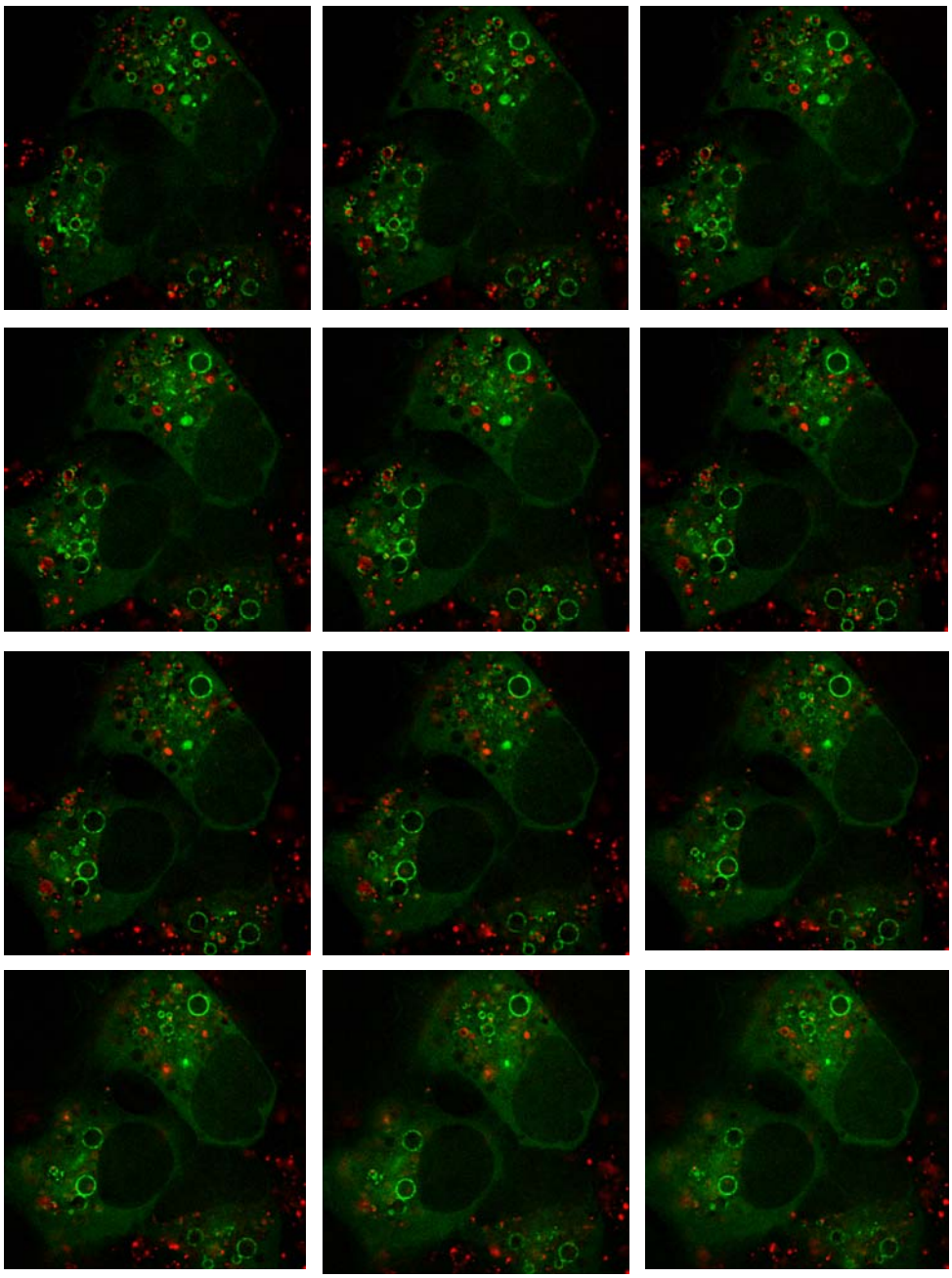

Fig 40: VPS4a E228Q does not largely co-localize with the lysosome marker LysoTracker® Red. HEK293 cells were transfected with GFP-VPS4a E228Q, stained with LysoTracker®, analyzed with a Zeiss Deltavision microscope, and the images were deconvolved.

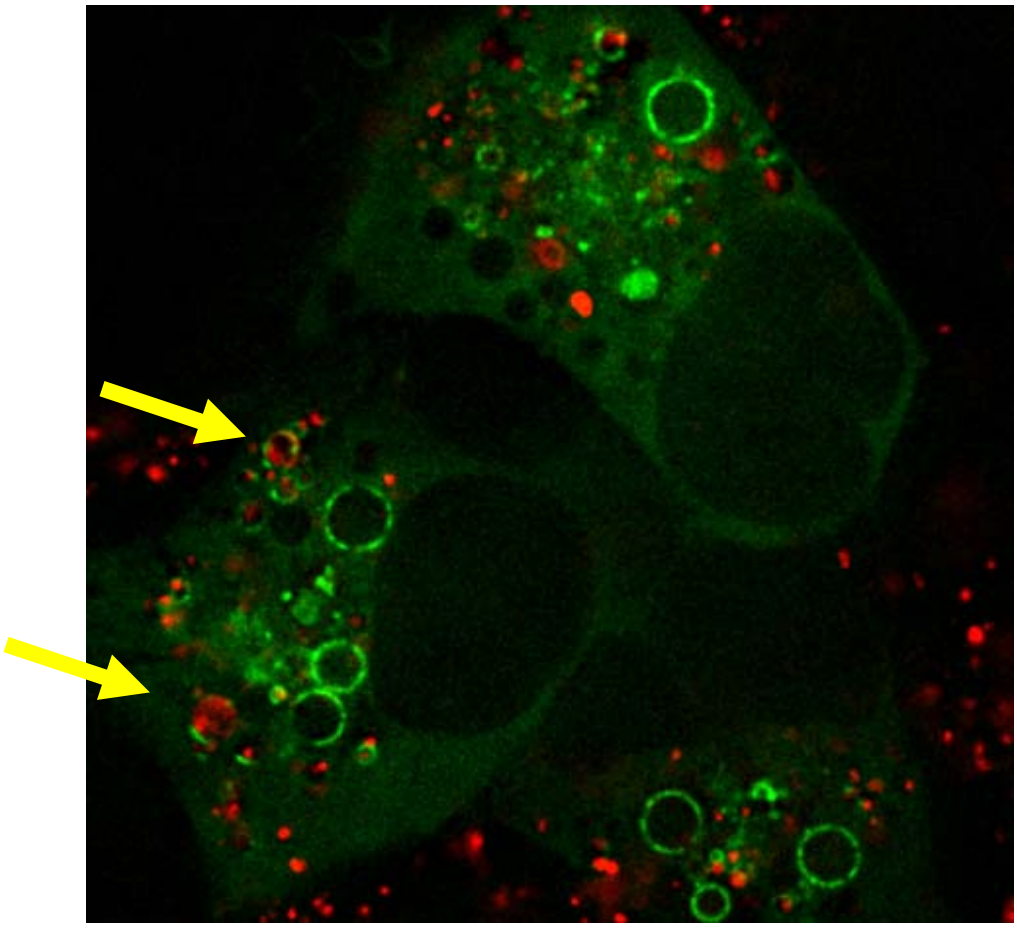

Fig 41: Larger image of one stack shown in Figure 40. Only a small subset of GFP-VPS4a E228Q localizes with LysoTracker® Red. See yellow arrows.

Chapter 5

Perspectives and Future Directions

Current Major Areas of WNK Research- Because mutations in WNK1 and WNK4 were found in patients with PHAII, focus has been placed on two major aspects of study concerning these kinases. Human geneticists have been attempting to correlate mutations in WNK promoters and genes to the severity of essential hypertension, and physiologists have been determining what ion channels and transporters WNK kinases regulate (discussed in Chapter 1).

In comparison to the amount of effort involved in these two fundamental areas, relatively little work has been conducted to understand how WNK kinases behave as enzymes and how they signal to influence the activity of the various channels and transporters. I predict that research groups will continue to use human genetic studies to link mutations in WNK kinases to other forms of hypertension besides PHAII and to use reconstitution studies to help identify the cell surface proteins that are regulated by each WNK family member. In addition, I predict the need to understand WNK kinase signaling and the mechanisms it utilizes to regulate the various channels and transporters will emerge and become another main focus of study. Our laboratory has been the major contributor of information concerning WNK biochemistry and signaling, but much work is still needed to connect these kinases to the regulation of blood pressure.

Correlating Mutations in WNK Kinases to Essential Hypertension- Because high blood pressure is a major health problem, better understanding the causes of essential hypertension has implications for developing treatments that

could benefit millions of people. As discussed previously, there have been a few population-based studies conducted to determine whether mutations in WNK1 and WNK4 are found in individuals that have no known genetic component leading to their high blood pressure. Two studies of Caucasians in Britain have suggested that mutations in WNK1 correlate with the severity of an individual's hypertension (Newhouse *et al.* 2005; Tobin *et al.* 2005).

It would be interesting to conduct further human genetic studies to determine whether mutations in WNK kinases are found in additional ethnic groups. Eventually, if more studies show mutations in WNKs are found in members of the general population who have high blood pressure, specific WNK SNPs and haplotypes may become genetic markers used to assess an individual's risk for developing hypertension and possibly the severity of the hypertension. If additional correlations are made, I anticipate that the WNK field will expand even further, and WNK kinases may become the focus of anti-hypertensive drug development.

Before an anti-WNK1 drug is developed, the target region needs to be identified. At this point it is premature to decide whether the kinase domain or a domain required for a particular protein-protein interaction would be the best target. Therefore, more studies are required to understand the importance of the WNK1 kinase domain and its binding partners in regulating ion homeostasis. The unique structure of the WNK catalytic domain provides a potentially reasonable

area to target since only WNK1, WNK2, WNK3 and WNK4 exhibit this atypical arrangement.

Regulation of Ion Channels and Transporters by WNK Kinases- Many reconstitution experiments in *Xenopus* oocytes and mammalian cell lines have been performed to identify ion transporters and channels that are regulated by WNK kinases and to determine whether the WNK-mediated effects are kinase dependent or independent (discussed in Chapter 1). In these assays, different WNK fragments or mutant WNKs are co-expressed with a given transporter or channel, and the cell surface expression and/or activity of the transporter or channel is measured.

Although these experiments have provided information about how WNK kinases may globally regulate blood pressure by identifying ion transporters and channels that are WNK-sensitive, there is relatively little information that connects each WNK to specific cell surface proteins. After more WNK substrates and interacting partners are identified, these variables should be included in the transporter and channel activity assays to determine their contribution to the WNK-mediated effects. In order to find these variables, more WNK1 characterization studies are critical and better reagents to study individual family members will be essential to this effort.

Potential Role of VPS4a in Regulating Ion Transporters and Channels- The identification of VPS4a as a WNK1 binding partner may provide a starting

point for deciphering how WNK1 regulates the cell surface presentation of ion transporters and channels. Because VPS4 plays a critical role in MVB formation and the degradation of plasma membrane proteins such as EGFR, it is likely VPS4a also promotes the down-regulation of ENaC, NCCT, NKCC, TRPV4 and KCC, proteins regulated by WNK1. To test this idea, VPS4a should be used as a variable in the channel and transporter activity assays, and if it is determined that VPS4a is involved in degrading these proteins, the impact of its interaction with WNK1 needs to be addressed. As described in Chapter 4, in collaboration with Chou-Long Huang's laboratory, I have tested whether VPS4 influences the surface expression and activity of the potassium channel ROMK, but results from these studies were inconclusive. Although VPS4a does not appear to play a role in regulating ROMK, it may modulate the activity of the other WNK1-sensitive cell surface proteins, ENaC, NCCT, NKCC and TRPV4

To test the role of the WNK1 interaction with VPS4a in modulating the plasma membrane localization of these channels and transporters, the cell surface localization of these proteins needs to be analyzed when the binding of WNK1 with VPS4a has been blocked. In order to do this, mutants of either protein that fail to bind to one another need to be generated. It would be useful to perform a random mutagenesis yeast-two-hybrid screen to identify point mutants that fail to interact with its binding partner. Once this has been conducted, the mutants can be over-expressed to override the function of the endogenous protein, or as an

alternative strategy, the fragment of WNK1 that binds to VPS4a can be over-expressed to disrupt the interaction between endogenous WNK1 and VPS4a.

One critical question is that if WNK1 does interact with VPS4a to regulate ion transporters and channels, is it a global regulator of intracellular trafficking or does it only modulate specific proteins? I predict that WNK1 is not a global regulator of lysosomal-mediated protein degradation. If it were, the PHAII patients would likely suffer a magnitude of problems as a consequence of having a perturbation in this critical pathway and WNK1 has not been identified by other groups as a contributor to this process. I anticipate that WNK1 will prove to be selective in what it may target for sorting through the endosomal pathway.

Acknowledgements

I would like to thank my mentor Melanie Cobb and my committee members Paul Sternweis, Joe Albanesi, Jim Waddle, and Mike White for their input and guidance and the Department of Defense for funding. I thank Bing-e Xu, Steve Stippec, Charles Heise, Byung-Hoon Lee, Xiaoshan Min, Wei Chen, Beth Levine, Wes Sundquist (U. of Utah), Jeff Frost (MD Anderson), and Masatoshi Maki (Nagoya U.) for various constructs and recombinant proteins and Wei Chen and Mark Henkemeyer for the mouse brain library. I thank Jill Reiter (Yale), Nita Maihle (Yale), Scott Emr (UCSD), and Markus Babst (U. of Utah) for antibodies. I thank Woody Wright, Jerry Shay, Richard Gaynor, and Orson Moe for cell lines. I thank Hongjun Sun and Yingming Zhao for their assistance with mass spectrometry. I thank Kate Luby-Phelps for her immense help with fluorescence microscopy and Abhijit Bugde for the many hours he spent creating the three-dimensional models. I thank the electron microscopy core facility for their help and guidance. I thank Colleen Vanderbilt who has been working with me for almost two years generating vast amounts of constructs and helping me with some of the yeast-two-hybrid experiments. I also thank Colleen Vanderbilt and Charles Heise for the many scientific discussions they had with me and Szu-wei Tu, a rotation student who analyzed the WNK1-VPS4a interaction in HeLa cells. Lastly, I think Dionne Ware for her mammoth amounts of administrative assistance.

Literature Cited

Anselmo, A.N., Earnest, S., Chen, W., Juang, Y.C., Kim, S.C., Zhao, Y., and M.H. Cobb. 2006. WNK1 and OSR1 regulate the Na+, K+, 2Cl- cotransporter in HeLa cells. *Proc. Natl. Acad. Sci.* **103:**10883-8.

Babst, M., Sato, T.K., Banta, L.M., and S.D. Emr. 1997. Endosomal transport function in yeast requires a novel AAA-type ATPase, Vps4p. *EMBO J.* **16:**1820-31.

Balasenthil, S., Sahin, A.A., Barnes, C.J., Wang, R.A., Pestell, R.G., Vadlamudi, R.K., and R. Kumar. 2004. p21-activated kinase-1 signaling mediates cyclin D1 expression in mammary epithelial and cancer cells. *J. Biol. Chem.* **279:**1422-8.

Banerjee, M., Worth, D., Prowse, D.M., and M. Nikolic. 2002. Pak1 phosphorylation on t212 affects microtubules in cells undergoing mitosis. *Curr. Biol.* **12:**1233-9.

Beeser, A., Jaffer, Z.M., Hofmann, C., and J. Chernoff. 2005. Role of group A p21-activated kinases in activation of extracellular-regulated kinase by growth factors. *J. Biol. Chem.* **280:**36609-15.

Beyer, A., Scheuring, S., Muller, S., Mincheva, A., Lichter, P., and K. Kohrer. 2003. Comparative sequence and expression analyses of four mammalian VPS4 genes. *Gene* **305:**47-59.

Cai, H., Cebotaru, V., Wang, Y.H., Zhang, X.M., Cebotaru, L., Guggino, S.E., and W.B. Guggino. 2006. WNK4 kinase regulates surface expression of the human sodium chloride cotransporter in mammalian cells. *Kidney Int.* **69:**2162-70.

Chen, W., Yazicioglu, M., and M.H. Cobb. 2004. Characterization of OSR1, a member of the mammalian Ste20p/germinal center kinase subfamily. *J. Biol. Chem.* **279:**11129-36.

Choate, K.A., Kahle, K.T., Wilson, F.H., Nelson-Williams, C., and R.P. Lifton. 2003. WNK1, a kinase mutated in inherited hypertension with hyperkalemia, localizes to diverse Cl- -transporting epithelia. *Proc. Natl. Acad. Sci.* **100:**663-8.

Chong, C., Tan, L., Lim, L., and E. Manser. 2001. The mechanisms of PAK activation. *J. Biol. Chem.* **276:**17347-53.

Cope, G., Murthy, M., Golbang, A.P., Hamad, A., Liu, C.H., Cuthbert, A.W., and K.M. O'Shaughnessy. 2006. WNK1 affects surface expression of the ROMK potassium channel independent of WNK4. *J. Am. Soc. Nephrol.* **17:**1867-74.

Dechert, M.A., Holder, J.M., and W.T. Gerthoffer. 2001. p21-activated kinase 1 participates in tracheal smooth muscle cell migration by signaling to p38 Mapk. *Am. J. Physiol. Cell Physiol.* **281:**C123-32.

Frost, J.A., Steen, H., Shapiro, P., Lewis, T., Ahn, N., Shaw, P.E., and M.H. Cobb. 1997. Cross-cascade activation of ERKs and ternary complex factors by Rho family proteins. *EMBO J.* **16:**6426-38.

Frost, J.A., Xu, S., Hutchison, M.R., Marcus, S., and M.H. Cobb. 1996. Actions of Rho family small G proteins and p21-activated protein kinases on mitogen-activated protein kinase family members. *Mol. Cell Biol.* **16:**3707-13.

Fu, Y., Subramanya, A., Rozansky, D., and D.M. Cohen. 2006. WNK kinases influence TRPV4 channel function and localization. *Am. J. Physiol. Renal Physiol.* **290:**F1305-14.

Fujita, H., Yamanaka, M., Imamura, K., Tanaka, Y., Nara, A., Yoshimori, T., Yokota, S., and M. Himeno. 2003. A dominant negative form of the AAA ATPase SKD1/VPS4 impairs membrane trafficking out of endosomal/lysosomal compartments: class E vps phenotype in mammalian cells. *J. Cell Sci.* **116:**401-14.

Gagnon, K.B., England, R., and E. Delpire. 2006. Volume sensitivity of cation-Cl- cotransporters is modulated by the interaction of two kinases: Ste20-related proline-alanine-rich kinase and WNK4. *Am. J. Physiol. Cell Physiol.* **290:**C134-42.

Garrus, J.E., von Schwedler, U.K., Pornillos, O.W., Morham, S.G., Zavitz, K.H., Wang, H.E., Wettstein, D.A., Stray, K.M., Cote, M., Rich, R.L., Myszka, D.G., and W.I. Sundquist. 2001. Tsg101 and the vacuolar protein sorting pathway are essential for HIV-1 budding. *Cell* **107:**55-65.

Golbang, A.P., Cope, G., Hamad, A., Murthy, M., Liu, C.H., Cuthbert, A.W., and K.M. O'Shaughnessy. 2006. Regulation of the Expression of the Na/Cl cotransporter (NCCT) by WNK4 and WNK1: evidence that accelerated dynamin-dependent endocytosis is not involved. *Am. J. Physiol. Renal Physiol.* [epub ahead of print].

Howard, T.L., Stauffer, D.L., Degnin, C.R., and S.M. Hollenberg. 2001. CHMP1 functions as a member of a newly defined family of vesicle trafficking proteins. *J. Cell Sci.* **114:**2395-404.

Hislop, J.N., Marley, A., and M. von Zastrow. 2004. Role of mammalian vacuolar protein-sorting proteins in endocytic trafficking of a non-ubiquitinated G protein-coupled receptor to lysosomes. *J. Biol. Chem.* **279:**22522-31.

Hurley, J.H., and S.D. Emr. 2006. THE ESCRT COMPLEXES: Structure and mechanism of a membrane-trafficking network. *Annu. Rev. Biophys. Biomol. Struct.* **35:**277-298.

Jaffer, Z.M., and J. Chernoff. 2002. p21-activated kinases: three more join the Pak. *Int. J. Biochem. Cell Biol.* **34:**713-717.

Jiang, Y., Ferguson, W.B., and J.B. Peng. 2006. WNK4 enhances TRPV5-mediated calcium transport: potential role in hypercalciuria of familial hyperkalemic hypertension caused by gene mutation of WNK4. *Am. J. Physiol. Renal Physiol.* [epub ahead of print].

Kahle, K.T., Gimenez, I., Hassan, H., Wilson, F.H., Wong, R.D., Forbush, B., Aronson, P.S., and R.P. Lifton. 2004. WNK4 regulates apical and basolateral Cl- flux in extrarenal epithelia. *Proc. Natl. Acad. Sci.* **101:**2064-9.

Kahle, K.T., Rinehart, J., de Los Heros, P., Louvi, A., Meade, P., Vazquez, N., Hebert, S.C., Gamba, G., Gimenez, I., and R.P. Lifton. 2005. WNK3 modulates transport of Cl- in and out of cells: implications for control of cell volume and neuronal excitability. *Proc. Natl. Acad. Sci.* **102:**16783-8.

Kahle, K.T., Wilson, F.H., Leng, Q., Lalioti, M.D., O'Connell, A.D., Dong, K., Rapson, A.K., MacGregor, G.G., Giebisch, G., Hebert, S.C., and R.P. Lifton. 2003. WNK4 regulates the balance between renal NaCl reabsorption and K+ secretion. *Nat. Genet.* **35:**372-6.

Katzmann, D.J., Odorizzi, G., and S.D. Emr. 2002. Receptor downregulation and multivesicular-body sorting. *Nat. Rev. Mol. Cell Biol.* **3:**893-905.

Kian Chua, P., Lin, M.H., and C. Shih. 2006. Potent inhibition of human Hepatitis B virus replication by a host factor Vps4. *Virology* **354:**1-6.

Knaus, U.G., Morris, S., Dong, H.J., Chernoff, J., and G.M. Bokoch. 1995. Regulation of human leukocyte p21-activated kinases through G protein--coupled receptors. *Science* **269:**221-223.

Landes Bioscience. *Macroautophagic Pathway.* Viewed 23 September 2006. http://www.ncbi.nlm.nih.gov/books/bv.fcgi?rid=eurekah.section.24953.

Lazrak, A., Liu, Z., and C.L. Huang. 2006. Antagonistic regulation of ROMK by long and kidney-specific WNK1 isoforms. *Proc. Natl. Acad. Sci.* **103:**1615-20.

Lee, B.H., Min, X., Heise, C.J., Xu, B.E., Chen, S., Shu, H., Luby-Phelps, K., Goldsmith, E.J., and M.H. Cobb. 2004. WNK1 phosphorylates synaptotagmin 2 and modulates its membrane binding. *Mol. Cell* **15:**741-51.

Lenertz, L.Y., Lee, B.H., Min, X., Xu, B.E., Wedin, K., Earnest, S., Goldsmith, E.J., and M.H. Cobb. 2005. Properties of WNK1 and implications for other family members. *J. Biol. Chem.* **280:**26653-8.

Leng, Q., Kahle, K.T., Rinehart, J., MacGregor, G.G., Wilson, F.H., Canessa, C.M., Lifton, R.P., and S.C. Hebert. 2006. WNK3, a kinase related to genes mutated in hereditary hypertension with hyperkalaemia, regulates the K+ channel ROMK1 (Kir1.1). *J. Physiol.* **571:**275-86.

Li, W., and H. She. 2000. **The** SH2 and SH3 adapter Nck: a two-gene family and a linker between tyrosine kinases and multiple signaling networks. *Histol. Histopathol.* **15:**947-55.

Licata, J.M., Simpson-Holley, M., Wright, N.T., Han, Z., Paragas, J., and R.N. Harty. 2003. Overlapping motifs (PTAP and PPEY) within the Ebola virus VP40 protein function independently as late budding domains: involvement of host proteins TSG101 and VPS-4. *J. Virol.* **77:**1812-9.

Lupas, A.N., and J. Martin. 2002. AAA proteins. *Curr. Opin. Struct. Biol.* **12:**746-53.

Malik, B., Price, S.R., Mitch, W.E., Yue, Q., and D.C. Eaton. 2006. Regulation of epithelial sodium channels by the ubiquitin-proteasome proteolytic pathway. *Am. J. Physiol. Renal Physiol.* **290:**F1285-94.

Min, X., Lee, B.H., Cobb, M.H., and E.J. Goldsmith. 2004. Crystal structure of the kinase domain of WNK1, a kinase that causes a hereditary form of hypertension. *Structure* **12:**1303-11.

Moriguchi, T., Urushiyama, S., Hisamoto, N., Iemura, S., Uchida, S., Natsume, T., Matsumoto, K., and H. Shibuya. 2005. WNK1 regulates phosphorylation of cation-chloride-coupled cotransporters via the STE20-related kinases, SPAK and OSR1. *J. Biol. Chem.* **280:**42685-93.

Morita, E., and W.I. Sunquist. 2004. Retrovirus budding. *Annu. Rev. Cell Dev. Biol.* **20:**395-425.

Mu, F.T., Callaghan, J.M., Steele-Mortimer, O., Stenmark, H., Parton, R.G., Campbell, P.L., McCluskey, J., Yeo, J.P., Tock, E.P., and B.H. Toh. 1995. EEA1, an early endosome-associated protein. EEA1 is a conserved alpha-helical peripheral membrane protein flanked by cysteine "fingers" and contains a calmodulin-binding IQ motif. *J. Biol. Chem.* **270:**13503-11.

Nakamichi, N., Murakami-Kojima, M., Sato, E., Kishi, Y., Yamashino, T., and T. Mizuno. 2002. Compilation and characterization of a novel WNK family of protein kinases in *Arabiodpsis thaliana* with reference to circadian rhythms. *Biosci. Biotechnol. Biochem.* **66:**2429-36.

Naray-Fejes-Toth, A., Snyder, P.M., and G. Fejes-Toth. 2004. The kidney-specific WNK1 isoform is induced by aldosterone and stimulates epithelial sodium channel-mediated Na+ transport. *Proc. Natl. Acad. Sci.* **101:**17434-9.

Newhouse, S.J.,Wallace, C., Dobson, R., Mein, C., Pembroke, J., Farrall, M., Clayton, D., Brown, M., Samani, N., Dominiczak, A., Connell, J.M., Webster, J., Lathrop, G.M., Caulfield, M., and P.B. Munroe. 2005. Haplotypes of the WNK1 gene associate with blood pressure variation in a severely hypertensive population from the British Genetics of Hypertension study. *Hum. Mol. Genet.* **14:**1805-14.

Nilius, B., Vriens, J., Prenen, J., Droogmans, G., and T. Voets. 2004. TRPV4 calcium entry channel: a paradigm for gating diversity. *Am. J. Physiol. Cell Physiol.* **286:**C195-C205.

Nishimoto, S., and E. Nishida. 2006. MAPK signalling: ERK5 versus ERK1/2. *EMBO Rep.* **7:**782-6.

Parrini, M.C., Matsuda, M., and J. de Gunzburg. 2005. Spatiotemporal regulation of the Pak1 kinase. *Biochem. Soc. Trans.* **33:**646-8.

Patton, G.S., Morris, S.A., Chung, W., Bieniasz, P.D., and M.O. McClure. 2005. Identification of domains in gag important for prototypic foamy virus egress. *J. Virol.* **79:**6393-9.

Pearce, D. SGK1 regulation of epithelial sodium transport. 2003. *Cell Physiol Biochem.* **13:**13-20.

Rashid, T., Banerjee, M., and M. Nikolic. 2001. Phosphorylation of Pak1 by the p35/Cdk5 kinase affects neuronal morphology. *J. Biol. Chem.* **276:**49043-52.

Rinehart, J., Kahle, K.T., de Los Heros, P., Vazquez, N., Meade, P., Wilson, F.H., Hebert, S.C., Gimenez, I., Gamba, G., and R.P. Lifton. 2005. WNK3 kinase is a positive regulator of NKCC2 and NCC, renal cation-Cl- cotransporters required for normal blood pressure homeostasis. *Proc. Natl. Acad. Sci.* **102:**16777-82.

Rossier, B.C. 2003. Negative regulators of sodium transport in the kidney: key factors in understanding salt-sensitive hypertension? *J. Clin. Invest.* **111:**947-50.

Scheuring, S., Rohricht, R.A., Schoning-Burkhardt, B., Beyer, A., Muller, S., Abts, H.F., and K. Kohrer. 2001**.** Mammalian cells express two VPS4 proteins both of which are involved in intracellular protein trafficking. *J. Mol. Biol.* **312:**469-80.

Schmitt, A.P., Leser, G.P., Morita, E., Sundquist, W.I., and R.A. Lamb. 2005. Evidence for a new viral late-domain core sequence, FPIV, necessary for budding of a paramyxovirus. *J. Virol.* **79:**2988-97.

Scott, A., Chung, H.Y., Gonciarz-Swiatek, M., Hill, G.C., Whitby, F.G., Gaspar, J., Holton, J.M., Viswanathan, R., Ghaffarian, S., Hill, C.P., and W.I. Sundquist. 2005a. Structural and mechanistic studies of VPS4 proteins. *EMBO J.* **24:**3658-69.

Scott, A., Gaspar, J., Stuchell-Brereton, M.D., Alam, S.L., Skalicky, J.J., and W.I. Sundquist. 2005b. Structure and ESCRT-III protein interactions of the MIT domain of human VPS4A. *Proc. Natl. Acad. Sci.* **102:**13813-8.

Strange, K., Denton, J., and K. Nehrke. 2006. Ste20-type kinases: evolutionarily conserved regulators of ion transport and cell volume. *Physiology* **21:**61-8.

Sudhof, T.C. 2002. Synaptotagmins: Why so many? *J. Biol. Chem.* **277:**7629-32.

Sun, X., Gao, L, Yu, R.K., and G. Zheng. 2006. Down-regulation of WNK1 protein kinase in neural progenitor cells suppresses cell proliferation and migration. *J. Neurochem.* [epub ahead of print].

Tanida, I., Ueno, T., and E. Kominami. 2004. LC3 conjugation system in mammalian autophagy. *Int. J. Biochem. Cell Biol.* **36:**2503-13.

Thebault, S., Hoenderop, J.G., and R.J. Bindels. 2006. Epithelial Ca2+ and Mg2+ channels in kidney disease. *Adv. Chronic Kidney Dis.* **13:**110-7.

Tobin, M.D., Raleigh, S.M., Newhouse, S., Braund, P., Bodycote, C., Ogleby, J., Cross, D., Gracey, J., Hayes, S., Smith, T., Ridge, C., Caulfield, M., Sheehan, N.A., Munroe, P.B., Burton, P.R., and N.J. Samani. 2005. Association of WNK1 gene polymorphisms and haplotypes with ambulatory blood pressure in the general population. *Circulation* **112:**3423-9.

Verissimo, F., and P. Jordan. 2001. WNK kinases, a novel protein kinase subfamily in multi-cellular organisms. *Oncogene* **20:**5562-9.

Verissimo, F., Silva, E., Morris, J.D., Pepperkok, R., and P. Jordan. 2006. Protein kinase WNK3 increases cell survival in a caspase-3-dependent pathway. *Oncogene* **25:**4172-82.

Vitari, A.C., Deak, M., Collins, B.J., Morrice, N., Prescott, A.R., Phelan, A., Humphreys, S., and D.R. Alessi. 2004. WNK1, the kinase mutated in an inherited high-blood-pressure syndrome, is a novel PKB (protein kinase B)/Akt substrate. *Biochem. J.* **378:**257-68.

Vitari, A.C., Deak, M., Morrice, N.A., and D.R. Alessi. 2005. The WNK1 and WNK4 protein kinases that are mutated in Gordon's hypertension syndrome phosphorylate and activate SPAK and OSR1 protein kinases. *Biochem. J.* **391:**17-24.

Wade, J.B., Fang, L., Liu, J., Li, D., Yang, C.L., Subramanya, A.R., Maouyo, D., Mason, A., Ellison, D.H., and P.A. Welling. 2006. WNK1 kinase isoform switch regulates renal potassium excretion. *Proc. Natl. Acad. Sci.* **103:**8558-63.

Wang, J., Frost, J.A., Cobb, M.H., and E.M. Ross. 1999. Reciprocal signaling between heterotrimeric G proteins and the p21-stimulated protein kinase. *J. Biol. Chem.* **274:**31641-7.

Wang, R.A., Mazumdar, A., Vadlamudi, R.K., and R. Kumar. 2002. P21-activated kinase-1 phosphorylates and transactivates estrogen receptor-alpha and promotes hyperplasia in mammary epithelium. *EMBO J.* **21:**5437-47.

Wang, Z., Yang, C.L., and D.H. Ellison. 2004. Comparison of WNK4 and WNK1 kinase and inhibiting activities. *Biochem. Biophys. Res. Commun.* **317:**939-44.

Wilson, F.H., Disse-Nicodeme, S., Choate, K.A., Ishikawa, K., Nelson-Williams, C., Desitter, I., Gunel, M., Milford, D.V., Lipkin, G.W., Achard, J.M., Feely, M.P., Dussol, B., Berland, Y., Unwin, R.J., Mayan, H., Simon, D.B., Farfel, Z., Jeunemaitre, X., and R.P. Lifton. 2001. Human hypertension caused by mutations in WNK kinases. *Science* **293:**1107-12.

Xie, J., Craig, L., Cobb, M.H., and C.L. Huang. 2006. Role of with-no-lysine [K] kinases in the pathogenesis of Gordon's syndrome. *Pediatr. Nephrol.* **21:**1231-6.

Xu, B., English, J.M., Wilsbacher, J.L., Stippec, S., Goldsmith, E.J., and M.H. Cobb. 2000. WNK1, a novel mammalian serine/threonine protein kinase lacking the catalytic lysine in subdomain II. *J. Biol. Chem.* **275:**16795-801.

Xu, B.E., Min, X., Stippec, S., Lee, B.H., Goldsmith, E.J., and M.H. Cobb. 2002. Regulation of WNK1 by an autoinhibitory domain and autophosphorylation. *J. Biol. Chem.* **277:**48456-62.

Xu, B.E., Stippec, S., Chu, P.Y., Lazrak, A., Li, X.J., Lee, B.H., English, J.M., Ortega, B., Huang, C.L., and M.H. Cobb. 2005a. WNK1 activates SGK1 to regulate the epithelial sodium channel. *Proc. Natl. Acad. Sci.* **102:**10315-20.

Xu, B.E., Stippec, S., Lazrak, A., Huang, C.L., and M.H. Cobb. 2005b. WNK1 activates SGK1 by a phosphatidylinositol 3-kinase-dependent and non-catalytic mechanism. *J. Biol. Chem.* **280:**34218-23.

Xu, B.E., Stippec, S., Lenertz, L., Lee, B.H., Zhang, W., Lee, Y.K., and M.H. Cobb. 2004. WNK1 activates ERK5 in a MEKK2/3-dependent mechanism. *J. Biol. Chem.* **279:**7826-31.

Yang, C.L., Angell, J., Mitchell, R., and D.H. Ellison. 2003. WNK kinases regulate thiazide-sensitive Na-Cl cotransport. *J. Clin. Invest.* **111:**1039-45.

Yang, C.L., Zhu, X., Wang, Z., Subramanya, A.R., and D.H. Ellison. 2005. Mechanisms of WNK1 and WNK4 interaction in the regulation of thiazide-sensitive NaCl cotransport. *J. Clin. Invest.* **115:**1379-87.

Yang, Z., Bagheri-Yarmand, R., Wang, R.A., Adam, L., Papadimitrakopoulou, V.V., Clayman, G.L., El-Naggar, A., Lotan, R., Barnes, C.J., Hong, W.K., and R. Kumar. 2004. The epidermal growth factor receptor tyrosine kinase inhibitor ZD1839 (Iressa) suppresses c-Src and Pak1 pathways and invasiveness of human cancer cells. *Clin. Cancer Res.* **10:**658-67.

Yeh, B.I., Sun, T.J., Lee, J.Z., Chen, H.H., and C.L. Huang. 2003. Mechanism and molecular determinant for regulation of rabbit transient receptor potential type 5 (TRPV5) channel by extracellular pH. *J. Biol. Chem.* **278:**51044-52.

Yeo, S.C., Xu, L., Ren, J., Boulton, V.J., Wagle, M.D., Liu, C., Ren, G., Wong, P., Zahn, R., Sasajala, P., Yang, H., Piper, R.C., and A.L. Munn. 2003. Vps20p and Vta1p interact with Vps4p and function in multivesicular body sorting and endosomal transport in Saccharomyces cerevisiae. *J. Cell Sci.* **116:**3957-70.

Yoeli-Lerner, M., and A. Toker. 2006. Akt/PKB signaling in cancer: a function in cell motility and invasion. *Cell Cycle* **5:**603-5.

Yoshimori, T., Yamagata, F., Yamamoto, A., Mizushima, N., Kabeya, Y., Nara, A., Miwako, I., Ohashi, M., Ohsumi, M., and Y. Ohsumi. 2000. The mouse SKD1, a homologue of yeast Vps4p, is required for normal endosomal trafficking and morphology in mammalian cells. *Mol. Biol. Cell* **11:**747-763.

Zambrowicz, B.P., Abuin, A., Ramirez-Solis, R., Richter, L.J., Piggott, J., BeltrandelRio, H., Buxton, E.C., Edwards, J., Finch, R.A., Friddle, C.J., Gupta, A., Hansen, G., Hu, Y., Huang, W., Jaing, C., Key, B.W., Kipp, P., Kohlhauff, B., Ma, Z.Q., Markesich, D., Payne, R., Potter, D.G., Qian, N., Shaw, J., Schrick, J., Shi, Z.Z., Sparks, M.J., Van Sligtenhorst, I., Vogel, P., Walke, W., Xu, N., Zhu, Q., Person, C., and A.T. Sands. 2003. Wnk1 kinase deficiency lowers blood pressure in mice: a gene-trap screen to identify potential targets for therapeutic intervention. *Proc. Natl. Acad. Sci.* **100:**14109-14.

Zhao, Z., and E. Manser. 2005. PAK and other Rho associated kinases- effectors with surprisingly diverse mechanisms of regulation. *Biochem. J.* **386:**201-214.

Zhang, S., Han, J., Sells, M.A., Chernoff, J., Knaus, U.G., Ulevitch, R.J., and G.M. Bokoch. 1995. Rho family GTPases regulate p38 mitogen-activated protein kinase through the downstream mediator Pak1. *J. Biol. Chem.* **270:**23934-6.

VITAE

Lisa Lenertz was born in Red Wing, Minnesota on October 15, 1978 to George and Yvonne Lenertz. She attended the University of Minnesota Duluth and earned a bachelor's of science in biochemistry. She entered the University of Texas Southwestern Graduate School of Biomedical Sciences in 2001 and married Kyle Lindemer on May 10, 2003. Kyle is currently in the Minnesota National Guard and a member of George Bush's imperialistic force in Iraq. They thankfully have no children but have six beautiful parrots.